①

S *CONSULTING*
 SERVICES

Donald L. Schilling Ph.D., P.E.

LEVEL

Hoffstot Lane
Sands Point, New York 11050

Telephone (516) 883-0760

AD A093851

Report   DAAB07-78-C-0173-0003

ADAPTIVE TECHNIQUES IN MULTICHANNEL TRANSMISSION

June 30, 1979

Final Report for Period 7 July 1978 - 30 June 1979

Prepared for
U.S. Army CORADCOM
Fort Monmouth, New Jersey 07703

DTIC
ELECTE
JAN 1 6 1981
C

DDC FILE COPY

81 1   15 055

S/C 395427

UNCLASSIFIED

REPORT DOCUMENTATION PAGE		READ INSTRUCTIONS BEFORE COMPLETING FORM
1 REPORT NUMBER DAAB07-78-C-0173	2. GOVT ACCESSION NO. AD-A093851	3. RECIPIENT'S CATALOG NUMBER
4 TITLE (and Subtitle) ADAPTIVE TECHNIQUES IN MULTI-CHANNEL TRANSMISSION		5. TYPE OF REPORT & PERIOD COVERED FINAL 1 July 1978 - 30 June 1979
		6. PERFORMING ORG. REPORT NUMBER DAAB07-78-C-0173
7. AUTHOR(s) L. MILSTEIN R. PETTIT S. RAPPAPORT D. L. SCHILLING		8. CONTRACT OR GRANT NUMBER(s) DAAB07-78-C-0173
9. PERFORMING ORGANIZATION NAME AND ADDRESS S CONSULTING SERVICES HOFFSTOT LANE, SANDS POINT, N.Y. 11050		10. PROGRAM ELEMENT, PROJECT, TASK AREA & WORK UNIT NUMBERS
11. CONTROLLING OFFICE NAME AND ADDRESS U.S. ARMY CORADCOM FORT MONMOUTH, NEW JERSEY 07703		12. REPORT DATE 30 June 1979
		13. NUMBER OF PAGES 95
14. MONITORING AGENCY NAME & ADDRESS(if different from Controlling Office)		15. SECURITY CLASS (of this report) UNCLASSIFIED
		15a. DECLASSIFICATION DOWNGRADING SCHEDULE

16. DISTRIBUTION STATEMENT (of this Report)

CORADCOM - INTERNAL

DISTRIBUTION STATEMENT A
Approved for public release;
Distribution Unlimited

17. DISTRIBUTION STATEMENT (of the abstract entered in Block 20, if different from Report)

18. SUPPLEMENTARY NOTES

19. KEY WORDS (Continue on reverse side if necessary and identify by block number)

SPREAD SPECTRUM TRACKING
FREQUENCY HOPPING PROCESSING GAIN
ACQUISITION

20. ABSTRACT (Continue on reverse side if necessary and identify by block number)

DD FORM 1473 EDITION OF 1 NOV 65 IS OBSOLETE

S/C 395 427

S CONSULTING
  SERVICES

Donald L. Schilling Ph.D., P.E.

Hoffstot Lane
Sands Point, New York 11050

Telephone (516) 883-0760

ABSTRACT

This report presents a new method of acquisition of a
spread spectrum signal. In addition, a comparison is
made between the error probability of several modulation/
spreading techniques as a function of the jammer-to-
signal (J/S) power ratio and the signal-to-noise (E_b/N)
ratio.

Table of Contents

I. SPREAD SPECTRUM COMMUNICATIONS: PART III

1.0 Minimum Shift Keying (MSK)--continued

In Part I we saw that MSK can be considered as a combined PSK/FSK modulation technique whose main advantages are that there is no phase discontinuity in the waveform, that the waveform is of constant amplitude and that it can be transmitted through a narrow band channel.

In this section we show that MSK can be considered to be a special form of QPSK which we call "QPSK with amplitude shaping." In addition, we describe the operation of a coherent MSK receiver which uses two coupled phase locked loops.

1.1 Demonstrating that MSK is a Special Form of QPSK

Figure 1.1 shows a technique for the generation of MSK. The incoming data $b(t)$, at the rate f_b, is demultiplexed into two bit streams b_o and b_e, each of which is at the rate $f_b/2$. The bit streams amplitude modulate, as shown in the figure, two sinusoids, one at the frequency f_H and the other at the frequency f_L. Note that the frequency difference

$$f_H - f_L = \frac{f_b}{2} \tag{1.1}$$

which is the rate at which $b_o(t)$ and $b_e(t)$ can change.

The MSK waveform $v_T(t)$ is readily found from Fig. 1.1 to be

$$v_T(t) = b_o(b_o \oplus b_e)\sin\omega_H t \; +$$
$$b_o(\overline{b_o \oplus b_e})\sin\omega_L t \tag{1.2}$$
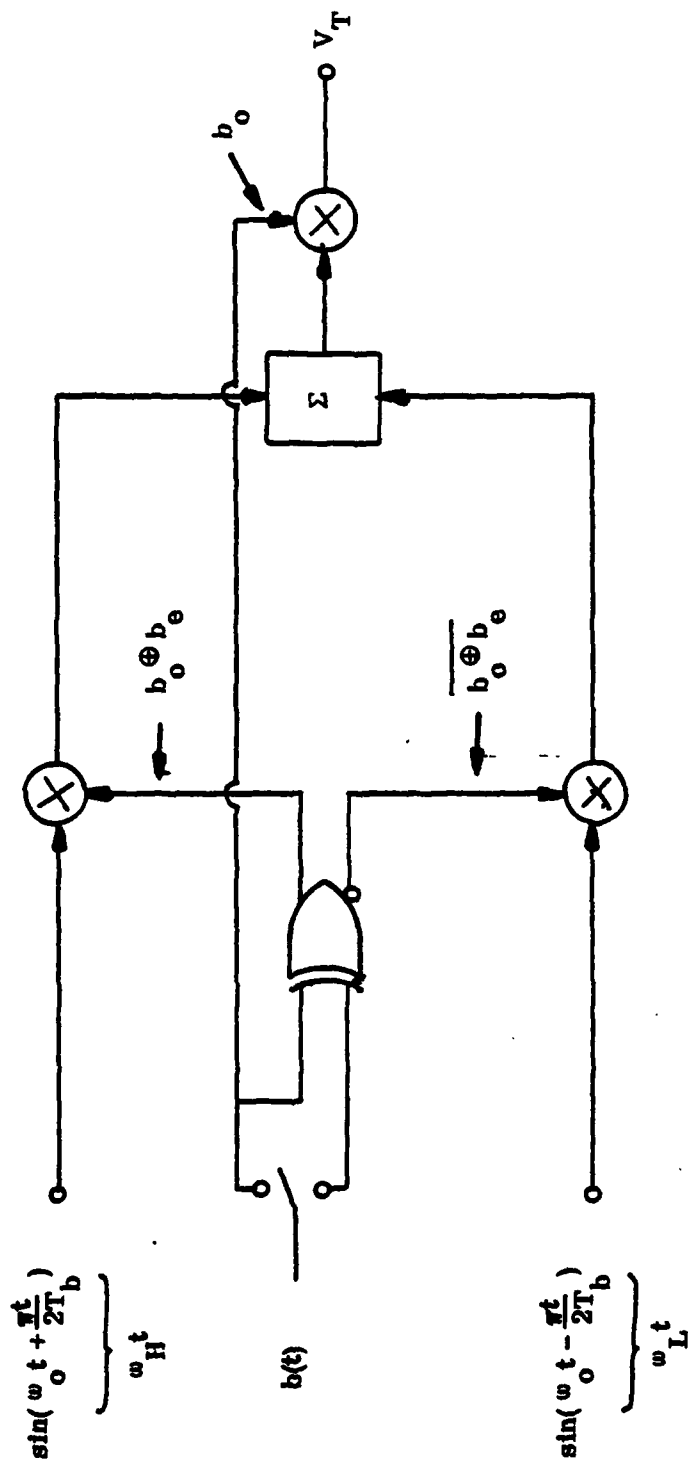
Fig. 1.1 Generation of MSK

where $\quad \overline{b_o \oplus b_e} = \begin{cases} 1 & \text{if} \quad b_o \neq b_e \\ 0 & \text{if} \quad b_o = b_e \end{cases}$

$\overline{b_o \oplus b_e} = \begin{cases} 0 & \text{if} \quad b_o \neq b_e \\ 1 & \text{if} \quad b_o = b_e \end{cases}$

and $\quad b_o$ is ± 1.

Thus,

$$v_T(t) = \begin{cases} b_o \sin \omega_H t & b_o \neq b_e \\ b_o \sin \omega_L t & b_o = b_e \end{cases} \quad\quad (1.3)$$

In Eq. (1.3) $v_T(t)$ looks like a PSK signal since $b_o(t)$ amplitude modulates a carrier, and also looks like FSK since there are two possible carrier frequencies.

Figure 1.2 illustrates our above discussion. In this figure we present $b_o(t)$ and $b_e(t)$ each waveform at a rate $f_b/2$. The two carrier frequencies f_H and f_L were chosen for simplicity such that

$$f_L = f_b \quad \text{and} \quad f_H = 3f_b/2 \quad\quad (1.4)$$

The MSK waveform $v_T(t)$ is shown. To see how $v_T(t)$ arises consider the time interval $0 \leq t \leq T_b$ in which $b_o = b_e = 1$. Since $b_o = b_e$ we transmit $\sin \omega_L t$ as shown. Now consider the interval $6T_b \leq t \leq 7T_b$. Here $b_o = \bar{b}_e = -1$. Since $b_o \neq b_e$ we transmit $b_o \sin \omega_H t$ and since $b_o = -1$ we transmit $-\sin \omega_H t$ during that interval.

Equation 1.2 can be rewritten, using the relations
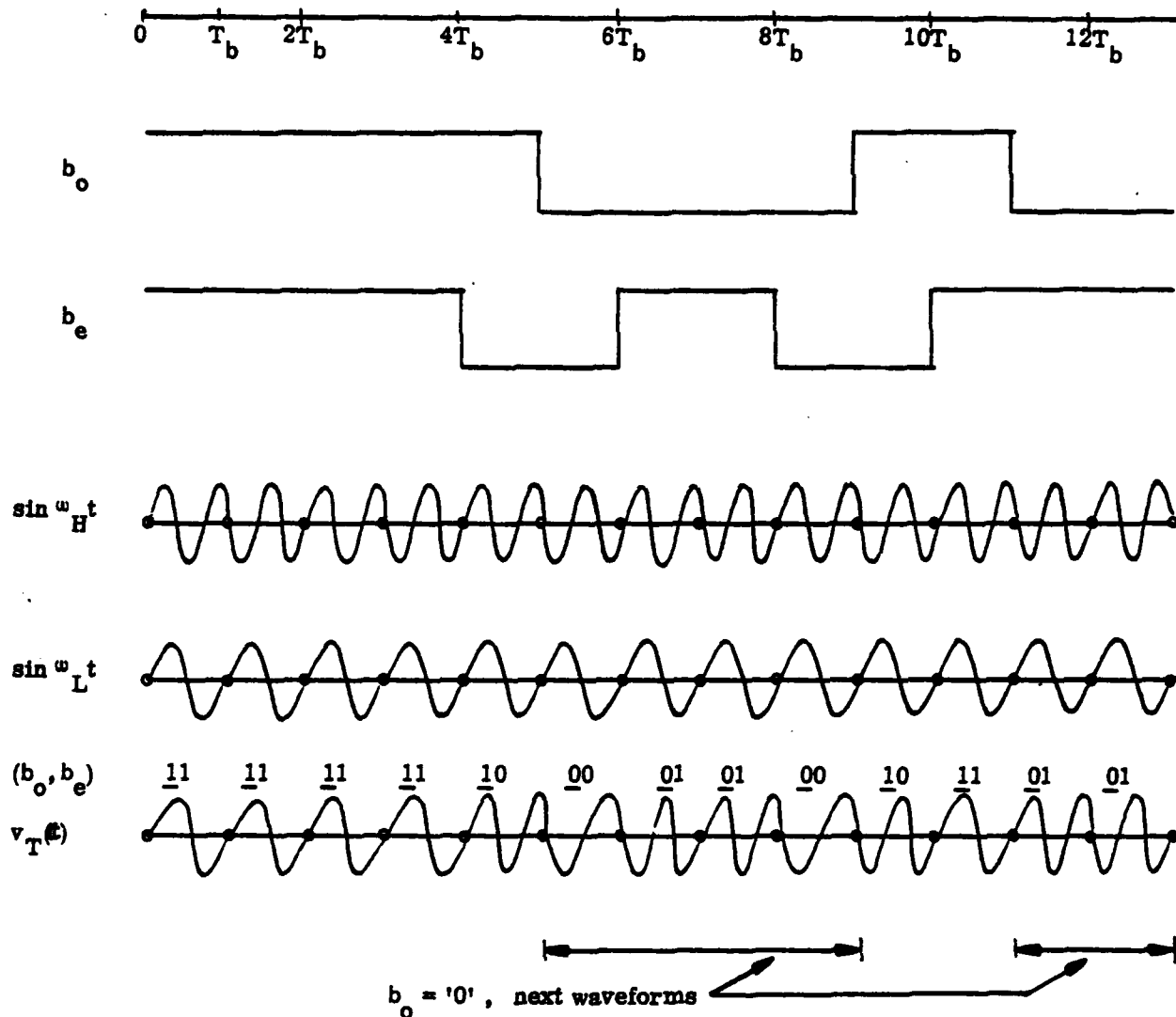
Fig. 1.2   MSK - example

$$f_H = f_0 + \frac{f_b}{4} \quad \text{and} \quad f_L = f_0 - \frac{f_b}{4} \tag{1.5}$$

and becomes

$$v_T(t) = \left(b_o(t) \cos \frac{\pi t}{2T_b}\right) \sin \omega_0 t - \left(b_e(t) \sin \frac{\pi t}{2T_b}\right) \cos \omega_0 t \tag{1.6}$$

Equation (1.6) is the equation of QPSK with sinusoidal amplitude shaping. The effect of the amplitude shaping is to decrease the bandwidth required for transmission. The error rate is that of QPSK.

1.2 Coherent Detection of MSK

The MSK signal, $v_T(t)$, can be detected using the circuit of Fig. 1.3. After squaring $v_T(t)$, the input to the phase-locked detector is (See Eq. 1.3)

$$v_{in} = v_T^2 = \begin{cases} \sin^2 \omega_H t & b_o \neq b_e \\ \sin^2 \omega_L t & b_o = b_e \end{cases} \tag{1.7}$$

Equation (1.7) can be written as (neglecting dc terms)

$$v_{in} = \cos\left(2\omega_0 t + (b_o \oplus b_e) \frac{\pi t}{T_b}\right) \tag{1.8}$$

The two oscillators VCO1 and VCO2 generate the two basic frequencies $f_b/2$ and $2f_0$, respectively. The outputs of VCO1 being

$$\begin{matrix} \cos \\ \sin \end{matrix} \left(\frac{\pi t}{T_b} + 2\phi\right)$$
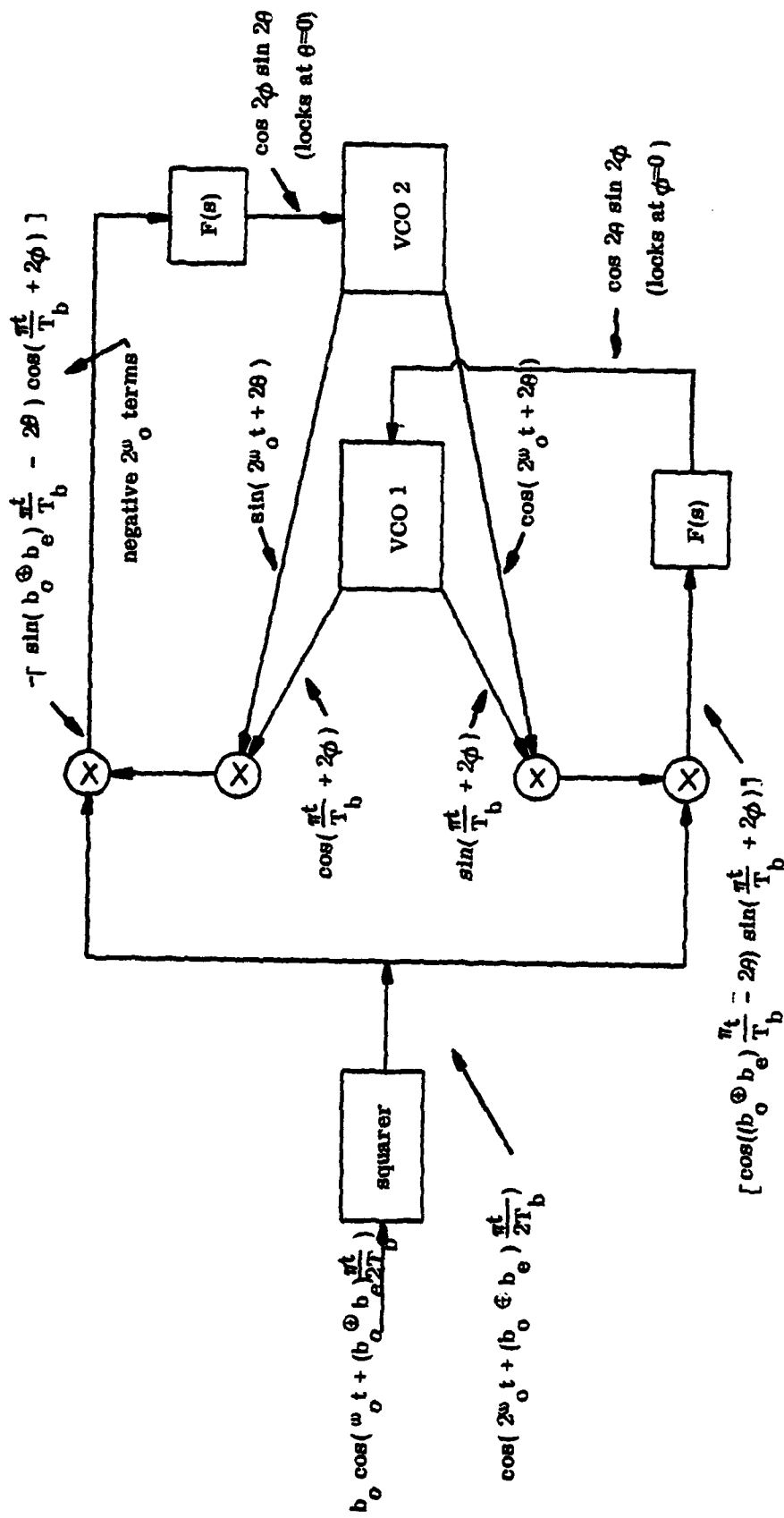
Fig. 1.3 Coherent detector for MSK

and the outputs of VCO2 being

$$\frac{\sin}{\cos}(2\omega_o t + 2\theta)$$

ϕ and θ being independent random variables which are forced to zero when phase locking occurs.

One of the terms obtained by multiplying the outputs of VCO-1, VCO-2 and V_{in} is

$$\cos(2\omega_o t + (b_o \oplus b_e) \frac{\pi t}{T_b}) \cos (\frac{\pi t}{T_b} + 2\theta) \sin(2\omega_o t + 2\theta)$$

Neglecting terms of frequency $2f_o$ and higher yields

$$- \sin ([b_o \oplus b_e] \frac{\pi t}{T_b} - 2\theta) \cos (\frac{\pi t}{T_b} + 2\phi).$$

The filter F(s) is a low pass filter designed to remove frequencies above $f_b/2$ (and of course f_o). Thus the output of the top filter which inputs VCO-2 is

$$\cos 2\phi \sin 2\theta$$

A stable steady-state is reached when $\theta = 0$. Similarly, as shown in Fig. 1.3, the input to VCO-1 is

$$\cos 2\theta \sin 2\phi$$

A stable steady state is reached when $\phi = 0$.

Coherent detection of the data is shown in Fig. 1.4. Here the incoming signal, before squaring is inputted to a correlator where it is correlated with the output of VCO-1 and

- MSK signal - $b_o(t) \cos \omega_o t \cos \frac{\pi t}{2T_b}$ + $b_e(t) \sin \omega_o t \sin \frac{\pi t}{2T_b}$

From VCO 2 after

frequency divider

$\cos(\omega_o t + \theta)$

$\cos(\frac{\pi t}{2T_b} + \phi)$

From VCO 1 after

frequency divider

$\int_0^{2T_b} dt$

$\int_0^{2T_b} dt$

b_o

b_e

b(t)

From VCO 2 after

frequency divider

$\sin(\omega_o t + \phi)$

$\sin(\frac{\pi t}{2T_b} + \phi)$

From VCO 1 after
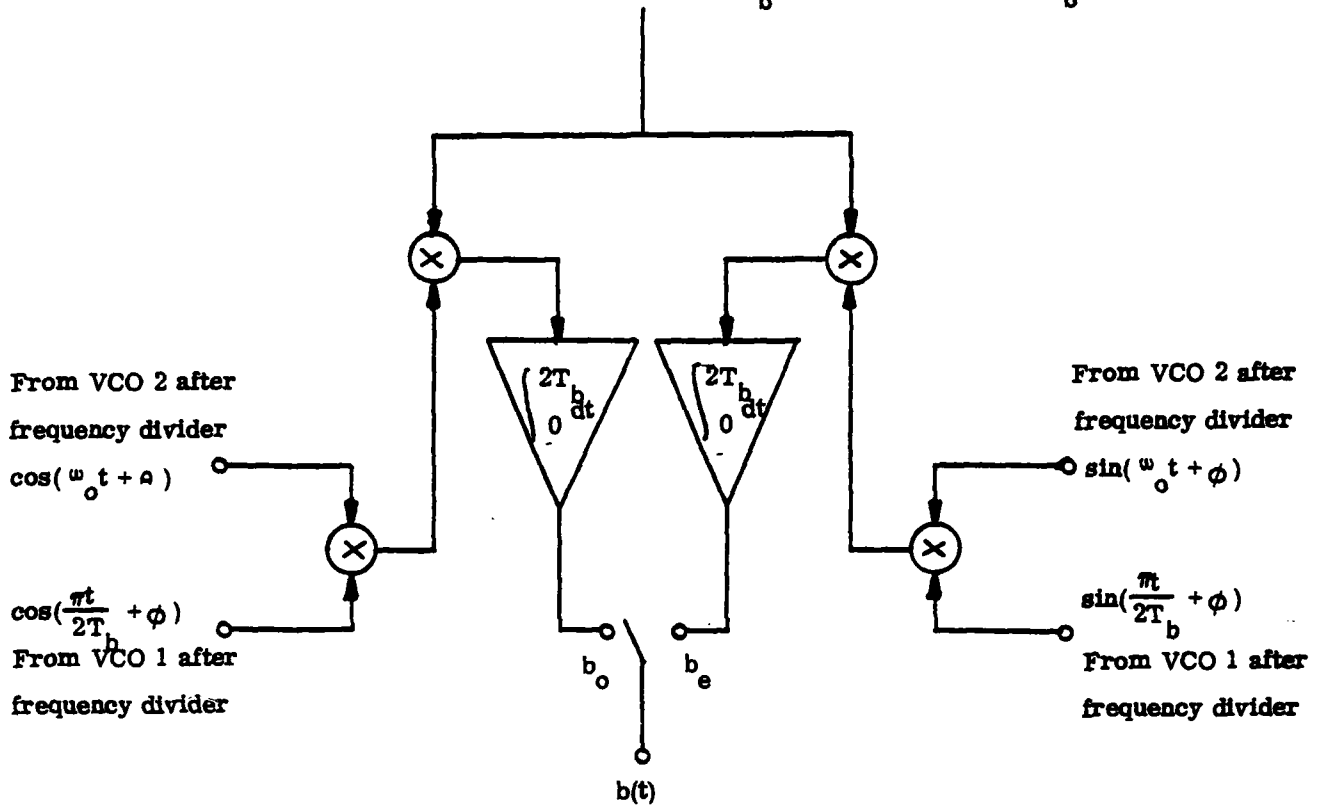
frequency divider

Fig. 1.4 Correlation to obtain b(t)

VOC-2 as shown. Note that the VCO outputs are taken after frequency division by 2. The resulting data b_o and b_e are then multiplexed to form the bit stream $b(t)$.

2.0   PN Sequence Acquisition

In this section we derive a "pseudo" PN sequence which yields worst-case acquisition times in a min-max sense.

2.1   Partial Correlation and the "Pseudo" PN Sequence

Figure 2.1 shows the incoming pn sequence $g(t+jT_c)$ being correlated with the local sequence $g(t)$. The partial correlation

$$R(j) = \sum_{i=0}^{\gamma} g(iT_c)g([i+j]T_c) \qquad (2.1)$$

where $\gamma < L$. When $\gamma = L$, $R_{\gamma=L}(j) = L$ if $j = 0$ and $R_\gamma(j) = -1$ if $j \neq 0$, i.e., there are only two possible values of $R_{\gamma=L}(j)$. When $\gamma < L$ such is not the case and there are a large number of values possible, depending on γ, j and the code length L.

During the acquisition process, a partial correlation, as shown in Fig. 2.1, occurs. After viewing γ chips, we decide whether or not we are synchronized. In making this determination, two possible errors can occur. The first type of error occurs when we are synchronized, but due to the input noise it appears as though we are not in "synch." The second type of error occurs when we are not synchronized but appear to be, due to the effect of the noise.

It is interesting to observe that even when there is no noise, the second type of error can occur if $\gamma < N$. This result is shown in Fig. 2.2. Here we see that if $j = 1$ and we

Input: $g(t+jT_c) + n_w(t)$

$g(t)$

$\sum_{i=1}^{\gamma}$

Output: $v_o(\gamma) = R_\gamma(J) + n_o(\gamma)$

Fig. 2.1 Partial correlation

$g(t+T_c)$: 0 1 1 1 1 . . . 1 1 0 |← N →|

$g(t)$: 0 1 1 1 . . . 1 1 1 0 |← N-1 →|
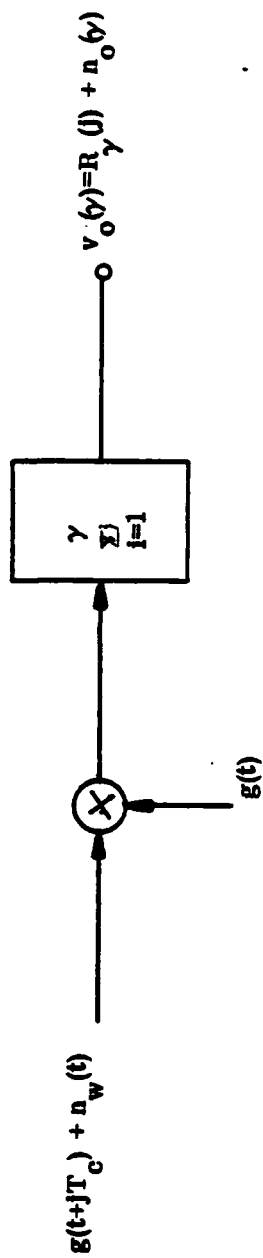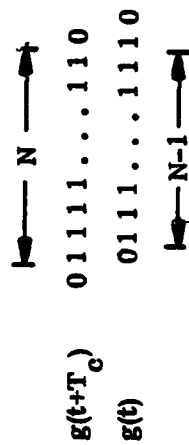
Fig. 2.2 Showing that a type 2 error can occur if $\gamma \leq N$

begin correlating at the start of the all -1 sequence of $g(t)$, then $R_\gamma(j) = \gamma$ so long as $\gamma < N$. Thus, in the worst case, even when no noise is present, $\gamma \geq N$.

The worst case partial correlation when the two sequences are not in synch, i.e. $j \neq 0$, is larger than any other partial correlation function. Hence

$$[R_\gamma(j)]_{worst\ case} \geq R_\gamma(j) \qquad (2.2)$$

The probability of either type of error is proportional to

$$d \equiv R_\gamma(0) - R_\gamma(j) \qquad (2.3)$$

Since d is smallest for the worst case $R_\gamma(j)$, the probability of error is largest.

We have invented a "pseudo" pn sequence having the same "run" characteristics as an ordinary pn sequence. However, the runs are reordered to produce a worst case $R_\gamma(j)$. The sequence is

$$g_p(t) = \underbrace{11...1}_{N}\ \underbrace{00...0}_{N-1}\ \underbrace{11...1}_{N-2}\ \underbrace{00...0}_{N-2}\ \underbrace{1...1}_{N-3}\ \underbrace{0...0}_{N-3}\ \underbrace{1...1}_{N-3}\ \underset{...}{...} \qquad (2.4)$$

(The runs are described in detail in Spread Spectrum (Part II). When $g_p(t+T_c)$ is correlated with $g_p(t)$, a worst case $R_\gamma(j)$ results. Typical results are shown in Fig. 2.3 and Fig. 2.4.

Fig. 2.4 shows the threshold voltage $V_T(\gamma)$ which is placed midway between $R_\gamma(0)$ and the worst case $R_\gamma(j)$. If the correlation output voltage $v_o(\gamma) > V_T$ we assume that we are
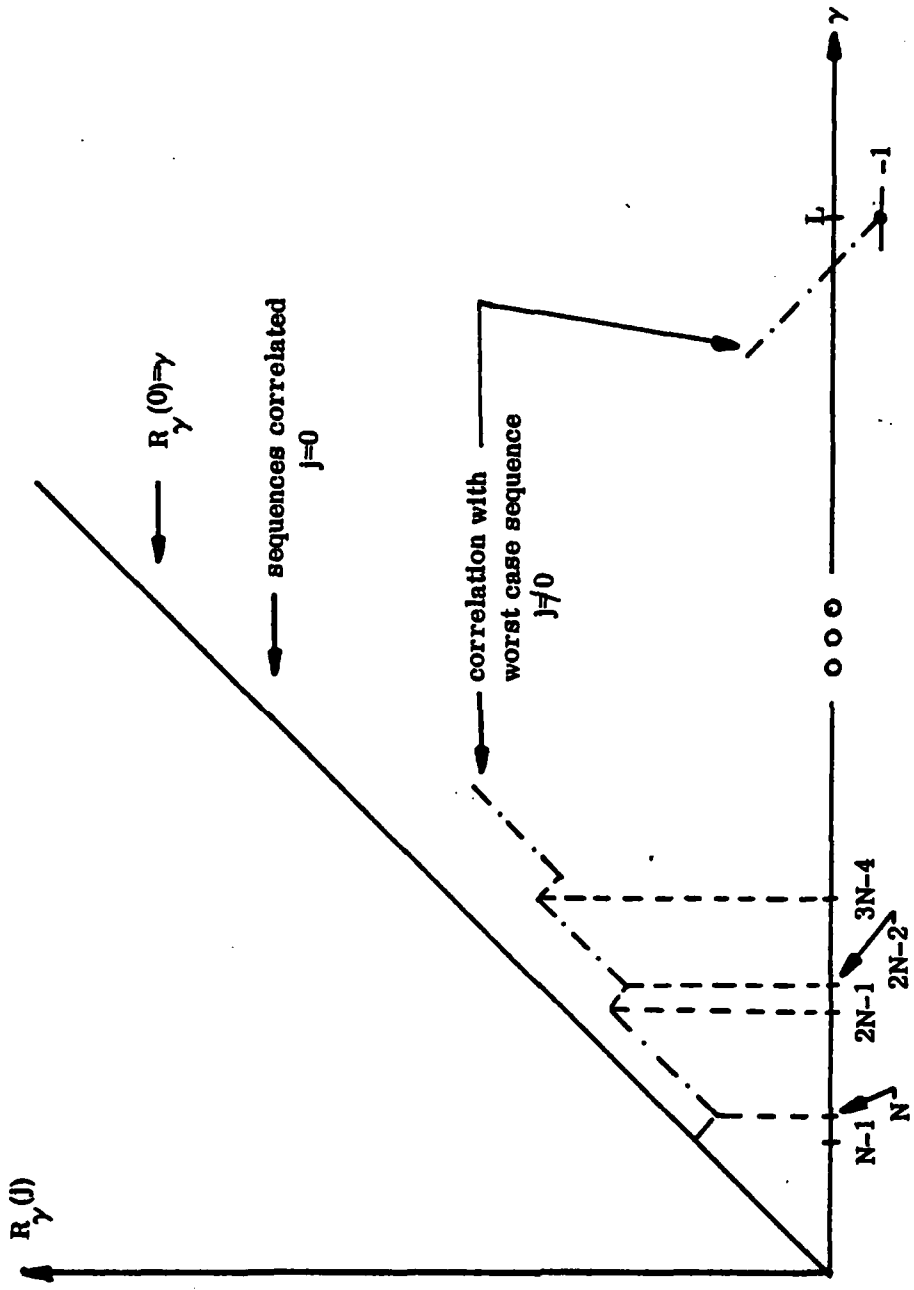
Fig. 2.3 Correlation for $\gamma \ll L$ using the worst case sequence
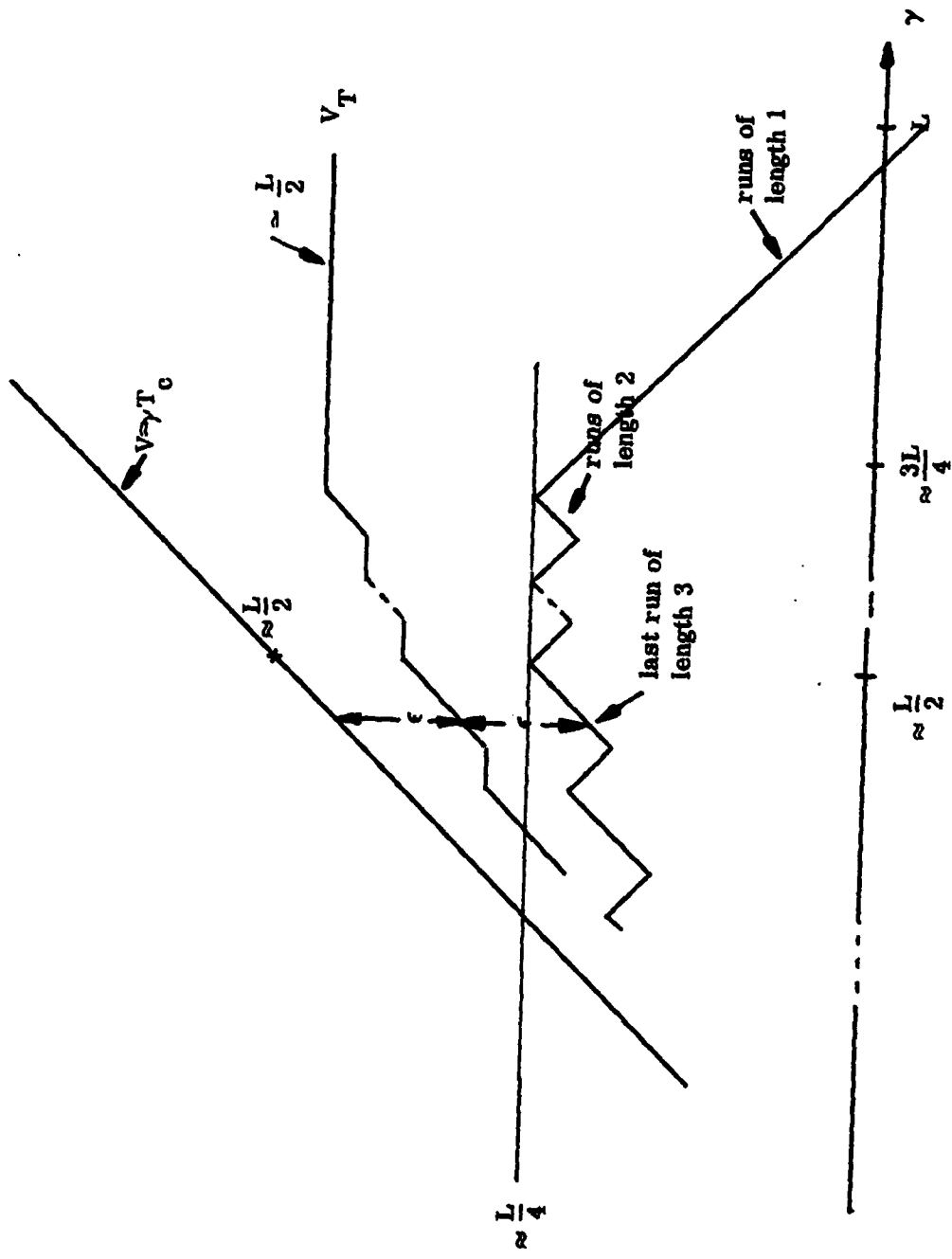
Fig. 2.4 Correlation for $\frac{L}{2} < \gamma \leq L$ using the worst case sequence

synchronized and if $v_o(\gamma) < V_T$ we assume that we are not in synch. The distance $d = 2\epsilon$ and therefore the probability of either type of error decreases with ϵ and hence with γ.

The relation between γ, ϵ and L is shown in Fig. 2.5 and, as expected, is highly nonlinear.

2.2 Probability of Error

If the incoming sequence is

$$v_{in}(t) = \sqrt{P_s}\, g(t) + n_w(t) \tag{2.5}$$

where $n_w(t)$ is white noise having a power spectral density $G_n(f) = \eta/2$, then assuming synchronization, we have

$$v_o(t) = \sqrt{P_s}\, \gamma\, T_c + n_o(\gamma) \tag{2.6}$$

The probability of error, P_e, is then

$$P_e = P(n_o > \sqrt{P_s}\, T_c \epsilon)$$

$$= \frac{!}{2\pi\sigma^2} \int_{\sqrt{P_s}\, T_c \epsilon}^{\infty} \exp(-n_o^2/2\sigma^2)\, dn_o \tag{2.7}$$

where $\sigma^2 = \eta\gamma T_c/2$

This expression can be formalized to

$$P_e = \frac{1}{2}\mathrm{erfc}\left[\frac{\epsilon^2}{L\gamma} \cdot \frac{LE_c}{\eta}\right]^{\frac{1}{2}} \tag{2.8}$$

For example, if L = 2047 and E_c/η = 0dB, then γ = 99 will
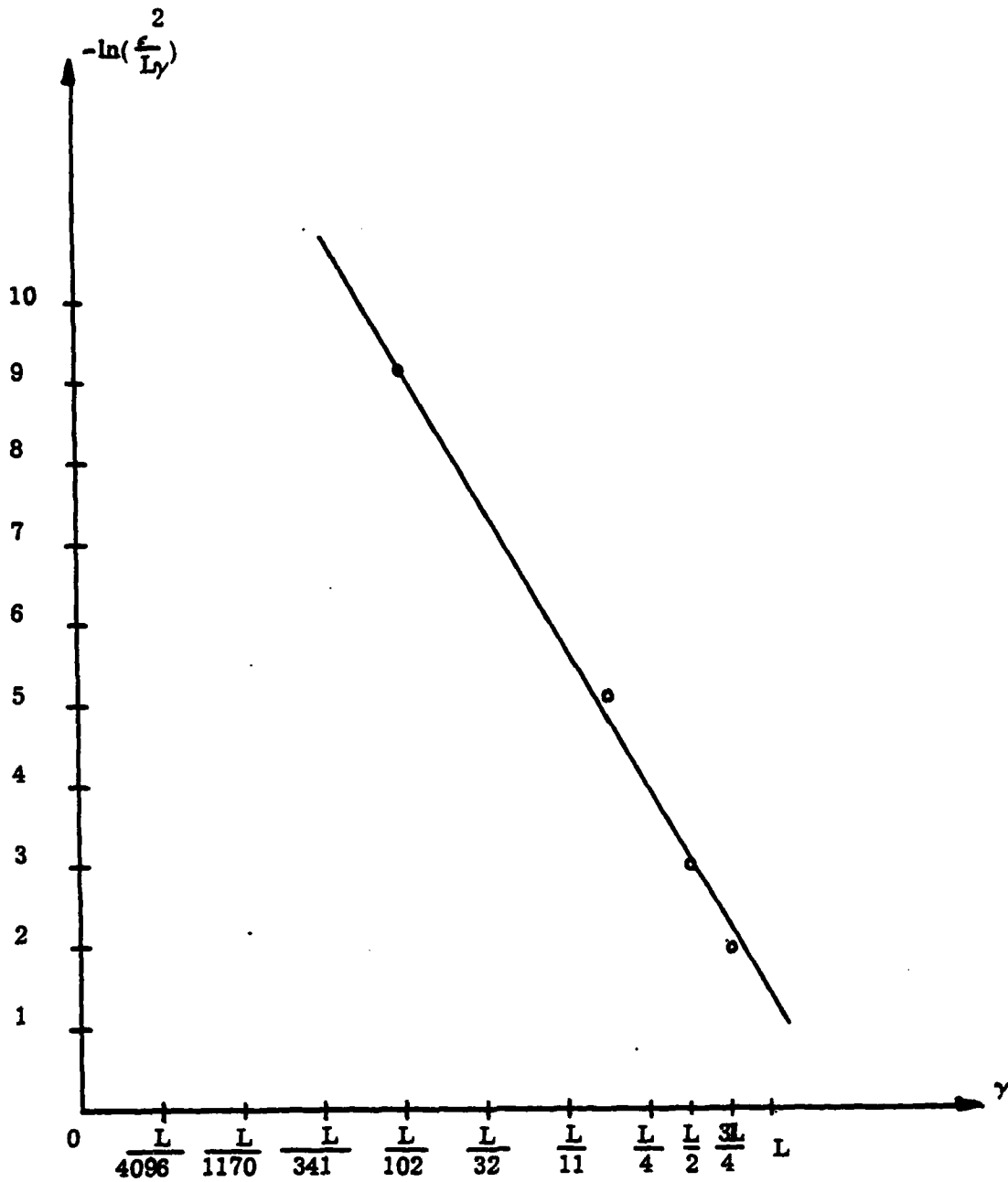
Fig. 2.5   Relationship between γ, ϵ and L

yield $P_e = 4 \times 10^{-2}$ and $\gamma = 383$ will yield $P_e = 10^{-5}$.

In general, Eq. (2.8) with Fig. 2.5 determines the acquisition time γ.

II. SYNCHRONIZATION OF SPREAD SPECTRUM SYSTEMS

1.0. INTRODUCTION

Pseudonoise (PN) modulation employing direct sequence phase modulation, or frequency and/or time hopping is sometimes used in spread spectrum communication systems to achieve systematic bandwidth spreading. Such waveforms are useful for a variety of reasons including anti-interference and anti-eavesdrop properties, power flux density reduction, low detectability, multiple access, and ranging. To a large extent the useful properties of such waveforms are due to their relatively long period when compared to a data bit and to their large bandwidth compared to that of the information signal.

While it is possible, at least in principle, for receivers in such systems to use completely passive matched filter structures for demodulating system waveforms, considerable reduction in the quantity and complexity of receiver hardward can often be realized if each receiver locally generates its own PN code and sychronizes it with that of the spread spectrum waveform which it receives (or wishes to receive).

Consider as a simple example a frequency hopped spread spectrum system using binary FSK on a carrier which is hopped over 512 distinct frequencies. In principle a receiver employing 1024 matched filters can be used to demodulate this waveform according to the same pattern, then when the two waveforms are synchronized, mixing the incoming signal with the

locally generated hopped signal "dehops" the carrier and produces a conventional BFSK waveform which can be detected using only two matched filters. Of course additional circuitry is needed to generate the receiver code, to dehop the incoming signal, and to maintain sychronization with the incoming code; however, for certain choices of system parameters, the exchange is often favorable. While rapidly advancing LSI technology may soon make such an exchange a moot point for these example parameters, the fact remains that the same technology will facilitate the sychronization implementation and will make feasible the development of systems to meet even more stringent requirements (more hopping frequencies, higher rates). Thus active generation of the local code by the receiver and synchronization with the incoming signal remains of interest. In tactical military communications, where system users are mobile, and communications among them is intermittent and characterized by frequent and possibly long periods of radio silence, the mechanism for achieving the necessary synchronization is a critical aspect of spread spectrum system design. In some applications frequency shifts due to the Doppler effect can introduce another dimension of uncertainty in addition to incoming code phase, however, in direct terrestrial communication among man-packs and ground vehicles this is not a major factor. On the other hand, high anti-jam requirements can slow synchronization considerably.

Specific synchronization requirements depend largely on the intended application; the sync subsystem often must be designed for worst case conditions in that application. The basic problem of synchronization is to adjust the timing, frequency and phase of the receiver's locally generated PN code to match that of the desired incoming signal. Often the sync process is considered to be composed of two parts; acquisition and tracking. Acquisition involves a search through the region of time-frequency undertainty and a determination that the locally generated code and incoming code are sufficiently closely aligned. Tracking is the process of maintaining the alignment of the two signals. This is usually accomplished using some type of feedback loop which also serves to reduce the alignment error remaining after the acquisition process.

A functional block diagram depicting the sychronization process is shown in Fig. 1. The operations shown would be needed regardless of which type of spread spectrum modulation were used but a more detailed block diagram would necessarily depend on specifics.

This chapter on Synchronization of Spread Spectrum Systems consists of two main parts. The first, comprised of Sections 2 and 3, presents an overview of code tracking and acquisition methods. The discussion is oriented but not limited to frequency hopped systems. Serial search, estimation
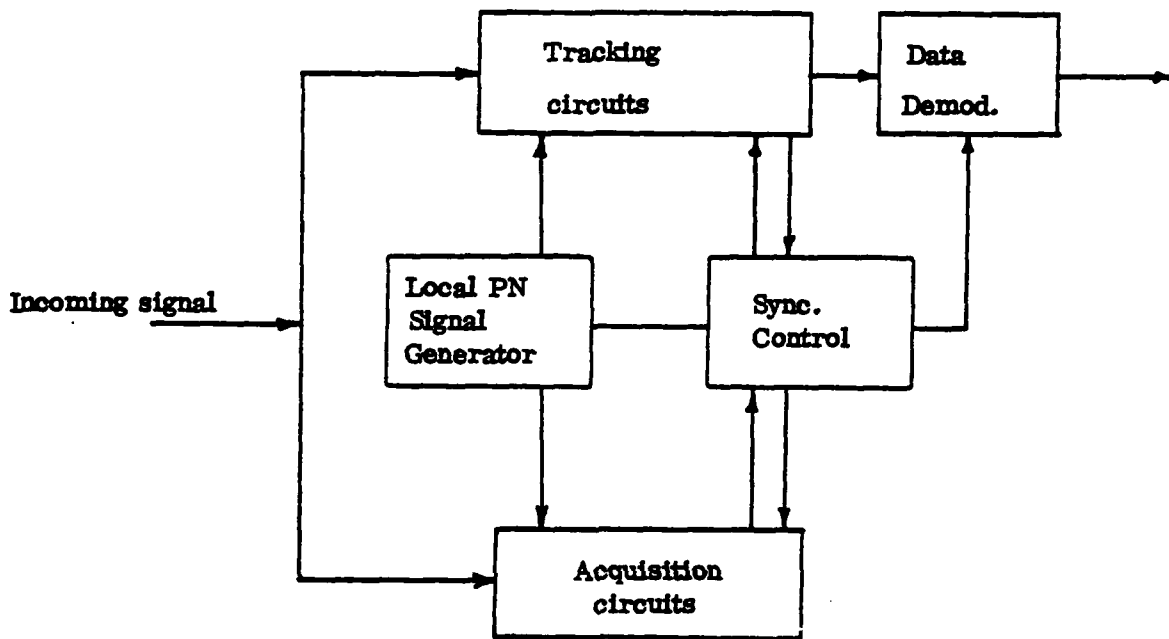
Fig. 1 Functional Diagram of Synchronization Subsystem.

procedures, parallel correlators, sequential detection, and matched filters for acquisition aiding are discussed. The second part, comprised of Section 4, describes a novel scheme for coarse acquisition of frequency hopped spread spectrum signals. The scheme consists of a two level acquisition process characterized by a passive correlator in tandem with a bank of active correlators. A threshold exceedance of the passive correlator innitiates an interval of active correlation if any of the active correlators are idle. The scheme combines the rapid search capability of passive correlation with the decision reliability of (long) active correlation; yet the number of active correlators can be much smaller than the number of cells to be searched. Using analytical models stemming from both queueing theory and from detection theory, the scheme is optimized and its performance in the presence of background noise with noise jamming and/or with cw jamming is analyzed. Performance curves and a discussion of results is presented for each type of jamming.

2.0   TRACKING

Synchronization aspects of the spread spectrum problem have often focused on direct sequence modulation systems with somewhat less attention to frequency hopped synchronizers. Furthermore, analyses often concentrate on either the tracking problem or on the acquisition problem.

For tracking direct sequence PN modulated signals a

delay locked loop (DLL) using envelope detectors is commonly used. Basically the loop operates by locally generating two (identical) PN signals which are delayed with respect to one another by one (or 2) chips. Each of these signals is correlated with the same incoming PN sequence and the difference of the envelopes is formed to produce an error signal proportional to the delay of the incoming signal. This error voltage is used to adjust the clocking rate of the locally generated signals. The basic configuration is shown in Fig. 2. The transient and steady state behavior of the DLL has been analyzed [1,2,3]. An alternative to the DLL is the tau-dither loop in which only a single correlator is required. In this configuration the timing of the locally generated PN signal is slowly dithered before correlation with the incoming signal. The dithering causes a coherent ripple at the dither frequency in the envelope of the correlated signal. The amplitude and phase of this ripple component is used to develop an error signal for the tracking loop [4,5]. The structure of the tau-dither loop is shown in Fig. 3. When frequency hopped spread spectrum signals are used the tracking loop could employ an early-late gate as shown in Fig. 4. The waveforms that would appear at various points in such a loop are shown in Fig. 5. The early-late (E-L) gating waveform is alternately negative and positive with the minus to plus transitions occurring simultaneously with the chip to chip frequency hopping instants of the locally generated
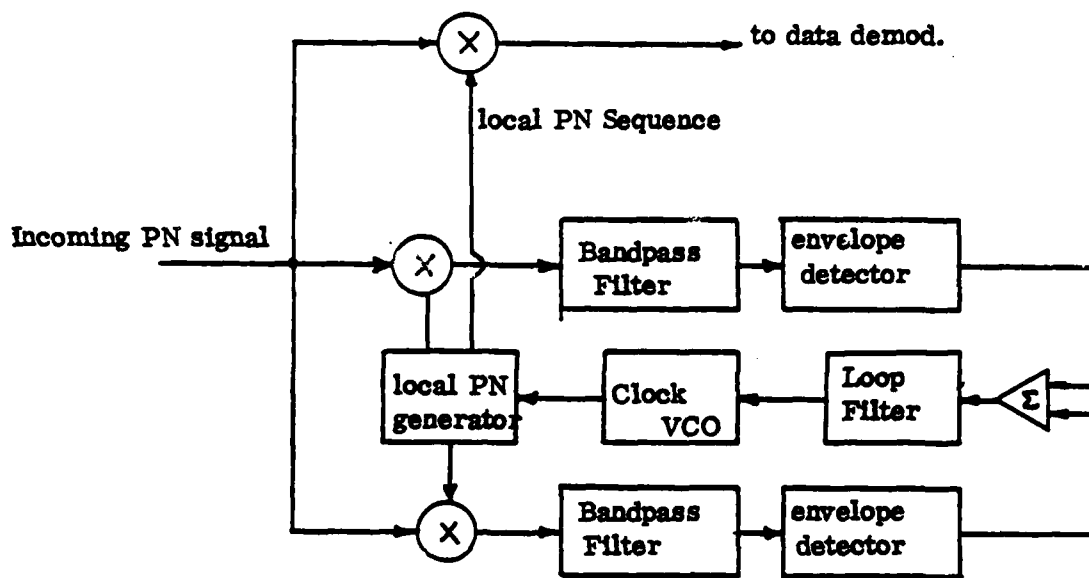
Fig. 2   Delay Locked Loop for Tracking Direct Sequence PN Signals.
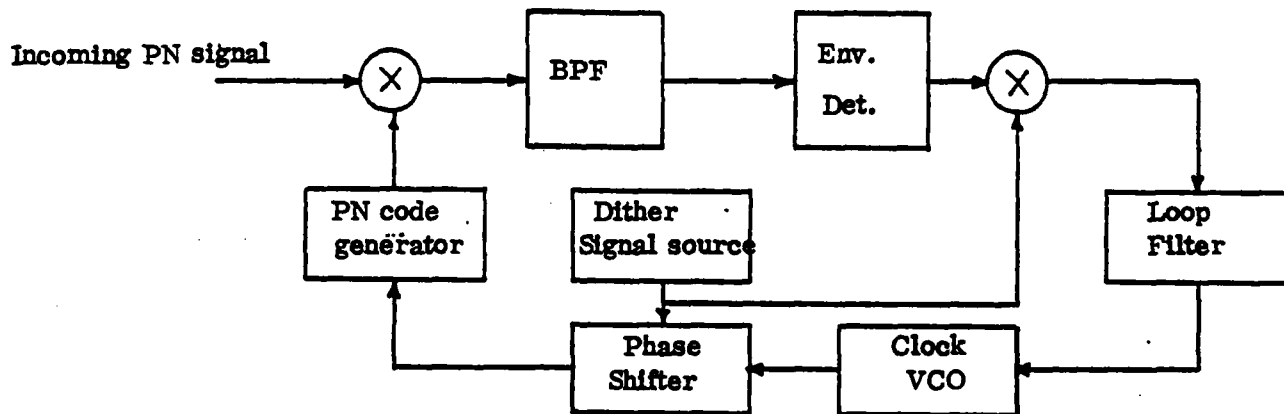

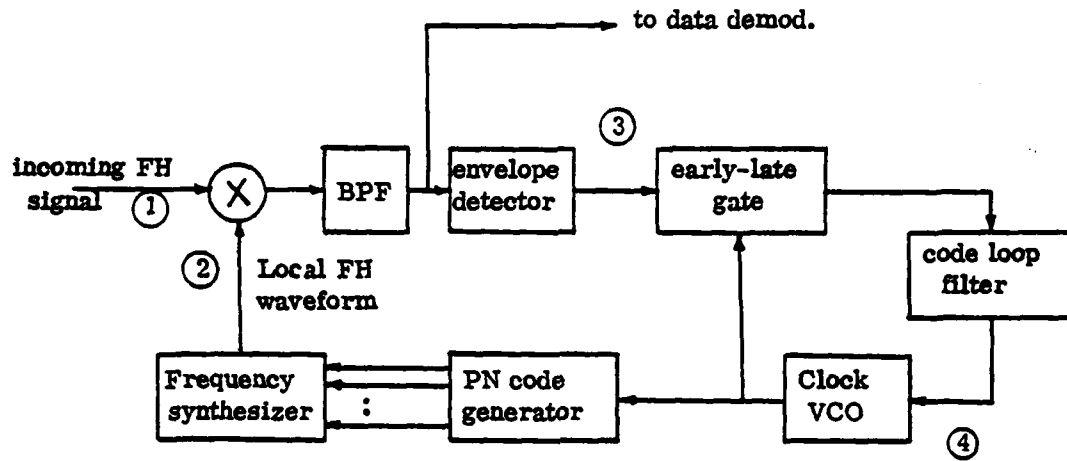Fig. 3.   Dithering Loop for Tracking Direct Sequence PN Signals.

Fig. 4   Tracking Loop for FH PN Signals Using an Early-Late Gate.
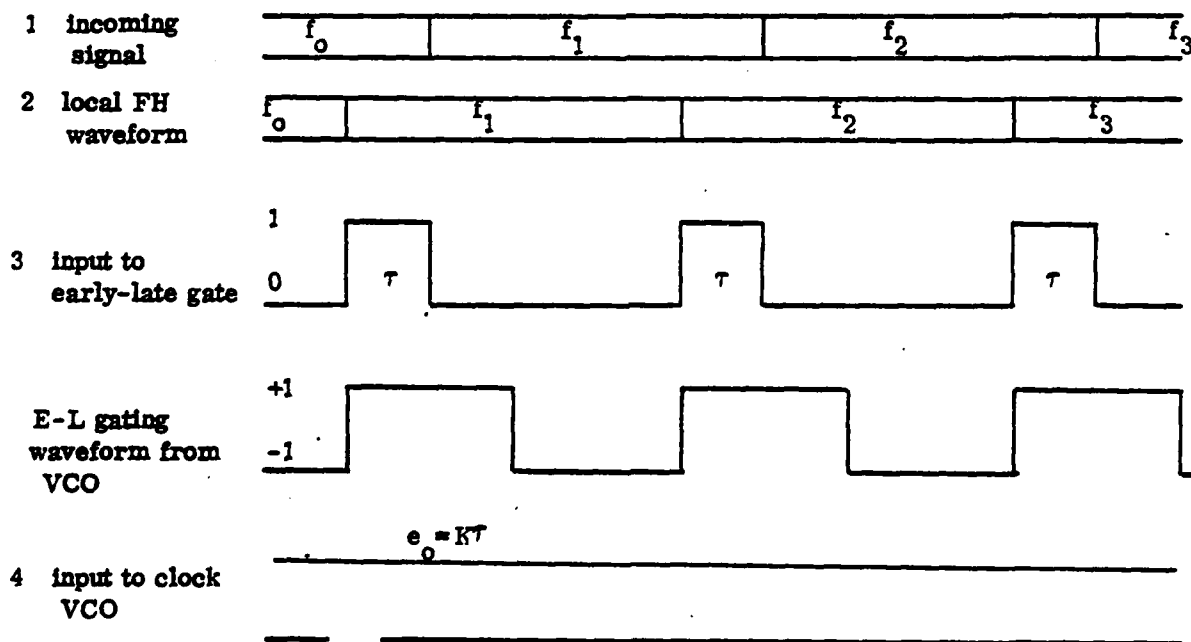
Fig. 5   Waveforms for Tracking a FH waveform Using an Early-Late gate

waveform. When the incoming signal is ahead of the local wave-
form by an amount τ $(\tau \leq \frac{1}{2}$ chip) it can be seen that the mixing
and envelope detection operations produce a pulsed waveform
at the chipping rate whose duty cycle is proportional to τ.
A D.C. signal e_0 which is proportional to τ will appear at
the input to the clock VCO. This signal is used to advance
or retard the local waveform if τ is positive or negative
respectively. When the incoming and locally generated FH
signals are _aligned_ the mixing and envelope detecting opera-
tions produce a D.C. or low frequency (much less than the
chipping rate) signal. When the output of the envelop detector
is gated by the E-L signal and integrated by the loop filter
a null signal is produced. If τ is positive, the VCO input
will be positive since the E-L gating input will also be
positive; however, if τ is negative, the E-L gating input will
be negative and the output of the E-L gate will be negative.
The error voltages vs. delay characteristic shown in Fig. 6
can be easily derived from the model waveforms sketched in
Fig. 5. From this characteristic it can be seen that the
pull in range for the loop is less than $\frac{1}{2}$ chip.

3.0 ACQUISITION

We now turn to the acquisition process, whose basic func-
tion is to bring the _incoming_ PN signal and the _locally gener-_
ated PN signal into sufficiently close alignment so that the
difference is within the pull in range of the tracking loop.
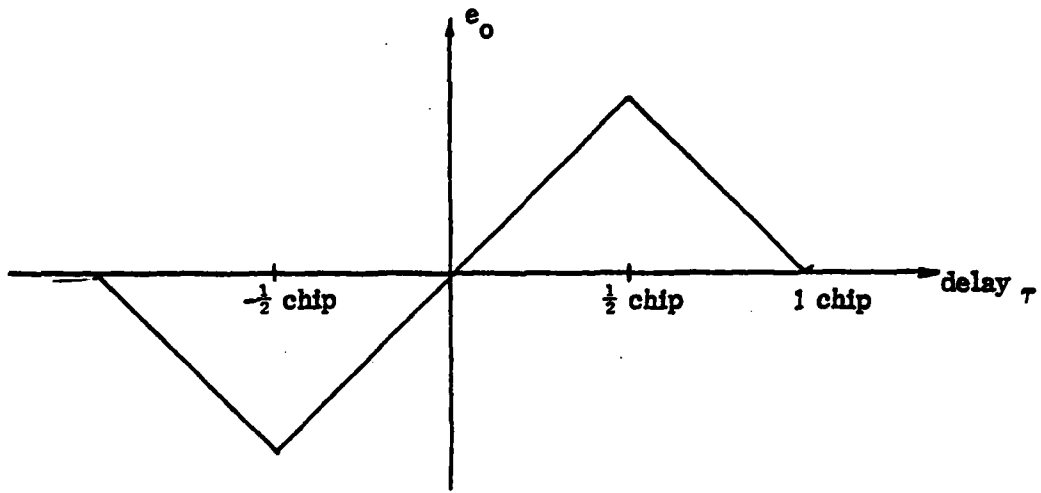
Fig. 6   Error Signal Voltage for FH Tracking Using an Early Late gate.

For tactical ground communication, Doppler shift will not be
a major factor but the user's receiver may be initially un-
synchronized. With moderately stable clocks that are readily
available the predominant uncertainty will therefore be that
of relative code epoch. We shall therefore focus on appro-
priate code acquisition techniques.

3.1 Serial Search--Detection of Coarse Alignment

The most straightforward strategy for long PN codes
using active correlation, is to use a simple serial search
until the correct code epoch is determined. A continuous
serial swept scheme has been considered for binary phase
encoded PN sequences and various in-lock detectors [6]. A
stepped serial search is essentially similar. The basic con-
figuration is shown in Fig. 7. In a stepped serial acquisi-
tion scheme the timing epoch of the local PN code is set and
the locally generated PN signal is correlated with the incming
PN signal. The envelope is extracted and compared to a
threshold at fixed "examination" intervals which are long
compared to a chip duration. If the threshold is not exceeded
the search control inhibits a clock pulse to the PN code
generator so that the local code phase slips to the next
cell (usually ½ chip) and the process is repeated. When
the incoming and local PN sequences are in coarse alignment
however, the threshold will be exceeded with high probability
and the local PN code will not be slipped; it will remain
in the same phase relative to the incoming signal. The search

incoming PN
signal ⊗ → BPF → envelope
detector → threshold

local PN
code ← search
control ←

Clock →

↓ sync
indicate
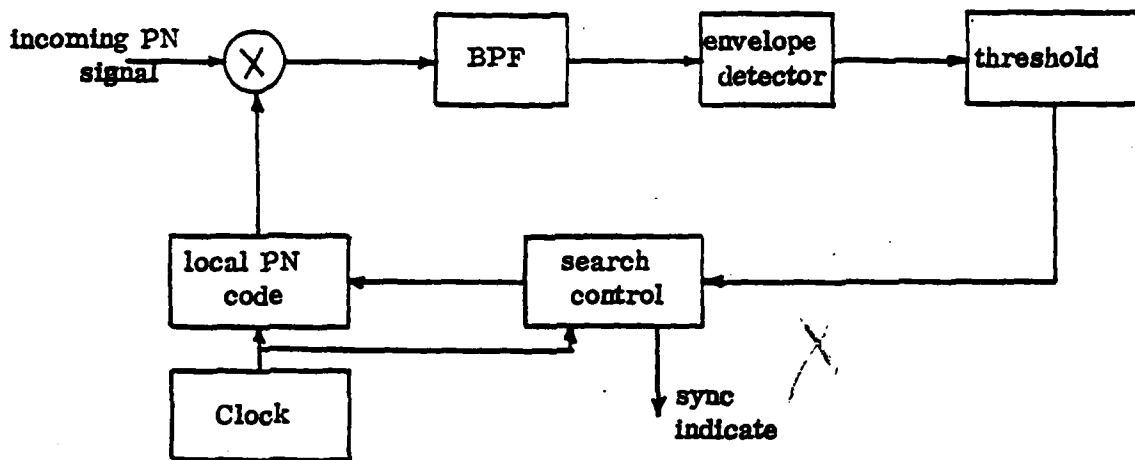
Fig. 7   Direct Sequence PN Acquisition Using Serial Search and
Active Correlation.

Incoming FH
signal ⊗ → BPF → Env.
det. → Integrator → threshold

reset

Frequency
Hopper

search
control

PN code
generator

Clock

→ sync
indicate
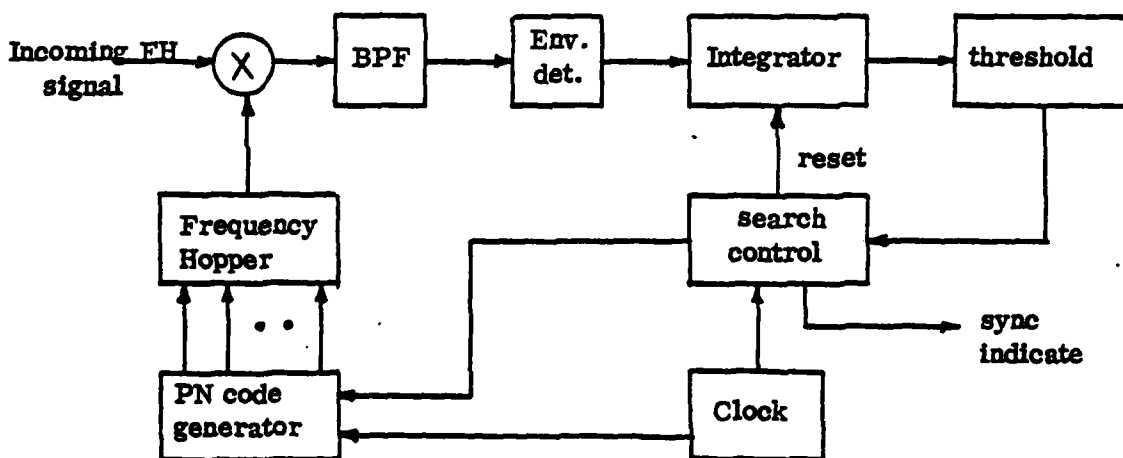
Fig. 8   FH PN Acquisition Using Serial Search.

will be stopped and tracking will be initiated. The ½ chip cell size is usually sufficient so that (a) coarse alignment will be detected with high probability and (b) the coarse alignment is small enough to be within the pull-in range of the tracking loop. Ideally, the examination intervals used should contain an integral multiple of PN code words so that full advantage of the autocorrelation properties of the PN sequence can be obtained. In practice an interval smaller than a single code-word period but still containing many chips is usually taken. This reduces the time required to inspect each cell although there will be a larger fraction of _false_ threshold exceedances. With an appropriate choice of parameters the net effect is to reduce the overall time needed for code acquisition. The same basic scheme can also be used to acquire frequency hopped signals in the configuration shown in Fig. 8. Here the state of the local PN code generator is used to activate the frequency hopper. When the local hopping is aligned with that of the incoming signal the input to the envelope detector is ideally a sinusoid at the IF frequency and the probability of threshold exceedance is high.

Minor (from an analytical viewpoint) variations of the scheme include alternative procedures for in-lock detection using (a) square law envelope detection (b) double threshold detection in which the output of the envelope detectors are quantized to two levels and the subsequent integrator "counts"

the number of such exceedances.

3.2 Mean-Acquisition Time

A rough estimate of the average acquisition time can be obtained as follows. We note that if T_e is the examination time for each cell and there are n cells to a chip, the scheme can search $1/nT_e$ chips/sec. If the initial code phase uncertainty is N_c chips, then n $N_c T_e/2$ seconds will be required on the average. This is optimistic because the occurrence of false alarms (which have been neglected) will slow the search and because <u>missed</u> detections of the "in alignment" condition will increase the acquisition time. Letting P_{FA} be the false alarm probability and assuming that each false alarm causes an additional examination of the same cell, the effective search rate will be $(1-P_{FA})/nTe$ chips/sec. The average time to search all N_c chips of the uncertainty region once is

$$T_s = \frac{n\ N_c\ T_e}{(1-P_{FA})} . \qquad (1)$$

Letting P_D be the probability of detecting the alignment condition,

$$\bar{T}_{acq} = \frac{T_s}{2} P_D + \frac{3T_s}{2} (1 - P_D)\ P_D + \frac{5T_s}{2} (1 - P_D)^2\ P_D + \ldots$$

$$= \frac{T_s P_D}{2} \sum_{i=0}^{\infty} (2i + 1)(1 - P_D)^i . \qquad (2)$$

With some algebraic manipulation the series can be summed
in closed form, yielding

$$T_{acq} = \frac{T_s}{2} \left(\frac{2 - P_D}{P_D} \right) \equiv \frac{n \, N_c \, T_e}{2(1-P_{FA})} \frac{(2 - P_D)}{P_D} . \qquad (3)$$

If the initial uncertainty region is large, this acquisition
time can be unsatisfactory. It is generally desirable to
make acquisition time as small as possible. Several ways to
reduce the acquisition time within the same basic framework
using serial code search are apparent:

(1) Increase P_D and/or decrease P_{FA} while other parameters
are held fixed. Thus optimum and near optimum configura-
tions for detecting the coarse alignment conditions are
of interest.

(2) Reduce the initial uncertainty region. This is accomp-
lished by using stable clocks at the transmitter and re-
ceiver and by as much prior agreement of code, frequency,
etc. as is practical.

(3) Increase the search rate. One possibility is to use
parallel correlation of the incoming signal with say k
delayed versions of the local replica code. By choosing
the largest of the correlator outputs and comparing it
to a detection threshold at the end of each decision
interval, T_e, a reduction in mean acquisition time by a
factor k can be expected. If k is equal to $n N_c$ the scheme
essentially performs a maximum likelihood of the incoming

code phase. A related method is to use digital time compression techniques with circuitry working at clock rates much faster than that of the incoming chip rate. Multiple looks at the same data in an interval T_e are then possible with the same effect as above but with less (though more sophisticated) hardware.

(4) Reduce the average time to examine a cell (dwell time). Perhaps the most straightforward way of accomplishing this is to use a passive correlation technique (matched filtering). A simple matched filter operates in real time so that n cells are examined every chip interval (instead of 1 cell every examination interval). The implementation of matched filters having large time-bandwidth products can be formidable however, so this approach is most commonly used in frequency hopped schemes and/or for partial correlation in conjunction with active correlation. We shall discuss this scheme further subsequently.

Another approach which can be used to reduce the average examination time employs sequential detection methods [7]. These methods stem from original work by Wald [8] and have also been applied to radar detection theory [9]. In the context of the serial code search the essence of the method is as follows. Most cells which are examined do not contain the correct code epoch and yet many such cells must be examined. Instead of examining each cell for a fixed period T_e, the decision voltage

is continually compared to a varying threshold during the
decision period and the cell is discarded if the voltage falls
below threshold anywhere in the interval. In this way many
cells can be discarded in less than T_e seconds with a net de-
crease in search time. In theory the test should continue
until the decision voltage either falls below a variable
threshold (cell is discarded) or it exceeds an upper variable
threshold (sync is declared). Under these conditions it is
possible to adjust the thresholds so that the corresponding
false alarm and false dismissal probabilities are as good as
those that can be obtained using a _fixed_ decision interval
which, however, will be larger than the _average_ decision inter-
val in the sequential test. In practice a truncated sequential
test is used in which a cell that is not discarded after a
fixed interval is accepted. The sequential detection serial
search approach is applicable to the various spread spectrum
systems and by itself has a number of variations. A digital
acquisition scheme using sequential detection for a frequency
hopped system is shown in Fig. 9. The scheme essentially keeps
a _running_ count of the fraction of incoming chips which _do_ _not_
exceed the hard quantizing threshold and moves to the next cell
as soon as this fraction falls _above_ some value. A cell that
is not dismissed, is accepted as the correct code epoch and
tracking is initiated.

3.3 Estimation Methods

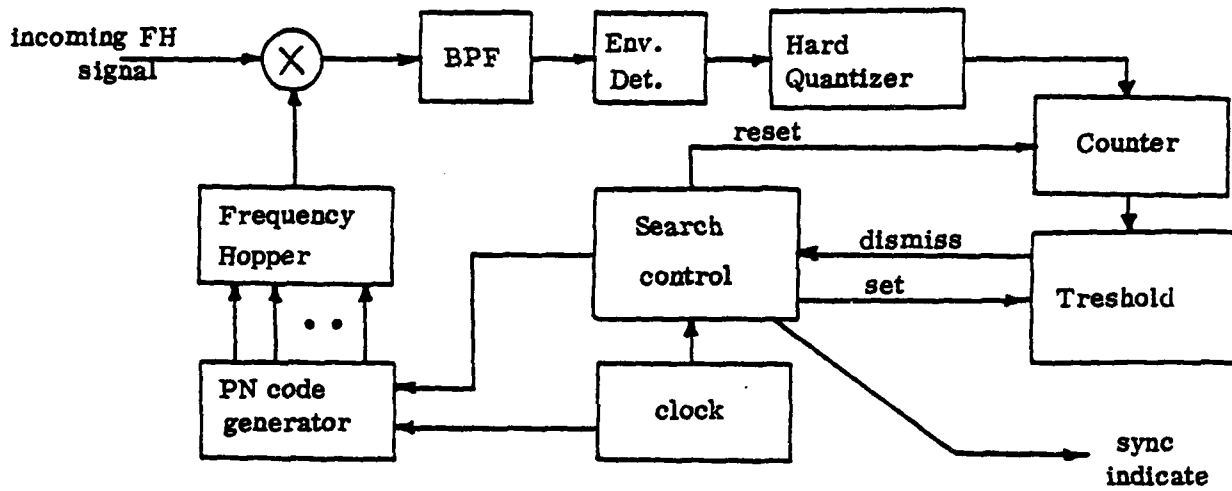An alternative to the basic idea of _serially_ searching

Fig. 9   FH PN acquisition using sequential detection
         and binary integration.

the cells for the correct code epoch has been proposed [10].
The method is based on sequentially estimating the present
state of an incoming PN stream by examining a small number of
input bits. The local PN generator is set to this state and
a statistical decision is made to determine if the incoming
code and local code are in coarse alignment. If the cell is
discarded a new estimate is made and the process is repeated.
A block diagram of the scheme is shown in Fig. 10.

The sequential estimation procedure has been compared
with stepped serial search when the only interference is back-
ground Gaussian noise. Significant improvement in mean acqui-
sition time has been shown for signal-to-noise ratios down to
-15dB. At a SNR of -10dB and for a shift register length
of 15 the estimation scheme has a mean acquisition time ap-
proximately one-twelfth that of a stepped serial search scheme.
It is important to note however that the estimation procedure
used presumes that the incoming PN signal was at video, that
additive Gaussian noise was the only interference, and that
video correlation was done. The implication for say, direct
sequence PN radio receivers, is that coherent carrier phase
tracking would have to be established before code acquisition,
to achieve the stated performance. While the basic principle
can be applied in other spread spectrum consifgurations, it
is clear that the scheme is extremely vulnerable to inter-
fering signals; it would try to acquire them. It is there-
fore not useful for multiple access or for tactical radio
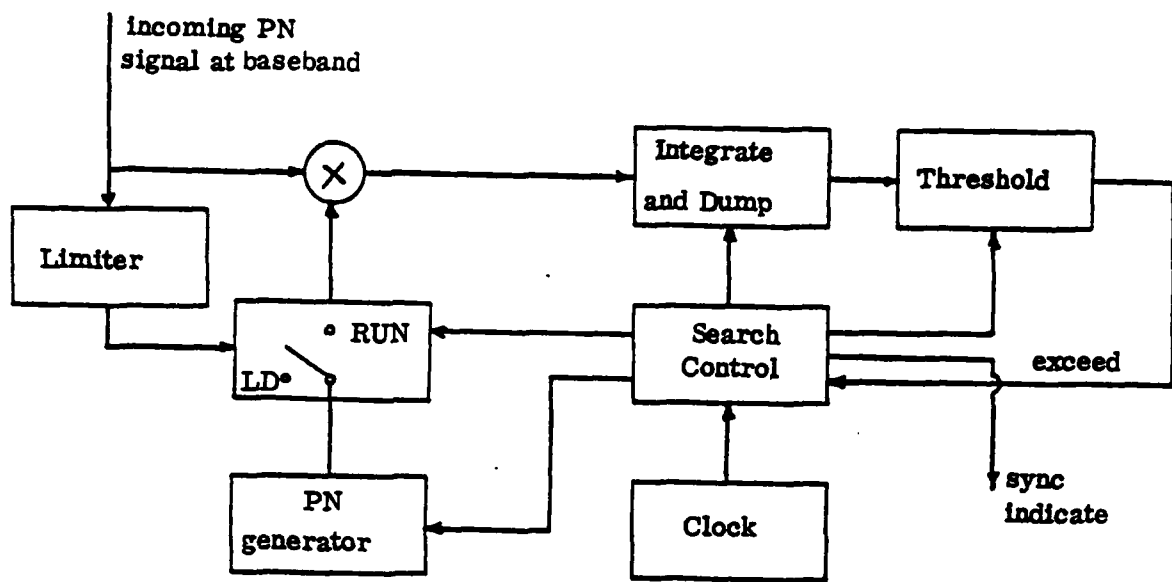
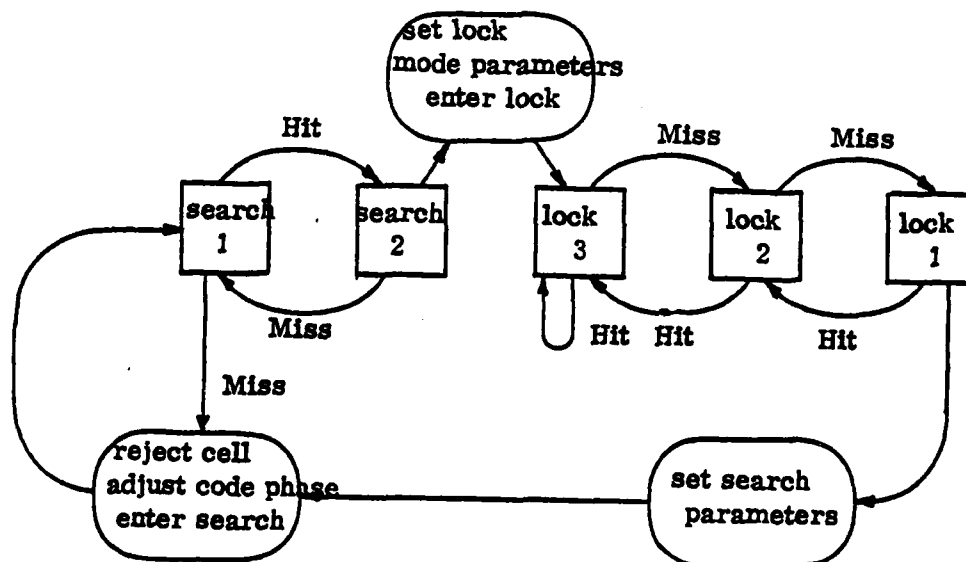Fig. 10 PN Acquisition by Sequential Estimation

Fig. 11 A Search-Lock algorithm for PN Acquisition

communication where intentional jamming or other PN signals are likely to be present.

Several schemes have been devised [11,12] that yield even additional improvements over Ward's basic sequential estimation scheme (in the same environment) but the basic limitation, vulnerability to interference, is not changed.

3.4 Search Control Algorithm

A serial search scheme for synchronization of direct sequence PN signals which uses a search control algorithm characterized by a finite state digital machine has been considered [13]. The strategy, which is depicted in Fig. 11, is analogous to a counter with four possible counts 0, 1, 2, and 3 and an initial count of 1. Upon inspecting a cell, a threshold exceedance, or hit, increases the count, while a miss causes a decrease. The lock mode is entered if the count reaches 3; the cell is rejected if the count reaches zero. System parameters, such as examination time and threshold, can depend on the state so that the transition from acquisition to tracking is "soft." The properties of finite Markov chains were used to analyze performance in a Gaussian noise environment. Explicit results for mean acquisition time and mean hold-in time are obtained. The methodology used can be applied to more complex situations including jamming, although this situation is not treated in the reference. A similar model is discussed in [14].

3.5 Matched Filter for Acquisition Aiding

As mentioned previously, a filter matched to the incoming code can theoretically provide rapid acquisition. However, since the implementation of such matched filters for long codes can be formidable, matched filtering is more easily incorporated as an acquisition aiding technique. In this application a sync preamble can be used which by prearrangement is the starting point for the known code. The matched filter is used to detect the presence of the preamble with high probability. A threshold exceedance at the matched filter output is used to start the receiver's code generator at the prearranged code phase. Active correlation over a longer code segment is then used to test the occurrence of coarse alignment. The basic scheme is sketched in Fig. 12. Simply the matched filter should detect the presence of the preamble very reliably with a small false alarm probability. In this way most of the code cells of the uncertainty region are correctly and rapidly rejected by the matched filter and only those that cause threshold exceedances at the output of the matched filter are put through the more stringent (and time consuming) active correlation test. The correct cell is likely to be one of these and will be more reliably detected by the active correlator which will also more reliabily discard false alarms. Generally the active correlator decision can be improved by increasing the correlation time. However, a false alarm from the matched filter will engage the active
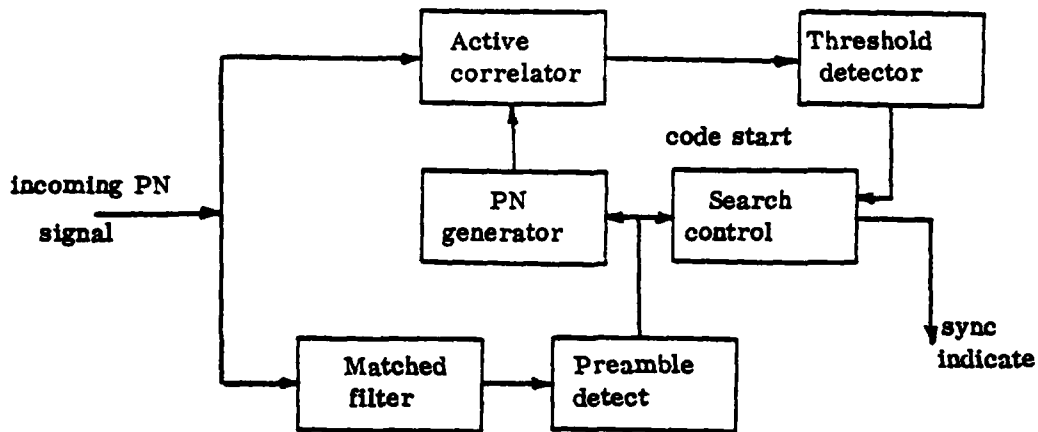
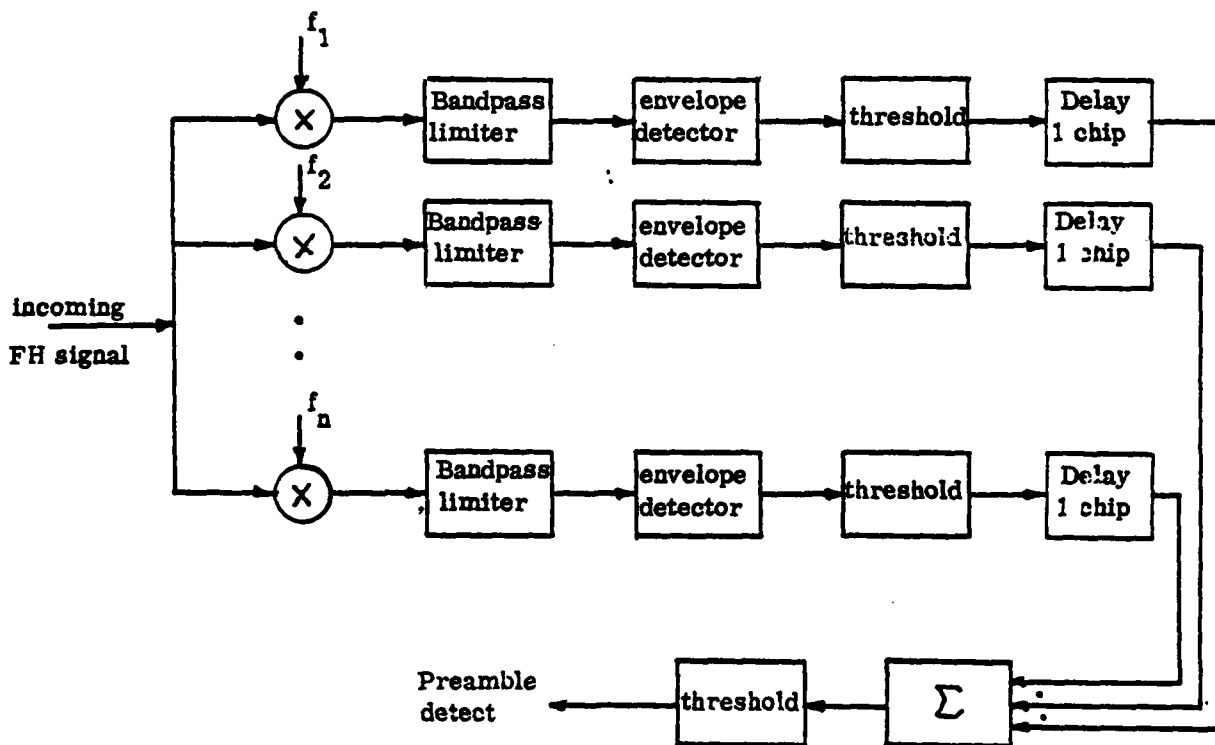Fig. 12 Matched Filter for Acquisition Aiding by Preamble Detection

Fig. 13 A Matched Filter Preamble Detector for Frequency Hopped System

jamming.

3. Uncertainty due to Doppler shift is negligible since mobility only at low speeds is involved. Relatively stable local clocks are used by the communicators. The predominant uncertainty between transmitting and receiving communicators is that of relative code phase.

4. The communicators are assumed to operate in a push to talk mode.

5. The communicators have a priori information about the PN code (hopping pattern) used; however, the specific (code) pattern is not known to any jammers. To maintain code security the code may be changed at previously agreed upon intervals using rough time of day information available to the users. The jammer(s) are therefore forced into a randomized jamming strategy to maximize their effectiveness.

6. The receiver does not know when a communication will begin; it must detect this from the transmission itself.

7. At the onset of each transmission a user will send a <u>leader</u> to facilitate acquisition by the receiver. This leader will consist of several repetitions of the hopped carrier pattern. We will refer to a <u>short</u> <u>segment</u> of one of a <u>"sync</u> <u>prefix</u>." In the acquisition scheme to be described the receiver

will detect the presence of this prefix using a
passive correlator (matched filter). At first one
is tempted to put the sync prefix at the very be-
ginning of the leader. However, a jammer could
then easily detect the "sync prefix" frequencies
since radio silence would always be broken by the
same sequence of pulses. Therefore the leader should
start at a random code phase but will include some
fixed number, $\underline{n}$, of sync prefixes each followed
by a long sequence of the hopped carrier code. The
structure of the message transmission leader is
shown in Fig. 14.

4.1 Description of the Acquisition Scheme

Suppose we have a spread spectrum system which employs
L, (L = m+k), frequencies in a "two level" coarse acquisition
procedure in the following way. A passive correlation is
used to detect the relatively short m hop sync prefix and
will generate code start signals for those hop intervals
in which its detection threshold is exceeded. The code start
signals are input to a bank of c active correlators as shown
in Fig. 15. Each code start signal will engage any (one)
active correlator that is idle, and cause it to cycle through
a sequence of k hops (k>>m). At the end of the k hops, the
output of the active correlator is compared with a second
threshold. A sync indication (to indicate tracking) is output
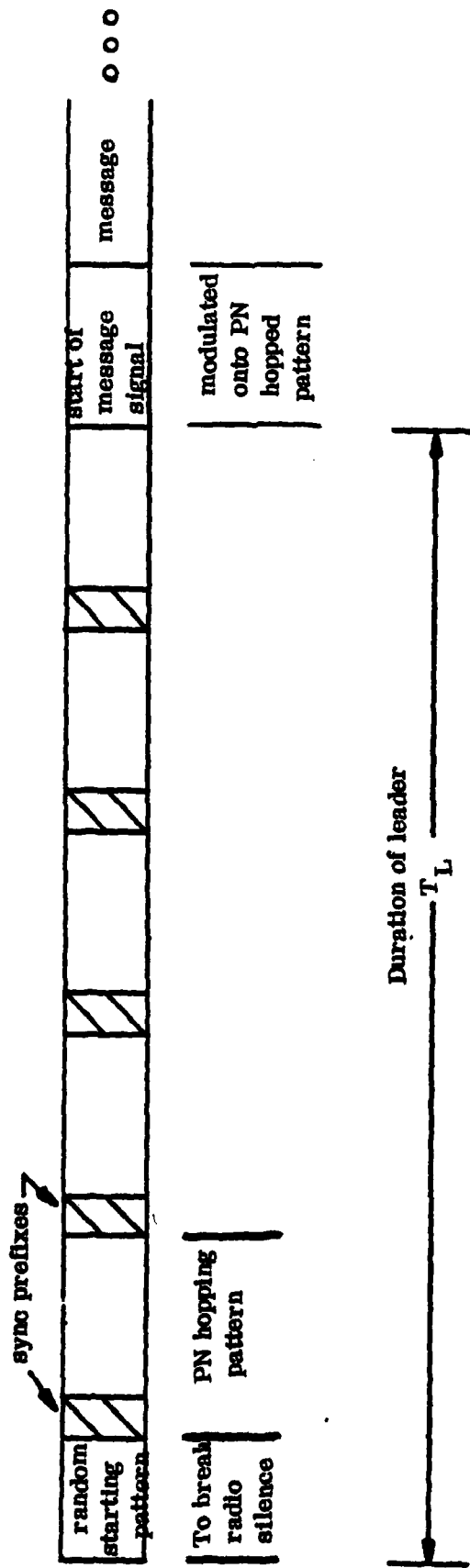
Fig. 14 Structure of message transmission leader
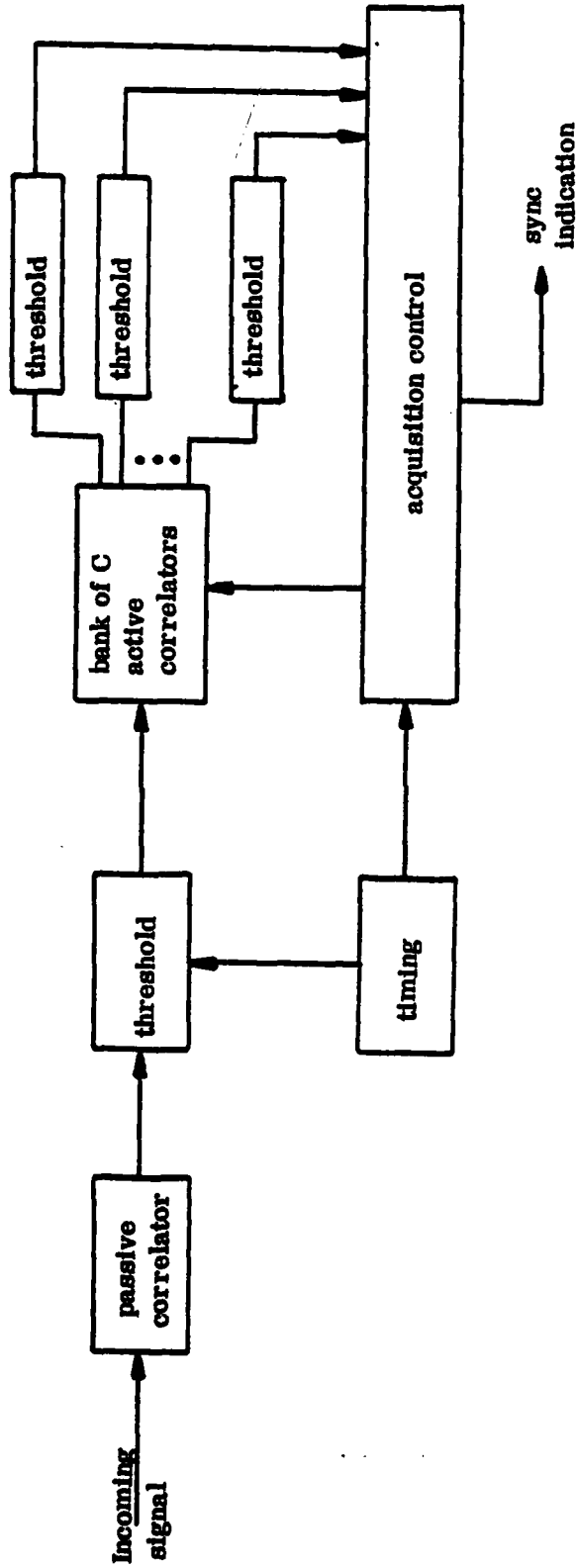
Fig. 15 A two level coarse acquisition scheme using a passive correlator and a bank of active correlators

if this second threshold is exceeded, otherwise the correlator
is again made available to the common bank. Code start
signals which find all active correlators engaged, are ignored.
Dismissal of a <u>valid</u> code start signal is one way in which
a sync prefix will be missed.

The threshold comparison at the correlator output for
either a passive or active correlator can be characterized
by the two probabilities P_{fa} (false alarm probability) and
P_{fd} (false dismissal probability) defined below:

$$P_{fa} = \text{Pr \{correlator (falsely) detects the in-sync}$$
$$\text{condition when in fact it is not present\}}$$

and

$$P_{fd} = \text{Pr \{correlator (falsely) dismisses the in-sync}$$
$$\text{condition when in fact it } \underline{is} \text{ present\}}$$

We shall denote passive correlator probabilities by P_{fa_1} and
P_{fd_1}; active correlator probabilities by P_{fa_2} and P_{fd_2}.

For the time being we shall assume that a message leader
contains only <u>one</u> <u>sync</u> <u>prefix</u> followed by the longer hopped
pattern and we shall focus on calculating the "miss" proba-
bility for this case. When the distinction between this
and the n repetitive case must be emphasized, we will call
this the <u>single</u> <u>copy</u> miss probability.

The passive correlator makes a threshold comparison
every hop interval, T_c. Therefore when no sync prefix is

present, false code start signals are generated at an average
rate of

$$\Lambda = P_{fa_1}/T_c = P_{fa_1} R_c \text{ sec}^{-1}, \tag{4}$$

where R_c is the hopping rate of the incoming code and P_{fa_1}
is the false alarm probability for the passive correlator.
Now, there are c active correlators and a code start signal
from the passive correlator engages an active correlator
for T_2 seconds, where $T_2 = kT_c$, if at least one active cor-
relator is not engaged.

We assume that false code start signals arrive (approxi-
mately) according to a Poisson point process with arrival
rate $\Lambda = P_{fa_1} R_c$. Then the activity of the bank of c active
correlators can be modelled as a queueing system with Poisson
arrivals; a finite number of servers, c; fixed holding times,
T_2, and no room for waiting. Specifically the correlator
bank behaves as an M/D/c/c queueing system. The load offered
to this queueing system is $a \equiv \Lambda T_2$. Substituting for Λ from
(4) and recalling that $T_2 = kT_c$ we find

$$a = P_{fa_1} R_c T_2 = P_{fa_1} R_c k T_c \equiv P_{fa_1} k. \tag{5}$$

With the correlator bank modelled in this way, the
probability that a code start signal finds all c correlators
engaged is just the blocking probability for this queue.
This is given by the Erlang B formula, B(c,a), where [14]

$$B(c,a) = \frac{(a^c/c!)}{\sum\limits_{k=o}^{c} (a^k/k!)} \quad , \quad c = 1,2,\ldots \quad (6)$$

which can be conveniently computed using the recursion formula

$$B(c,a) = \frac{aB(c-1,a)}{C + aB(c-1,a)} , \quad (7)$$

beginning with $B(o,a) \equiv 1$.

Now a single copy message leader can be missed in a number of ways. These are:

(a) The passive correlator falsely dismisses the m hop sync prefix when it occurs. The probability of this event is P_{fd_1}.

(b) The passive correlator detects the m hop sync prefix and thereby generates a correct code start signal; however, the code start signal finds all active correlators engaged and is therefore ignored. The probability of this event is $(1-P_{fd_1})B(c,a)$.

(c) The passive correlator detects the m hop sync prefix and generates a true code start signal at a time when at least one of the active correlators is idle. An active correlator is therefore engaged for this true code start signal, but after correlation over the succeeding k hop intervals, the in-sync condition is falsely dismissed. The probability of this event is $(1-P_{fd_1})(1-B(c,a))P_{fd_2}$.

The events (a), (b) and (c) above are mutually exclusive
and therefore the single copy miss probability is given by

$$P_{miss} = P_{fd_1} + (1-P_{fd_1})[B(c,a) + (1-B(c,a))P_{fd_2}] \qquad (8)$$

where $a \equiv P_{fa_1} k$.

A false lock will occur if <u>all</u> of the following events
occur:

    (a) the passive correlator generates a false code
        start signal

    (b) the code start signal finds at least one active
        correlator idle

    (c) the active correlator that is engaged by this
        false code start signal <u>falsely</u> detects the in
        sync condition.

Thus the probability of false lock is

$$P_{false\ lock} = P_{fa_1} P_{fa_2} (1-B(c,a)). \qquad (9)$$

When the false code start signals arrive, according to a
Poisson process and under the assumption of white Gaussian
noise the events (a), (b) and (c) above are statistically
independent, hence the multiplication in (9) is justified.
In practical cases of interest $B(c,a) \ll 1$, hence

$$P_{FL} \equiv P_{fa_1} P_{fa_2} \qquad (10)$$

is a <u>tight</u> <u>upper</u> <u>bound</u> on the false lock probability given

by (9).

EXAMPLE: PASSIVE & ACTIVE CORRELATOR STRUCTURES

In order to demonstrate the applicability of this scheme
we will consider synchronization of a frequency hopped system.
The essential structure of the passive correlator considered
is shown in Figure 16. Effectively it performs square law
integration of the envelopes of the outputs of m bandpass
limiters centered at the hop frequencies in the sync prefix.
The structure shown is a near optimal noncoherent detector.
for detecting the hopped sequence f_1, f_2, f_3,...f_m in a
background of white gaussian noise.

We have included a limiter in each arm of the passive
correlator to preclude the possibility that a strong cw
jamming signal will generate an inordinate number of false
code start signals by jamming only one frequency. The limiting
level should be set slightly above that of the envelope of
the received desired signal. In this way, for example, the
impact of a single cw jamming tone, <u>however</u> <u>strong</u>, will
be limited. To increase its effectiveness a jammer must
jam a number of different frequencies. However, since the
specific frequencies used for sync are unknown to him he
is forced to a random selection of frequencies in the band
and therefore with nonzero probability will expend some of
his power ineffectively jamming some frequencies which are
not used for synchronization anyway.

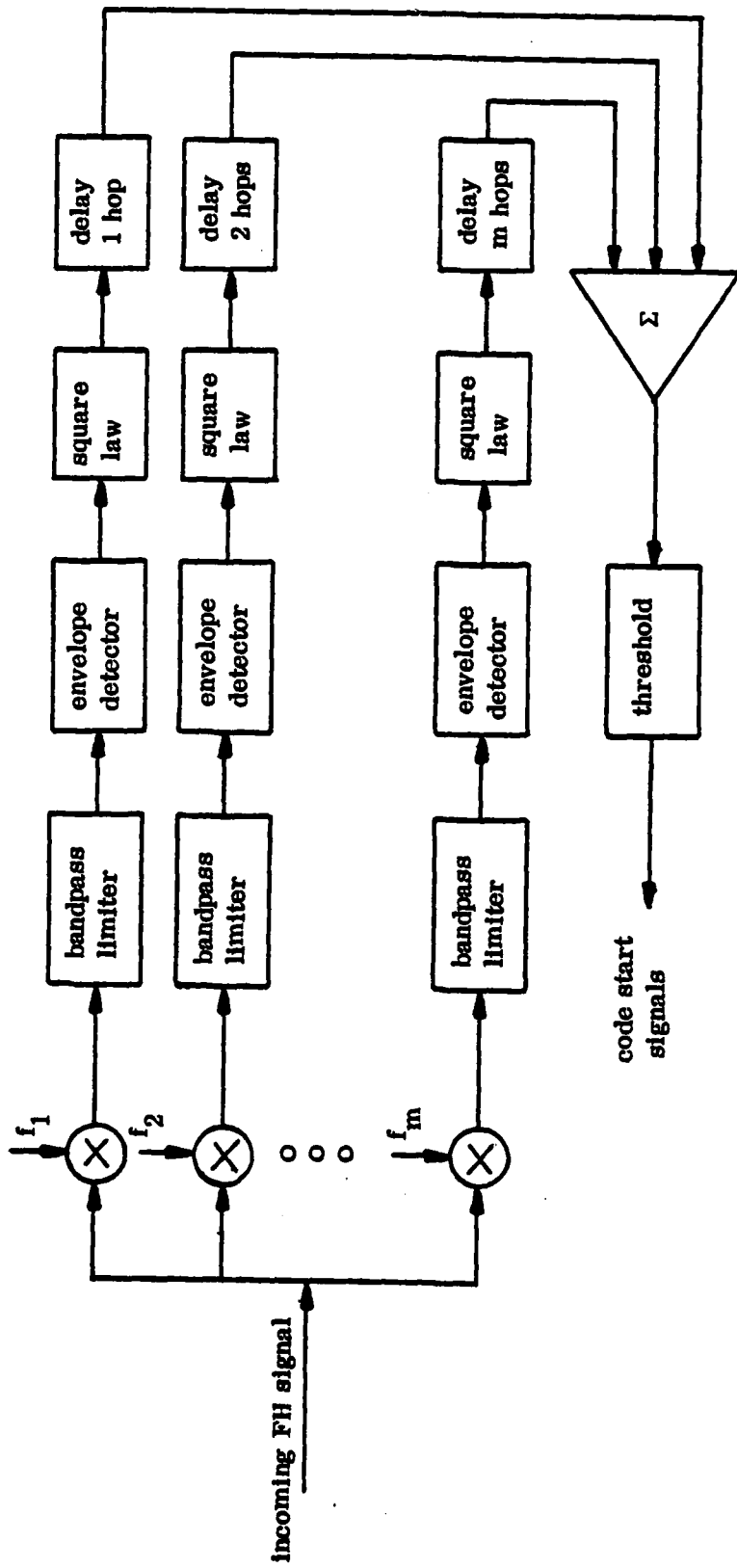The active correlator shown in Fig. 17 also forms the

Fig. 16 Passive correlator structure for two level coarse acquisition scheme

sum of squares of envelopes but this is done temporally by active correlation rather than spatially. In this way integration can be performed over a large number of chips without the need for a huge bank of matched filters.

4.2 <u>Performance in the Presence of Background Noise and Noise Jamming</u>

The performance of the proposed acquisition structure in the presence of gaussian noise is analyzed in this section. The gaussian noise may be due to receiver noise, to intentional noise jamming, or to a mixture of the two. Therefore, the model and the results obtained in this section are applicable in two realistic situations which are distinguished only by values that certain parameters assume. These are: a) performance in a benign environment, characterized by high input SNR, and b) performance in the presence of wideband noise jamming, characterized by low input SNR.

To express the one sided noise power spectral density, let P_j be the total noise jamming power. Since this must be spaced over the L frequency slots of the system, the jamming noise power per slot is P_j/L. The effective one sided noise power spectral density at the receiver is therefore

$$\eta = N_o + (P_j/2R_c) \tag{11}$$

where N_o is the thermal noise component and $P_j/2R_c$ is the jamming component. If $P_j = 0$ only background noise is present.

Assuming that the interference (noise + jamming) is

gaussian, the voltage input to the threshold device shown
in Fig. 16 is the sum of squares of m Rician variates when
the desired sync prefix is, in fact, present. The probability
that ths sync prefix is falsely dismissed when it is present
is just the probability that the voltage does not exceed
the threshold. This probability is given by the complement
of the generalized Q function. Specifically the false dis-
miss probability can be expressed as

$$P_{fd_1} = 1 - Q_m(s_1, \ell_1) \tag{12}$$

where $Q_M(a,b)$ is the generalized Q function defined by

$$Q_M(a,b) = \int_b^\infty \zeta(\zeta/a)^{M-1} \exp[-(a^2+\zeta^2)/2] I_{M-1}(a\zeta) d\zeta, \tag{13}$$

$$M = 1,2,\ldots; \quad a,b \geq o,$$

$$S_1 = \sqrt{2m(E_c/\eta)}$$

E_c = received signal energy per hop

and η is the effective one sided noise spectral density as
in (11). The complementary generalized Q function will be
denoted $Q_M^C(a,b)$. Thus

$$Q_M(a,b) + Q_M^C(a,b) \equiv 1. \tag{14}$$

The argument ℓ_1 appearing in (12) is the normalized passive
correlator threshold. That is, the sum of squared Rician
voltages is compared with the voltage threshold $2R_c\ell_1^2\eta$ and
a code start signal is generated in each hop for which the

threshold is exceeded.

The probability that the passive collector threshold is exceeded when the sync prefix is not present is given by

$$P_{fa_1} = Q_m(o, \ell_1). \tag{15}$$

In a similar way the probability that an active correlator (shown in Fig. 17), which has been correctly started, dismisses the sync signal when in fact it is present is given by

$$P_{fd_2} = 1 - Q_k(s_2, \ell_2) \tag{16}$$

where

$$s_2 = \sqrt{sk(E_c/\eta)}$$

and ℓ_2 is the normalized threshold to which the test statistic is compared.

In implementation the sum of squared Rician variables accumulated at the active correlator output is compared with the threshold $2R_c \ell_2^2 \eta$. A sync indication is made and the system's tracking function is engaged if this threshold is exceeded. The probability that a falsely started active correlator generates exceedance of the ℓ_2 threshold is

$$P_{fa_2} = Q_k(o, \ell_2). \tag{17}$$

When this occurs tracking will be initiated and a lock indication will be made (though false).

It is important to note, in evaluating the probabilities

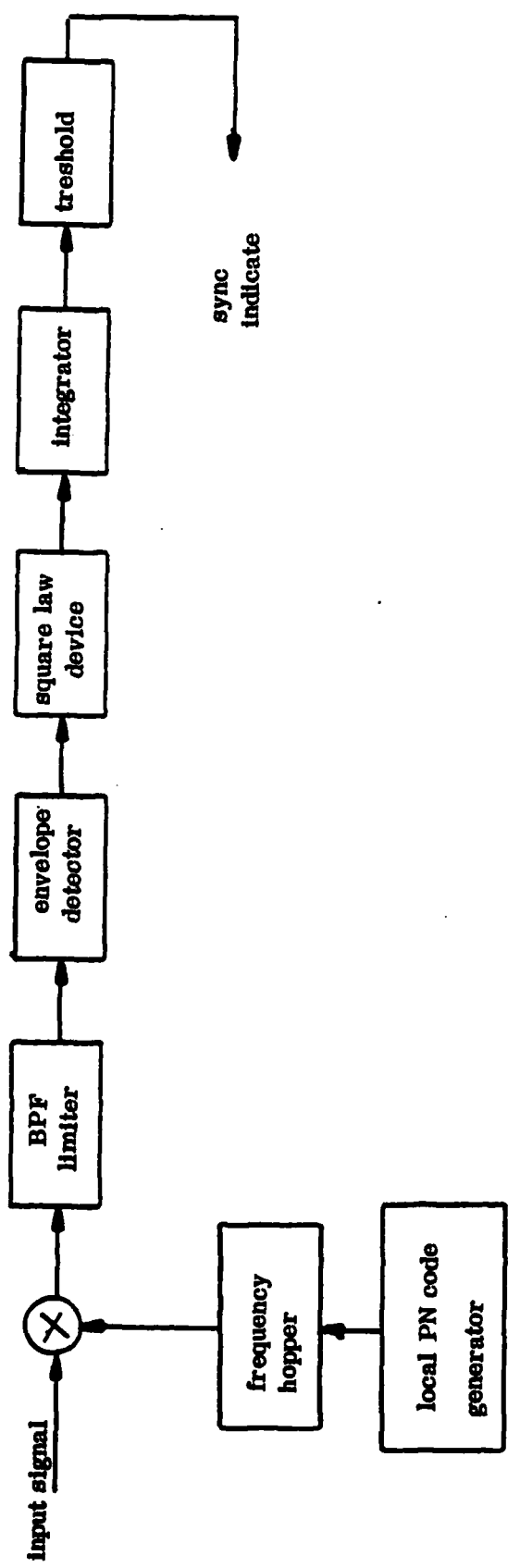Input signal → ⊗ → BPF limiter → envelope detector → square law device → integrator → treshold

frequency hopper → ⊗

local PN code generator → frequency hopper

sync indicate

Fig. 17 Active correlator structure for two level coarse aquisition scheme

P_{fa_1}, P_{fa_2}, P_{fd_1}, and P_{fd_2}, that these quantities will gener-
ally be small. To maintain accuracy, care must be taken in
the computational approach. Thus, for example, if P_{fd_1} is
small, $Q_M(s_1, \ell_1) \approx 1$, and calculation of P_{fd_1} using the RHS
of (12) expressed as a small difference between relatively
large numbers will yield inaccurate results. A direct
evaluation of the complementary Q function $Q_M^C(a,b)$ is prefer-
able in this case. A more complete discussion of the compu-
tational approach and the approximations used is given sub-
sequently. When the false alarm, false detection and blocking
probabilities are calculated, the "single copy" miss prob-
ability P_{miss}, and the upper bound on false lock probability,
P_{FL} can be calculated using (9) and (10).

Threshold Optimization

The terms appearing in the expressions for P_{miss} and P_{FL}
depend on the quantities m, k, E_c/η, c, ℓ_1, and ℓ_2. When
other parameters are known, suitable choices for the thresholds
ℓ_1 and ℓ_2 can be considered.

It can be seen that increasing ℓ_1 will reduce P_{fa_1} and
the "load offered" to the bank of active correlators. The
probability that a code start signal will find all correla-
tors engaged will therefore decrease. An increased ℓ_1, how-
ever, also implies a larger probability that the passive
correlator will miss the sync prefix when it is in fact present
(i.e. P_{fd_1} increases). These opposing effects lead to con-
sideration of optimizing the threshold settings.

With m, k, c, and E_c/η given, it is meaningful to seek those thresholds ℓ_1 and ℓ_2 which minimize the miss probability, P_{miss}, subject to the constraint that the probability of false lock is below some specified value. Mathematically the problem is to find

$$\min_{\ell_1,\ell_2} P_{miss}(\ell_1,\ell_2) \qquad (18)$$

subject to the constraint

$$P_{FL}(\ell_1,\ell_2) \leq \text{constant} \equiv 10^{-p} \qquad (19)$$

where $p > o$.

The solution to this minimization problem yields the minimum "single copy" miss probability, P^O_{miss} and the two optimizing <u>normalized</u> thresholds ℓ_1, and ℓ_2. In an actual system the required threshold would be set relative to an <u>estimated</u> noise background level which may introduce some additional uncertainty [16]. The optimum performance described here serves as a bench mark for system comparisons. The procedure used to solve the stated minimization problem is described in Section 6.0 (Appendix I).

Relation to Acquisition Time

In the scheme under consideration each transmission is initiated by a <u>leader</u> consisting of n full cycles of a long PN hopped signal pattern. The length of this leader is a form of system "overhead." Just prior to data transmission

a sequence of digits modulating the spread spectrum waveform
will be used to indicate the beginning of data (or voice)
transmission. To successfully demodulate the message the
intended receiver must acquire the PN signal prior to this
"start of data" sequence. Thus the length of the leader
represents the <u>maximum</u> time that the receiver has for code
acquisition, and this time must be sufficiently long for the
intended receiver to acquire it with high probability. With
n replications of the PN hopped pattern in the leader, the
receiver will have n opportunities for acquisition. The
probability that the receiver will <u>not acquire</u> a transmitted
leader is given approximately by

$$P_{NA} \approx (P^O_{miss})^n. \tag{20}$$

The average length of the leader, in seconds, is

$$T_L = (n+\tfrac{1}{2}) L/R_c \tag{21}$$

where

R_c = hopping rate in hops/sec

L = number of hopping frequencies

n = number of repetitions in a leader.

This format includes a component of average length $L/2R_c$
to account for the random code starting phase used to break
radio silence (see Fig. 14). It follows from (20) and (21)
that one can expect roughly an exponential decrease in P_{NA}
as the duration of the leader is increased by more repetitions.

As an example for $L = 256$ and $R_c = 100$ khps the duration of a leader is $T_L = (2.56)(n+\frac{1}{2})$ msec. Thus with $n = 4$, leader durations of about 15 msec can be used yielding $P_{NA} < 10^{-2}$ even for single copy P^o_{miss} as high as 0.3.

Discussion of Results Obtained for Noise Jamming

Minimum miss probability calculations were evaluated by the method described for two sets of system parameters. One set is for a system with 256 hopping frequencies, and one for a system with 512 hopping frequencies. A value of $P_{FL} \leq 10^{-8}$ was taken as an illustration. The resulting performance curves are shown in Figures 18 and 19. It can be seen from these figures that the probability of not acquiring a transmitted leader can be reduced by increasing either n or c or both. The use of a moderate number of active correlators (say 5 to 10) yields considerable improvement in performance with "diminishing returns" for higher values of c. Several replications of the hopped pattern and sync prefix in the leader can yield substantial reductions in miss probability P_{NA} especially when used in conjunction with the active correlator bank. Except for the case of very low values of hop energy to noise density ratio, E_c/η, we found that the minimum miss probabilities obtainable are very insensitive to the values of P_{FL}. Essentially the same miss probabilities were shown to apply for values even as low as 10^{-20} or smaller. This is because for sufficiently high E_c/η the quantity P_{fd_2} drops out of the expression for P_{miss}. In this case P_{miss}

is (for the given parameter shown) essentially determined by ℓ_1 while both ℓ_1 and ℓ_2 affect P_{FL}. Thus within a broad range ℓ_2 can be chosen to set the false lock probability quite small. In our calculations it was convenient to keep $P_{FL} \leq 10^{-8}$ as indicated in Figs. 19 and 19, but somewhat smaller values of P_{FL} can yield essentially the same miss probabilities for the chosen parameters.

Miss probabilities less than 10^{-2} are easily obtained for $E_c/\eta > -/dB$, with only two replications and five active correlators; substantially better performance is attainable for reasonable parameter choices.

4.3 Performance in Background Noise and CW Jamming

To consider the impact of CW jamming on the proposed acquisition scheme consider a jammer which places CW jamming tones in J of L (L=m+k) frequency slots of the system. We assume that the jammer does not know which frequency slots are used for active or passive correlation and that it places these jamming tones randomly. Because of the receiver's hard limiting in the frequency channels of the passive and active correlators, a jammer will be most effective if the strength of each jamming tone is just greater than that of the signal. Thus the jammer to signal power ratio is J. It is unlikely that the envelope of the two or more equal sinusoids of random phase will be smaller than that of one of them. Therefore the

Fig. 18 Minimum miss probabilities in gaussian noise
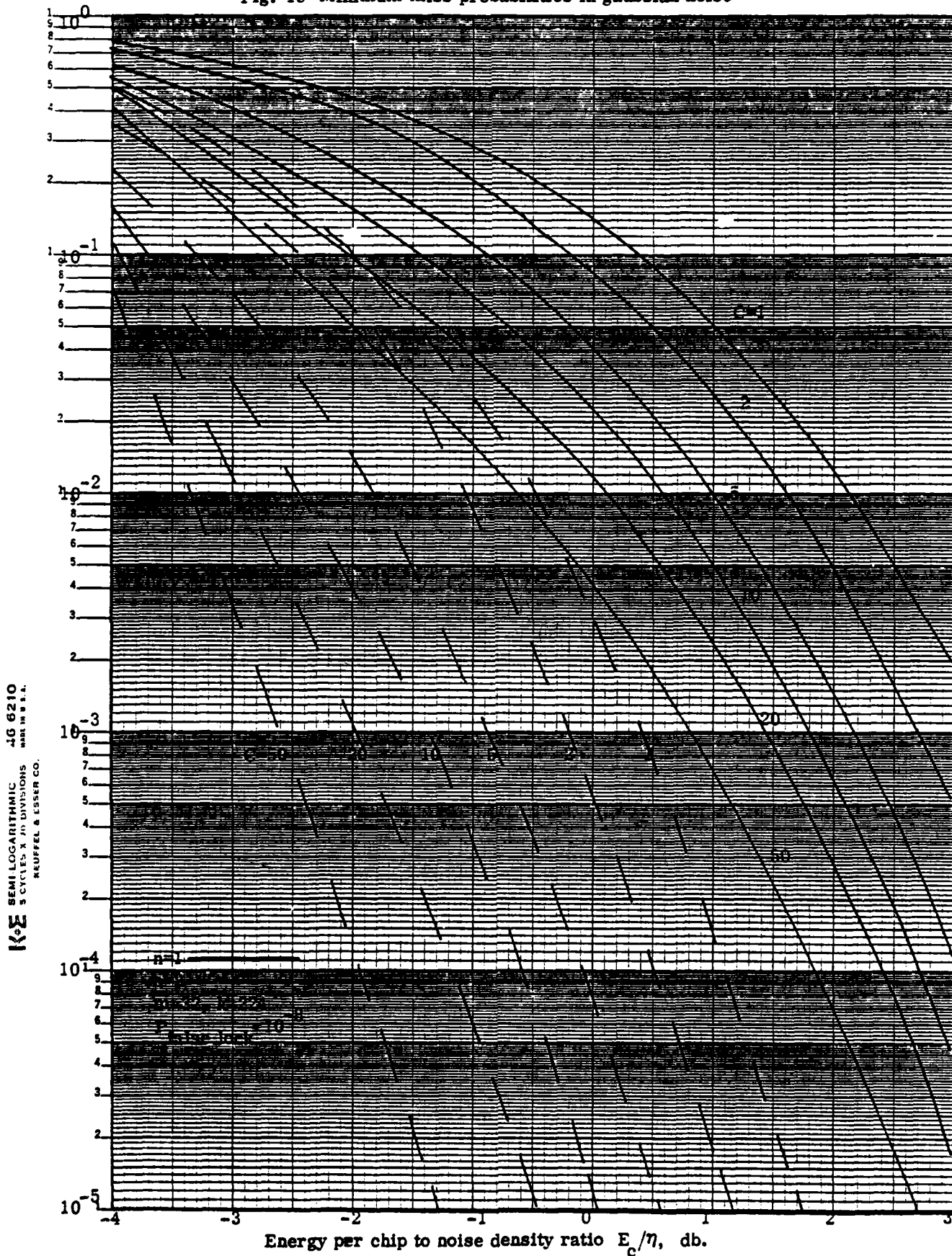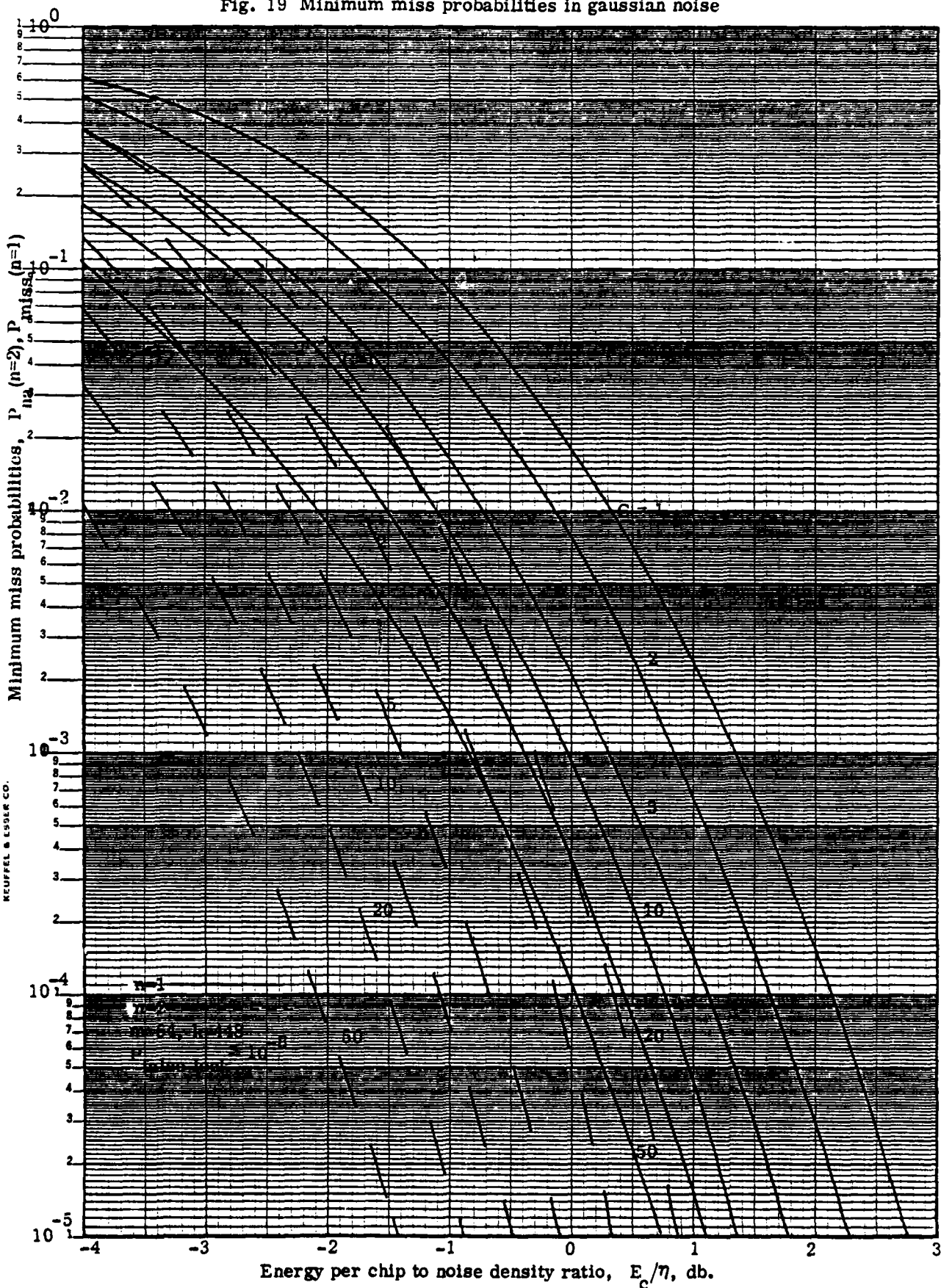
Energy per chip to noise density ratio E_c/η, db.

Fig. 19 Minimum miss probabilities in gaussian noise

Minimum miss probabilities, $P_{ma}(n=2)$, $P_{miss}(n=1)$

Energy per chip to noise density ratio, E_c/η, db.

effect of CW jamming is to increase the probabilities of threshold exceedances regardless of whether the prefix _is_ or _is not_ present.

Therefore, the strategy and major impact of CW jamming is to increase the rate at which false code start signals are generated and to increase the probability of false lock. The increased loading of the active correlators due to _false_ code start signals results in an increased probability that a _correct_ code start signal will find all correlators busy and that the prefix will be missed; however, the jamming will tend to increase the probability of successfully detecting a true code start signal _which_ _does_ in fact _engage_ an active correlator.

For an approximate analysis of acquisition performance in the presence of CW jamming it will be assumed that if two or more sinusoids occupy the same frequency slot in addition to the background noise, the hard limiting operation and envelope detection process produce an envelope which is essentially that of a single sinusoid in gaussian noise. Let ν_1 and ν_2 be the respective fractions of passive correlator and active correlator frequencies which are jammed. Recalling that the jammer to signal ratio is J, and that the jammer is attempting to jam as many frequencies as possible, we have

$$\nu_1 m + \nu_2 k = J \tag{22}$$

To obtain specific results we further assume that the detection thresholds at the receiver have been set to optimize

performance in a noise background alone as in Section 4.2.
We define these optimum thresholds for the passive and the
active correlators, as ℓ_1^* and ℓ_2^* respectively. If the
presence of randomly placed CW jamming tones causes the
fraction ν_1 of the passive correlator frequencies to be jammed,
the probability of generating a false code start signal will
be

$$P_{fa_1} = Q_m(s_1\sqrt{\nu_1}, \ell_1^*) \tag{23}$$

while the false dismissal probability

$$P_{fd_1} = Q_m^c(s_1, \ell_1^*). \tag{24}$$

Similarly the probability of a false exceedance of the
active correlator's threshold will be

$$P_{fd_2} = Q_k(s_2\sqrt{\nu_2}, \ell_2^*) \tag{25}$$

and the false dismissal probability at the second
threshold is

$$P_{fd_2} = Q_k^c(s_2, \ell_2^*) \tag{26}$$

where

$$s_1 = \sqrt{2m(e_c/\eta)} \tag{2&}$$

and

$$s_2 = \sqrt{2k(E_c/\eta)} \tag{28}$$

The resulting single-look miss probability becomes

$$P_{miss} = Q_M^c(s_1, \ell_1^*) + [1-Q_k^c(s_2, \ell_2^*)](B(c,a) + (1-B(c,a)Q_k^c(s_2, \ell_2^*)] \tag{29}$$

where

$$a = kQ_m(s_1\sqrt{\nu_1}, \ell_1^*). \tag{30}$$

The probability of false lock is bounded by

$$P_{FL} = Q_m(s_1\sqrt{\nu_1}, \ell_1^*) \; Q_k(s_2\sqrt{\nu_2}, \ell_2^*). \tag{31}$$

In a CW jamming environment with a jammer to signal ratio of J one may have equal fractions ν_1 and ν_2, that is

$$\nu_1 = \nu_2 = J/(m+k) \tag{32}$$

If n prefix repetitions are used in the leader, then the miss probability is reduced because there would be n opportunities for acquisition of the leader rather than only one. If independent looks are assumed, as might become reasonable for long hopping sequences and some false alarm rates the single copy miss probability will be raised to the nth power as before.

Discussion of Results for CW Jamming

The impact of CW jamming on acquisition performance of the proposed scheme is shown for the illustrative parameters in Figs. 20 and 21. The two figures are qualitatively the same but the smaller miss probabilities achievable from the 512 hop system is apparent. If a receiver has c active correlators in its bank and attempts to set thresholds which are optimum for this c in a noise environment the resulting thresholds will be quite low ·and performance will rapidly deteriorate

when CW jamming arises. A more conservative strategy is for
a receiver with say 10 active correlators to set its detec-
tion thresholds higher (say optimum for c = 3). When CW
jamming arises the increased rate of false code start signals
will then not overload the active correlator bank until the
jammer to signal ratio, JSR, is quite high.

Figs. 20 and 21 depict system performance as a function
of JSR, and for values of E_c/η and c. It can be seen that
this strategy will maintain P_{miss} at an essentially fixed
value as jamming increases up to a value determined largely
by c. Beyond this point, the miss probability rises rapidly.
(Note only E_c/η = OdB is shown in Fig. 21 for convenience of
scale.)

Figure 22 shows the accompanying impact on false lock
probabilities, where the thresholds were set on the basis of
P_{FL} = 10^{-8} to provide a conservative (high) characterization.

5.0 CONCLUDING REMARKS

The proposed scheme combines the advantages of the rapid
search time of passive correlation with the decision reli-
ability of long sequence active correlation. By sharing a
common bank of active correlators among arriving code start
signals, a significant reduction in hardware is possible com-
pared with a full L chip parallel correlator structure.

The two level scheme has been analyzed using queueing
theory and detection theory methodology. The results indicate

Miss probability

$E_b/n = 0$ db $C = 2$ 5   10   20

m=32, k=224, L=256

$C = 8$, PRI/ΔT = 192
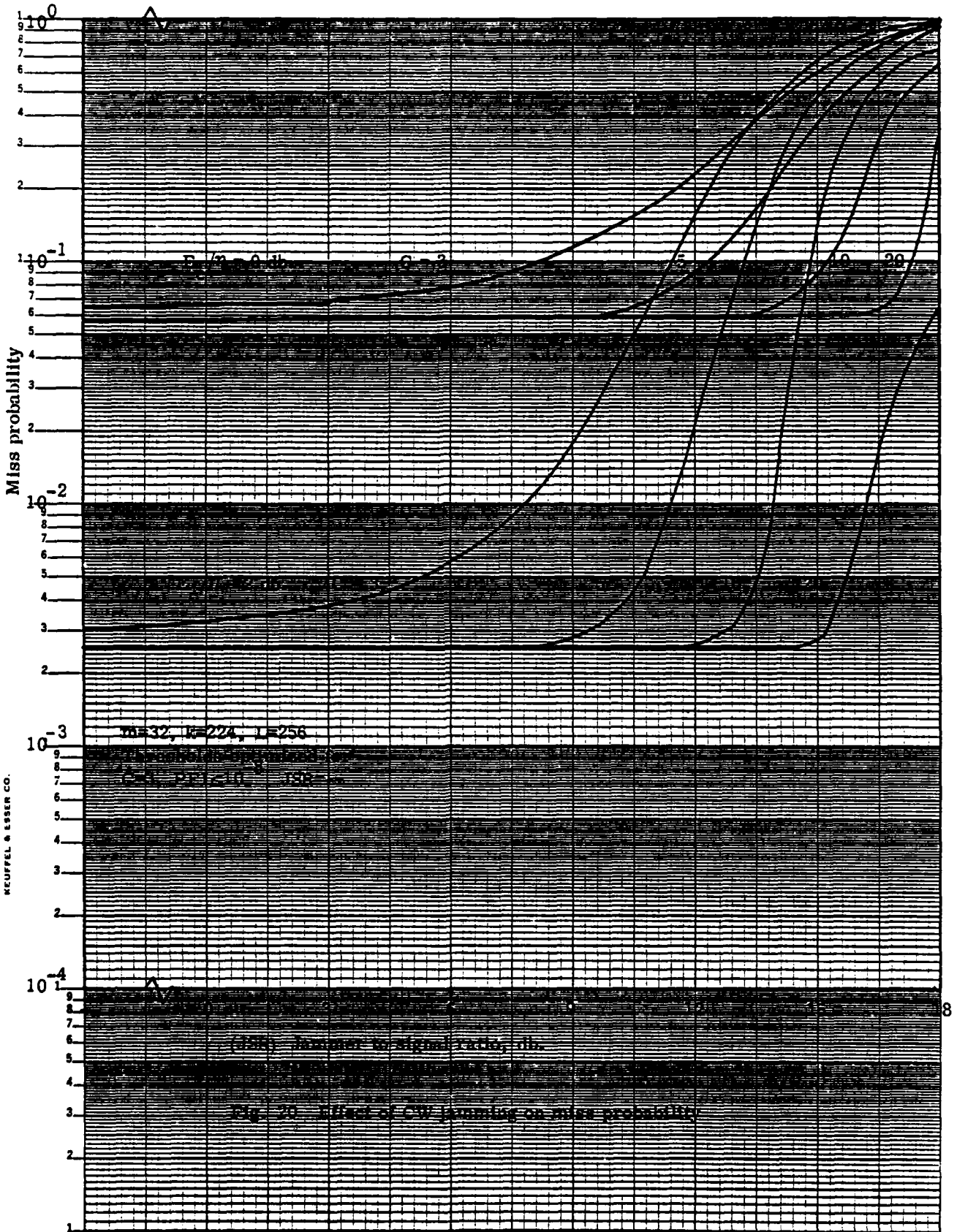
(JSR) Jammer to signal ratio, db
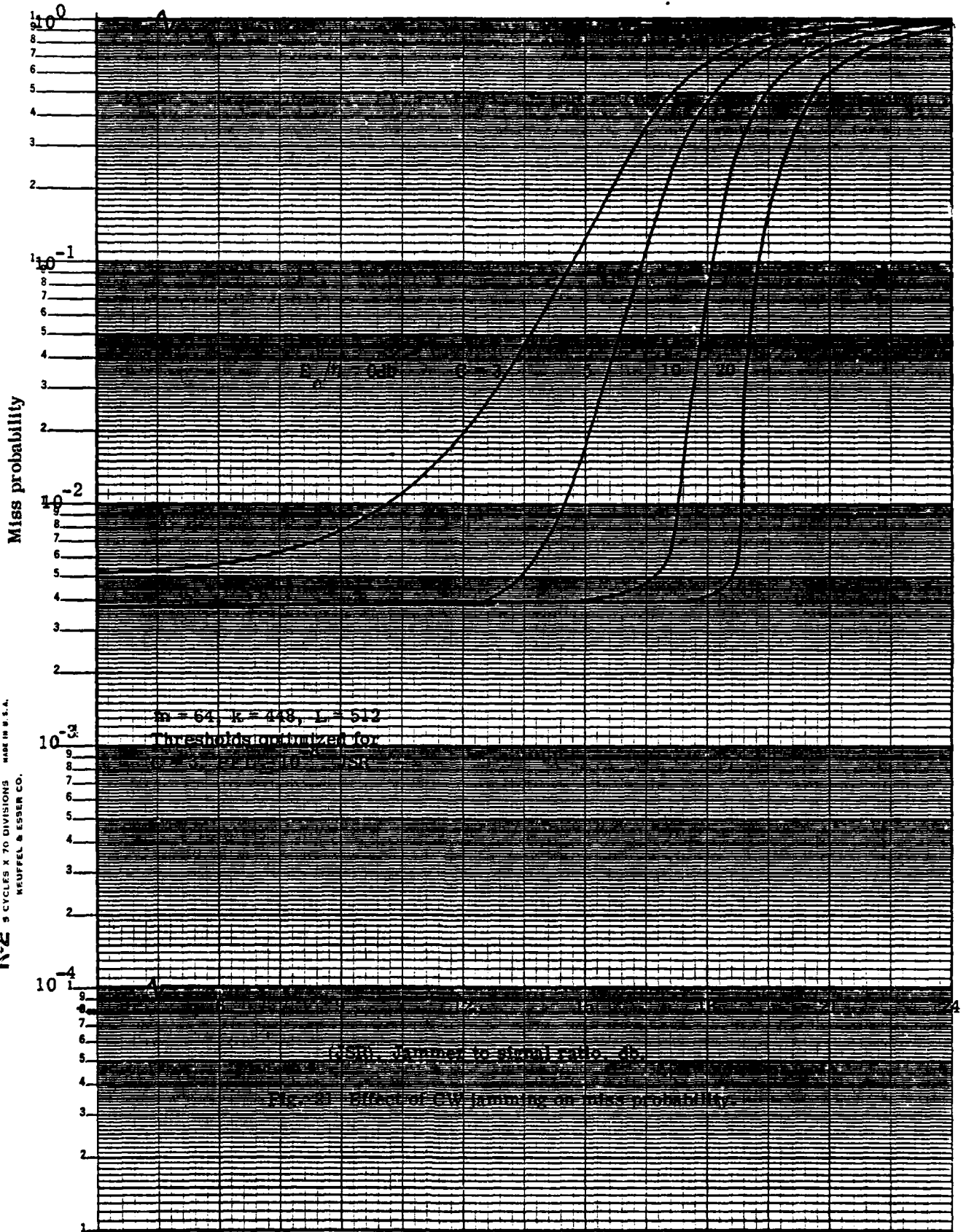
Fig. 20 — Effect of CW jamming on miss probability

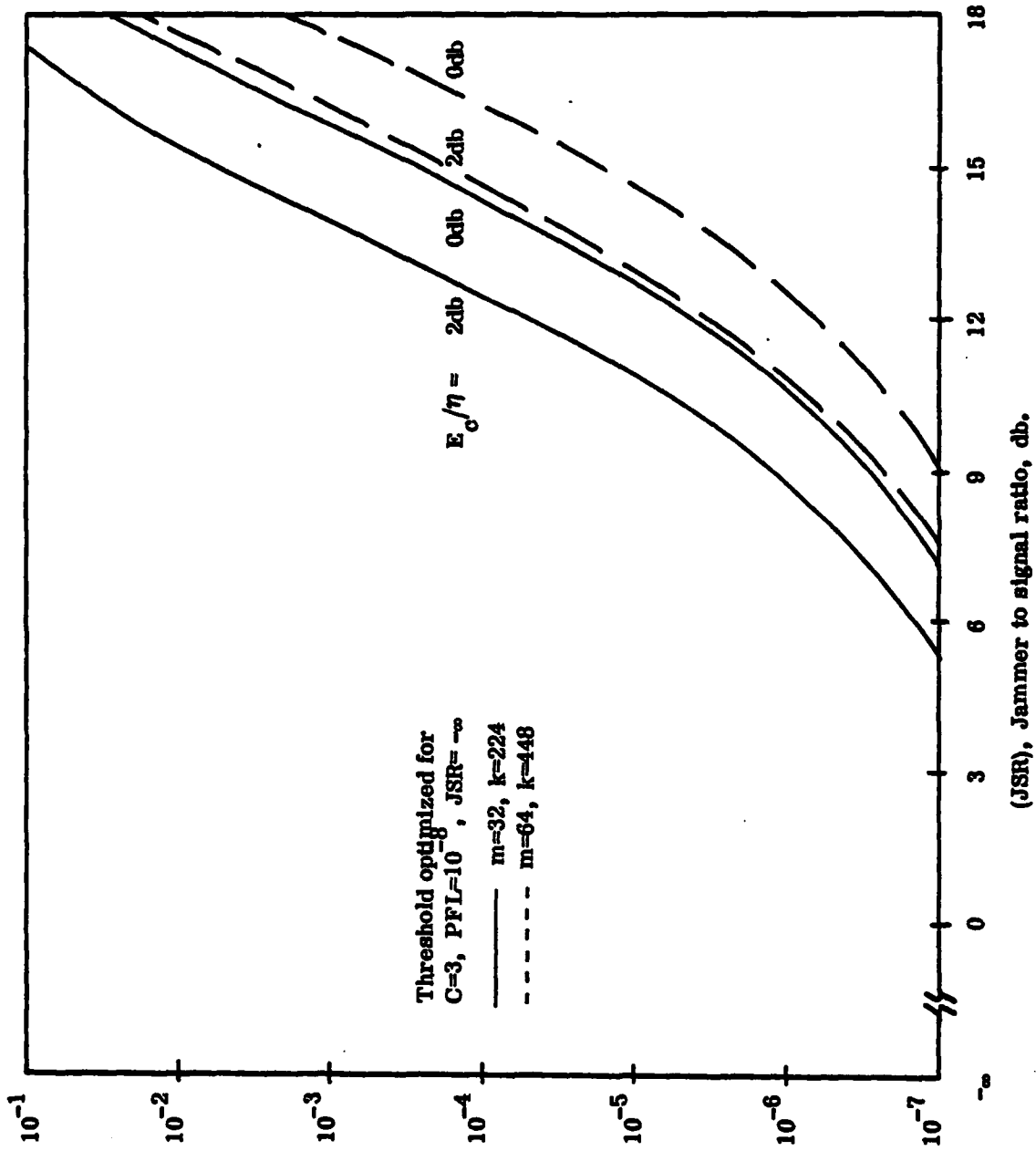Fig. 31 Effect of CW jamming on miss probability.

Fig. 22 Effect of CW jamming on false look probability

that an active correlator bank of moderate size and several
replications of the hopping pattern in the transmission
leader can yield small miss and false lock probabilities.

Performance of the acquisition structure in a CW jamming
environment shows that a relatively fixed level of miss
probability can be maintained over a wide jamming threat by
appropriately setting detection thresholds.

6.0 APPENDIX I

Overall Description of Computational Method

The following method was used to find P_{miss}^{O} which is
the minimum "single copy" miss probability, subject to the
"soft inequality" constraint $P_{FL} \leq 10^{-p}$ as described in (18)
and (19). For each given parameter set, consisting of m,
k,c, and E_c/η, two minimizations were done. The first was
a constraint minimization mathematically stated as follows:

A.
$$\min_{\ell_1, \ell_2} P_{miss}(\ell_1, \ell_2) \tag{A1.1}$$

subject to the equality constraint

$$P_{FL}(\ell_1, \ell_2) = 10^{-p} \tag{A1.2}$$

This was recast as a single variable minimization over
ℓ_1 without a constraint. The equality constraint (A1.2) was
treated as an implicit equation for ℓ_2 as a function of ℓ_1.
This implicit equation was solved using an iteration procedure

at each step of the minimization. Specifically the recast
problem can be stated as

$$\min_{\ell_1} P_{miss}(\ell_1, \ell_2(\ell_1)) \qquad (A1.3)$$

where $\ell_2(\ell_1)$ is that ℓ_2 which for given ℓ_1 satisfies (A1.2).

In this way a simple one dimensional search was used to
find the optimum ℓ_1 with ℓ_2 found by numerical solution of an
implicit equation. For these minimizing values of ℓ_1 and ℓ_2
the value of P_{FL} was then evaluated using (10), (15), and
(17).

When this was complete an <u>unconstrained</u> two dimensional
minimization was performed to find

$$B. \qquad \min_{\ell_1, \ell_2} P_{miss}(\ell_1, \ell_2).$$

For the minimizing values of ℓ_1 and ℓ_2 the value of P_{FL} was
found as before. If this was less than or equal to the
specified $10^{-\bar{P}}$ then the desired solution to the soft inequality
problem is the solution to B. Otherwise the desired solution
is the solution to A.

7.0 <u>APPENDIX II</u>

<u>Calculation of False Dismissal and False Alarm Probabilities</u>

An exact calculation of the required dismissal and false
alarm probabilities which involve evaluation of the generalized
Q function and/or its complement can itself be a formidable

task. A number of papers in the technical literature address the problem of computing Q_M [17,18]. For our purposes we found it convenient to approximate these quantities by appropriate values of the cumulative normal distribution. This approximation is good if M is large (which is generally the case of interest here), and it has also been used [19] in developing theoretical performance of radar receivers using noncoherent square law integration of received pulses. Transliterating from [19] we used the following approximation

$$Q_M(a,b) \approx \text{erfc}(y) \tag{A2.1}$$

where the function erfc(.) denotes the complementary error function defined by

$$\text{erfc}(u) \triangleq \frac{1}{\sqrt{2\pi}} \int_u^\infty e^{-\xi^2/2} \, d\xi \tag{A2.2}$$

and y is given by

$$y = \frac{b^2 - a^2 - 2M}{2\sqrt{\alpha^2 + M}}$$

It is noted that if $y = 0$, then (within the accuracy of the erfc approximation) Q_M and Q_M^c are each approximately equal to 0.5. Since both of these functions are needed to determine P_{miss} and $P_{false\ lock}$, and since usually P_{miss} will be small in the range of interest, care must be taken in their computation to maintain accuracy in the final answer. For $y > 0$

we have $Q_M(a,b) < Q_M^C(a,b)$, while for $y < 0$ the inequality is reversed. To avoid the loss of significant figures when Q_M or Q_M^C is small, we calculated

$$Q_M(a,b) = \text{erfc}(y) \tag{A2.4}$$

for $y > 0$ and then found Q_M^C by subtracting from unity. For $y < 0$ we first calculated

$$Q_M^C(a,b) = \text{erfc}(|y|) \tag{A2.5}$$

and then found Q_M by subtracting from unity.

8.0 REFERENCES

1. Spilker, J.J., Jr., "Delay-Lock Tracking of Binary Signals," IEEE Transactions on Space Electronics and Telemetry, Vol. SET-9, March 1963, pp. 1-8.

2. Gill, W.J., "A Comparison of Delay-Lock Tracking Loop Implementations," IEEE Transactions of Aerospace and Electronic Systems, Vol. AES-2, July 1966, pp. 415-523.

3. Nielson, P.T., "On the Acquisition Behavior of Delay Lock Loops," IEEE Transactions on Aerospace and Electronic Systems, Vol. AES-11, May 1975, pp. 415-417.

4. Hartman, H.P., "Analysis of Dithering Loop for PN Code Tracking," IEEE Transactions on Aerospace and Electronic Systems, Vol. AES-10, no. 1, January 1974, pp. 2-9.

5. Dixon, R.C., Spread Spectrum Systems, Wiley: New Yo York, 1976.

6. Sage, G.F., "Serial Synchronization of Pseudonoise Systems," IEEE Transactions on Communication Technology, Vol. COM-12, pp. 123-127, December 1964.

7. Cahn, C.R., "Spread Spectrum Applications and State-of the-Art Equipments," in Agard Lecture Series No. 58, AD-766-914.

8. Wald, A., Sequential Analysis, Wiley: New York, 1947.

9. DiFranco and Rubin, Radar Detection, Prpentice Hall, 1968, pp. 556ff.

10. Ward, R.B., "Acquisition of Pseudonoise Signals by Sequential Estimation," IEEE Transactions on Communication Technology, Col. COM-13, no. 4, December 1965, pp. 474-483.

12. Ward, R.B., and Yiu, K.P., "Acquisition of Pseudonoise Signals by Recursion-Aided Sequential Estimation," IEEE Transactions on Communications, Vol. COM-25, no. 8, pp. 784-794, August 1977.

13. Hopkins, P.M., "A Unified Analysis of Pseudonoise Synchronization by Envelope Correlation," IEEE Transactions on Communications, Vol. COM-25, no. 8, pp. 770-778, August 1977.

14. Holmes, J.K., and Chen, C.C., "Acquisition Time Performance of PN Spread-Spectrum Systems," IEEE Transactions on Communications, Vol. COM-25, no. 8, pp. 778-783, August 1977.

15. R.B. Cooper, <u>Introduction of Queueing Theory</u>, Macmillan: New York, 1972.

16. S.S. Rappaport, "On Practical Setting of Detection Thresholds," Proc. IEEE, vol. 57, no. 8, pp. 1420-1421, August 1969.

17. S.S. Rappaport, "Computing Approximations for the Generalized Q-function and Its Complement," IEEE Trans. on Info. Theory, Vol. IT-17, no. 4, pp. 497-498, July 1971.

18. C.W. Helstrom, "Approximate Evaluation of Detection Probabilities in Radar and Optical Communications," IEEE Trans. on Aerospace   Electronic Systems, Vol. AES-14, July 1978.

19. C.W. Helstrom, <u>Statistical Theory of Signal Detection</u>;
     Pergamon: London, 1968.

III. <u>INVESTIGATION OF ECM/ECCM FOR TACTICAL COMMUNICATION</u>
<u>SYSTEMS</u>

1.0 <u>Introduction</u>

In this final report, we discuss the significance of the
results presented in the previous interim report [1], cover-
ing susceptibility analyses for binary FH/DS NCFSK and DPSK,
and extend those results to cover the general M-ary cases
for these conventional digital modulation techniques. In
addition, new analytical results are presented for the
susceptibility analysis of Minimum Shift Keying (MSK).

The objective of this section is to find valid and useful
analytical measures of system vulnerability and weaknesses, in
order to make wise choices of signaling methods for future
systems and to discover needed modifications to existing
systems for the jamming environments in which they will operate.
In addition, the results provide information for choosing
jamming waveforms and strategies for attacking the communica-
tion systems of an enemy.

Computer simulations, and controlled field and laboratory
measurements are very useful and necessary to confirm and
verify theoretical results. To the extent possible, however,
theoretical susceptibility analyses should be carried out.
These require accurate mathematical models of the system and
the operating environment. It would, of course, be desirable
to be able to determine an "optimum" system for a particular

environment, and to find an "optimum" jamming waveform/
strategy for a particular system. It is not feasible at this
time to obtain such general analytical results which hold for
all possible modulation methods, spread-spectrum techniques,
jamming waveforms and strategies, etc. Nor is it feasible
to attempt analysis for interference environments which
simultaneously encompass jamming, multipath, noise, distortions,
nuclear effects, inter-symbol interference, fading, mutual
interference, etc. The approach taken in this study involved
selecting a variety of modulation methods, the most common
spreading techniques, and representative jamming waveforms,
with susceptibility evaluations carried out for these cases.
Emphasis here is on jamming, but background noise is also in-
cluded in all cases, to provide performance bounds and means
for comparisons.

2.0 Discussion of Results for Binary FH/DS NCFSK and DPSK

These very complete and detailed results, described in
the earlier report, are significant in two ways. Their
greatest significance lies in the analytical approaches taken,
as they provide the basis for similar investigations for other
systems. Many of the noise, signal, and jamming models are
the same as needed for other studies. The approach of first
finding "building block" error probabilities which do not
incorporate spread-spectrum effects is a key one. These are
then appropriately modified to incorporate frequency-hopping,

direct-sequence spreading, and hybrid FH/DS spreading. The
other main point of significance is noted from sample curves
presented earlier. For convenience in this discussion, one
of these sets is reproduced here--Figure 1, for partial-band
tone jamming of frequency-hopped binary NCFSK. For a basis
of comparison, the set includes the non-hopped case ($N_s = 2$)
and an example of hopping ($N_s = 1000$). Several representative
cases of the partial-band strategy are included ($K_s = 1, 2, 100, 500, 1000$).

Some very interesting points can be observed for this
sample set. For example, with frequency-hopping based on a
factor of 500 increase in bandwidth (1000 frequency slots
instead of 2 required for binary FSK), a "processing gain" of
27dB results. However, the actual "gain" is very much depen-
dent upon the partial-band strategy adopted by the jammer and
upon the value of error-probability which represents the
"jammed" condition for a particular system. Some highly
critical systems may, for example, have their effectiveness
significantly reduced even for a relatively low error rate.
On the other hand, there are other systems which can tolerate
much higher error-rates before losing effectiveness. Let us
now look at the case of 10^{-4} for the error-probability of
significance. Notice that curve A (no frequency-hopping,
both slots have jamming tones) indicates a value of approxi-
mately 8dB for the corresponding S/J power ratio (S is aver-
age signal power and J is total average jamming power). For
frequency hopping over 1000 slots and jamming tones now in
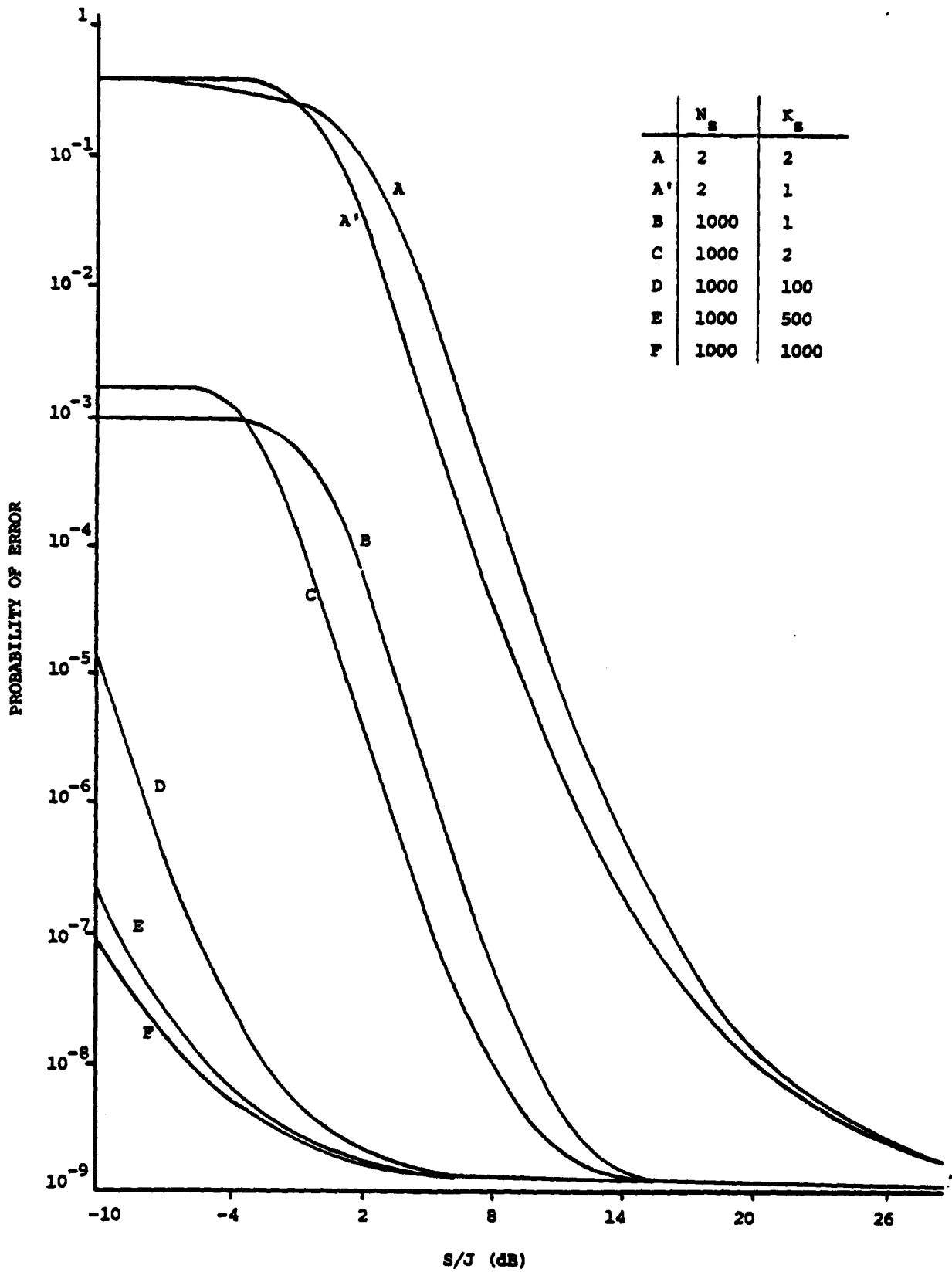
FIG. 1. TONE JAMMING (S/N = 16 dB)

all of these (curve F), the value of S/J is approximately -19dB. Thus, for the same value of S, a jammer must supply 27 dB of additional power, but only if he chooses to spread his energy into all frequency slots. This is the only case for which "process gain" has meaning with frequency-hopping. Choosing frequency hopping as the spread-spectrum technique does not alone force the jammer into spreading his energy over the entire band. Suppose, for this example, that he instead chooses to concentrate his energy into one slot at a time (perhaps on a hopping basis also). Curve B then is the appropriate one, showing a value of approximately 1 dB for S/J. Comparison with curve A', which also represents one plot jammed but without an increase in N_s, shows only about 6 dB as the "actual gain." Comparison again with curve A shows approximately 7 dB as the gain attributable to frequency-hopping. For this strategy the jammer increases the peak power of his transmission. There are, of course, many strategies in between those of curves B and F, with curves C, D, and E being representative. The jammer thus, at least conceptually, has the ability to adopt partial-band strategies which involve some increase in peak power and/or average power and reduce the actual gain provided by frequency-hopping to a value, in decibels, which may be much lower than that indicated by the "process-gain" rule-of-thumb value.

Note another effect, however, Curve B reaches a plateau at a lower level than curve C, which in turn has a

lower maximum probability-of-error than curve D, etc. Thus,
if the tolerable error rate is higher than the maximum
allowed by curve B (perhaps due to added error-correcting
coding), a jammer is then forced to operate on another curve
and the actual "gain" is increased. In conclusion, it is
apparent from this set of curves which are based on the ana-
lytical results given, that "process gain" may not be of
great significance when referring to frequency-hopping, due
to the wide number of possibilities open for use by a jammer,
with corresponding actual "gains" which vary over a wide range.
Many trade-offs are involved, whose understanding requires
results such as these.

A similar sample set of curves for FH/DS binary DPSK is
given in Figure 2. These are for the noise jamming case, with
parameter values as shown on the graph. Similar conclusions
result for these curves as in the FSK set. The analytical
results for binary FH/DS DPSK reported earlier provide the
basis for generating similar curves for all significant choices
of the underlying parameters.

We now generalize these binary results to the more general
M-ary cases. This is given in the next sections.

3.0 M-ary FH/DS NCFSK

The analysis of partial-band noise or CW-tone jamming for
hybrid frequency-hopped/direct-sequence-spread M-ary NCFSK
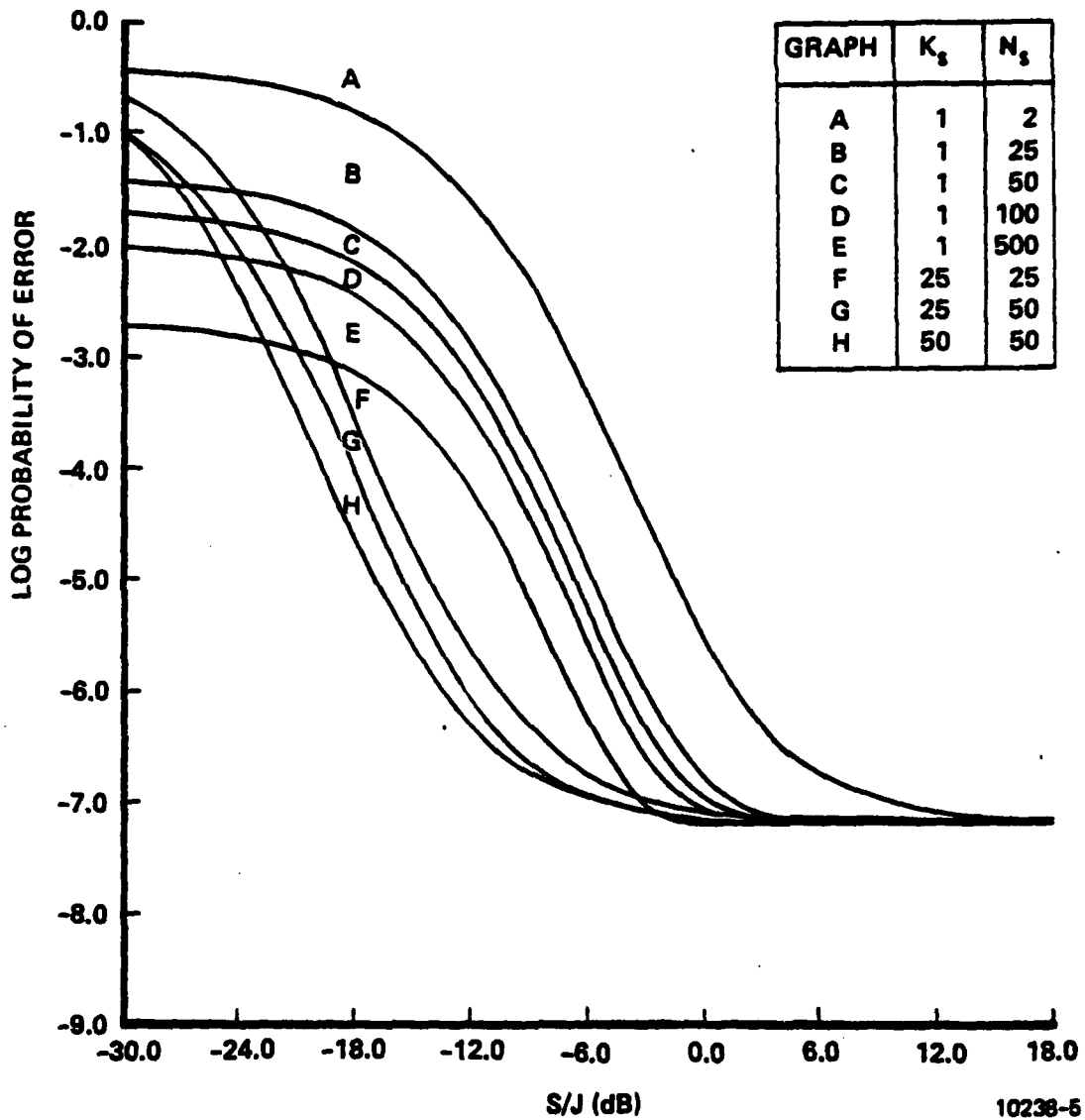utilizes the same approach which proved useful in the binary

Figure 2 . Dependence of the Log Probability of Error Versus S/J on $\bar{N}_s$ and K_s ($1 \leq K_s \leq 50$): DS/FH, Binary DPSK; Noise Jamming; S/N = 12 dB, R_c/R_i = 31

cases described earlier. Some of these results were described in a recent paper by Pettit [3].

Because of requirements to increase the number of information bits per second per Hertz of bandwidth, higher-order-alphabet systems are being used or planned for. This makes it necessary to derive methodology which permits the same type of extensive susceptibility investigations as was made possible for those binary cases. Since the signal, system and noise models for M-ary NCFSK are straightforward extensions of those adopted for the binary case, no additional elaboration on these points is given. Instead, we will concentrate in this section on the analytical steps taken in deriving the methodology, and on the final results concerning probability of symbol-error as a function of important system and environment parameters. The basic receiver is modeled as M parallel branches, each consisting of a bandpass filter (centered at the M signaling frequencies, respectively) and envelope detector. (This is, of course, the de-spread portion of the receiver.) The receiver's output is based on which detector has the largest value at the sampling time (every T_b seconds).

Two discrete probabilities are needed in order to account for frequency-hopping effects. We again let N_s be the total number of frequency slots available for the pseudo-random selection of M (M $\leq$ N_s) for signaling (one of the M is selected according to the data to be transmitted). Also, we let K_s

be the number of frequency slots which contain jamming signals, with $1 \leq K_s \leq N_s$. If j represents the number out of K_s that overlap the M signaling slots, the two required discrete probabilities are given below.

$$P \left\{ \begin{array}{l} j \text{ of } K_s \text{ overlap the M signaling slots and none} \\ \text{of the j is in the data slot} \end{array} \right\}$$

$$= P_{jo}$$

$$= \frac{\dfrac{N_s!(M-j)}{j!(K_s-j)!(M-j)!(N_s-M-K_s+j)!M}}{\begin{pmatrix} N_s \\ K_s \end{pmatrix} \cdot \begin{pmatrix} N_s \\ M \end{pmatrix}} \tag{1}$$

Also,

$$P \left\{ \begin{array}{l} j \text{ of } K_s \text{ overlap the M signaling slots and one} \\ \text{of the j is in the data slot} \end{array} \right\}$$

$$= P_{j1}$$

$$= \frac{\dfrac{N_s!j}{j!(K_s-j)!(M-j)!(N_s-M-K_s+j)!M}}{\begin{pmatrix} N_s \\ K_s \end{pmatrix} \cdot \begin{pmatrix} N_s \\ M \end{pmatrix}} \tag{2}$$

In the above, $\binom{a}{b}$ represents the binomial coefficient given by $\dfrac{a!}{b!(a-b)!}$.

From (1) and (2), and the total-probability formula, the symbol error-probability for frequency-hopping is given by

$$P(err) = \sum_{j=j_{min}}^{j_{max}} \left\{ P_{jo} \cdot P(err \mid none\ of\ j\ in\ data\ slot) \right.$$

$$\left. + P_{ji} \cdot P(err \mid one\ of\ j\ in\ data\ slot) \right\}$$

(3)

where j_{max} is the smaller of M and K_s, and j_{min} is zero for $N_s - K_s \geq M$ and j_{min} is $M + K_s - N_s$ for $N_s - K_s < M$.

The determination of the two required conditional probabilities of (3) is based on the recognition that the random variables involved are Rayleigh-Rician mixtures. The rather lengthy mathematical steps required will not be reproduced here, in order that the final results can be emphasized. The two equations are given below.

$P(err \mid none\ of\ j\ in\ data\ slot)$

$$= 1 - \sum_{i=0}^{i} \sum_{\ell=0}^{M-j-1} (-1)^{i+\ell} \cdot \binom{j}{i} \cdot \binom{M-j-1}{\ell} \cdot \left[\frac{N + \frac{J}{K_s}}{(\ell+i+1)N + (\ell+1)\frac{J}{K_s}} \right]$$

(4)

$$\cdot \exp\left[-\frac{S}{N} \left\{ \frac{(\ell+i)N + \ell\frac{J}{K_s}}{(\ell+i+1)N + (\ell+1)\frac{J}{K_s}} \right\} \right]$$

P(err|one of j in data slot)

$$= 1 - \sum_{i=0}^{j-1} \sum_{\ell=0}^{M-j} (-1)^{i+\ell} \cdot \binom{j-1}{i} \binom{M-j}{\ell} \cdot \left[\frac{N}{(\ell+i+1)N + \ell \frac{J}{K_s}} \right] \cdot$$

(5)

$$\cdot \exp \left[-\left\{ \frac{S}{N+\frac{J}{K_s}} \cdot \frac{(\ell+i)N + \frac{J}{K_s}}{(\ell+i+1)N + \ell\frac{J}{K_s}} \right\} \right]$$

A compact form for the error-probability of interest in this frequency-hopping case is given by

P(err) = P_e(MNCFSK, PB-Noise, FH)

$$= 1 - \frac{N_s!}{M \cdot \binom{N_s}{K_s} \cdot \binom{N_s}{M}} \cdot \sum_{j=j_{min}}^{j_{max}} \left\{ \frac{(M-j)(N+\frac{J}{K_s})}{g(j;K_s,M,N_s)} \cdot f_1(j;K_s,M,S,N,J) \right.$$

(6)

$$\left. + \frac{j \cdot N}{g(j;K_s,M,N_s)} \cdot f_2(j;K_s,M,S,N,J) \right\}$$

where the following definitions apply:

$$g(j;K_s,M,N_s) = j! \, (K_s-j)! \, (M-j)! \, (N_s-M-K_s+j)!$$

(7)

$$f_1(j;K_s,M,S,N,J)$$

$$= \sum_{i=0}^{j} \sum_{\ell=0}^{M-j-1} (-1)^{i+\ell} \cdot \frac{\begin{bmatrix} j \\ i \end{bmatrix} \cdot \begin{bmatrix} M-j-1 \\ \ell \end{bmatrix}}{(\ell+i+1)N + (\ell+1)\frac{J}{K_s}}$$

(8)

$$\cdot \exp\left[-\frac{S}{N} \left\{ \frac{(\ell+i)N + \ell\frac{J}{K_s}}{(\ell+i+1)N + (\ell+1)\frac{J}{K_s}} \right\} \right]$$

$$f_2(j;K_s,M,S,N,J)$$

$$= \sum_{i=0}^{j-1} \sum_{\ell=0}^{M-j} (-1)^{i+\ell} \cdot \frac{\begin{bmatrix} j-1 \\ i \end{bmatrix} \cdot \begin{bmatrix} M-j \\ \ell \end{bmatrix}}{(\ell+i+1)N + \ell\frac{J}{K_s}}$$

(9)

$$\cdot \exp\left[-\left(\frac{S}{N+\frac{J}{K_s}} \right) \left\{ \frac{(\ell+i)N + \ell\frac{J}{K_s}}{(\ell+i+1)N + \ell\frac{J}{K_s}} \right\} \right]$$

The above results provide the means for complete investigation
of the effects of partial-band noise-jamming of M-ary NCFSK.
In order to also incorporate direct-sequence spreading, along
with frequency-hopping for the equations above, it is neces-
sary only that every term $\frac{J}{K_s}$ be replaced by $\frac{J}{K_s} \cdot \frac{R_I}{R_c}$. The
spreading-code "chip" rate is R_c, and R_I is the information-
symbol rate. Thus we have now completed the task of generaliz-
ing to the M-ary NCFSK case to cover noise-jamming. The tone-
jamming case is now discussed.

Equations (1), (2), and (3) still apply, but alternates
to (4) and (5) are required. Again we recognize that the ran-
dom variables are Rayleigh-Rician mixtures, along with uniform
random variables representing the phase angles of the jamming
tones. There is some convenience for this case in treating
correct-symbol probabilities instead of error-probabilities.
The resulting conditional probabilities, given below, could
not be evaluated in closed form, leading to a simplification
in the form of bounds which are tight for the cases of inter-
est.

The equations for frequency hopping are:

P(cor|none of j in data slot)

$$
= \int_0^\infty \frac{r}{N} \cdot \exp\left(-\frac{A_s^2 + r^2}{2N}\right) \cdot I_0\left(\frac{rA_s}{N}\right) \left[1 - Q\left(\frac{A_j}{\sqrt{N}}, \frac{r}{\sqrt{N}}\right)\right]^j \cdot
$$

(10)

$$
\cdot \left[1 - \exp\left(-\frac{r^2}{2N}\right)\right]^{M-j-1} \cdot dr
$$

P(cor|one of j in data slot)

$$
= \frac{1}{\pi} \int_{\theta=0}^\pi \int_{r=0}^\infty \frac{r}{N} \cdot \exp\left(-\left(\frac{r^2 + A_s^2 + 2A_s A_j \cos\theta + A_j^2}{2N}\right)\right) \cdot
$$

(11)

$$
\cdot I_0\left[\frac{r}{N}(A_s^2 + 2A_s A_j \cos\theta + A_j^2)^{\frac{1}{2}}\right] \cdot \left[1 - Q\left(\frac{A_j}{\sqrt{N}}, \frac{r}{\sqrt{N}}\right)\right]^{j-1} \cdot
$$

$$
\cdot \left[1 - \exp\left(-\frac{r^2}{2N}\right)\right]^{M-j} \cdot dr \cdot d\theta
$$

Equations (10) and (11), weighted by (1) and (2), respectively, and summed over j yields P(cor) for this case. Since this produces a somewhat unwieldy expression for computer evaluation which is repeated many times, a simple and accurate approximate solution was sought. The result is based on the fact that the Q-function is a probability, and therefore is a non-negative number which cannot exceed unity. Therefore,

$$\left[1 - Q\left(\frac{A_j}{\sqrt{N}}, \frac{r}{\sqrt{N}} \right) \right]^j \le 1 - \delta \cdot Q\left(\frac{A_j}{\sqrt{N}}, \frac{r}{\sqrt{N}} \right) \qquad (12)$$

where

$$\begin{aligned} &= 0, \quad \text{for } j = 0 \\ &= 1, \quad \text{for } j \ne 0 \end{aligned} \qquad (13)$$

A lower bound for this expression is obtained from Taylor's Series, giving

$$\left[1 - Q\left(\frac{A_j}{\sqrt{N}}, \frac{r}{\sqrt{N}} \right) \right]^j \ge 1 - j \cdot Q\left(\frac{A_j}{\sqrt{N}}, \frac{r}{\sqrt{N}} \right) \qquad (14)$$

(In equation (11), the exponent is j-1 instead of j). The resulting upper-bound expression is

$$P_u(cor) = \sum_{j=j_{min}}^{j_{max}} \sum_{\ell=0}^{M-j-1} P_{jo} \cdot \frac{(-1)^\ell}{\ell+1} \cdot \binom{M-j-1}{\ell} \cdot \exp\left[-\left(\frac{\ell}{\ell+1}\right) \frac{S}{N}\right] \cdot$$

$$\cdot f_3(\ell;\delta,K_S,S,N,J)$$

(15)

$$+ \sum_{j=j_{min}}^{j_{max}} \sum_{\ell=0}^{M-j} P_{ji} \cdot \frac{(-1)}{\ell+1} \binom{M-j}{\ell} \cdot \exp\left[-\left(\frac{\ell}{\ell+1}\right)\left(\frac{S}{N} + \frac{J}{K_S N}\right)\right]$$

$$\cdot \frac{1}{\pi} \int_{\theta=0}^{\pi} \exp\left[-\left(\frac{2\ell}{\ell+1}\right)\left(\frac{S}{N} \cdot \frac{J}{K_S N}\right)^{\frac{1}{2}} \cos\theta\right] \cdot f_4(\ell;\delta_1,\theta,K_S,S,N,J) \cdot d\theta$$

For the above

$$\delta = 0, \quad \text{for } j = 0 \tag{16}$$
$$= 1, \quad \text{for } j > 0$$

and

$$\delta_1 = 0, \quad \text{for } j = 1 \tag{17}$$
$$= 1, \quad \text{for } j > 1$$

Also

$$f_3(\ell;\delta,K_S,S,N,J)$$

$$= 1 - \delta \cdot \left\{ \left(\frac{1}{\ell+2}\right) \cdot \left[1-Q\left\{\left[\frac{2}{(\ell+1)(\ell+2)} \cdot \frac{S}{N}\right]^{\frac{1}{2}}, \left[\frac{2(\ell+1)}{(\ell+2)K_S} \cdot \left(\frac{J}{N}\right)\right]^{\frac{1}{2}}\right\}\right] \right.$$

(18)

$$\left. + \left(\frac{\ell+1}{\ell+2}\right) \cdot Q\left\{\left[\frac{2(\ell+1)}{(\ell+2)K_S} \cdot \left(\frac{J}{N}\right)\right]^{\frac{1}{2}}, \left[\frac{2}{(\ell+1)(\ell+2)} \cdot \left(\frac{S}{N}\right)\right]^{\frac{1}{2}}\right\}\right\}$$

and

$$f_4(\ell; \delta_1, \theta, K_S, S, N, J)$$

$$= 1 - \delta_1 \cdot \left\{ \left(\frac{1}{\ell+2}\right) \cdot \left[1 - Q \left\{ \left[\frac{2}{(\ell+1)(\ell+2)} \cdot \left(\frac{S}{N} + \frac{2}{\sqrt{K_S}} \left[\frac{S}{N} \cdot \frac{J}{N} \right]^{\frac{1}{2}} \cos\theta + \frac{J}{K_S N} \right) \right]^{\frac{1}{2}}, \right. \right. \right.$$

$$\left. \left[\frac{2(\ell+1)}{(\ell+2)K_S} \cdot \left(\frac{J}{N} \right) \right]^{\frac{1}{2}} \right\} \right]$$

(19)

$$+ \left(\frac{\ell+1}{\ell+2}\right) \cdot Q \left\{ \left[\frac{2(\ell+1)}{(\ell+2)K_S} \cdot \left(\frac{J}{N} \right) \right]^{\frac{1}{2}}, \right.$$

$$\left. \left. \left[\frac{2}{(\ell+1)(\ell+2)} \cdot \left(\frac{S}{N} + \frac{2}{\sqrt{K_S}} \left[\frac{S}{N} \cdot \frac{J}{N} \right]^{\frac{1}{2}} \cos\theta + \frac{J}{K_S N} \right) \right]^{\frac{1}{2}} \right\} \right\}$$

To obtain P_L(cor), the lower bound, use equation (15) except replace δ by j in (18), and replace δ_1 by j-1 in (19). That is,

$$P_L(\text{cor}) = P_u(\text{cor}) \Big|_{\substack{\text{let } \delta = j \\ \delta_1 = j-1}}$$

As before, to modify the above frequency-hopping results to accommodate FH/DS, merely replace $\frac{J}{K_S}$ by $\frac{J}{K_S} \cdot \frac{R_I}{R_c}$. This completes the development and discussion for M-ary FH/DS NCFSK. In the next section we will summarize corresponding results for M-ary FH/DS DPSK.

4.0 M-ary FH/DS DPSK

The susceptibility analysis for this case is very complex
[2]. Additional complications arise due to the two time-inter-
vals which must be considered with DPSK, one providing the
phase reference for the other. Even though more-exact ex-
pressions can be found for the special binary and quaternary
cases, the emphasis here is on a general set of results which
hold for M-ary signaling. For tractable results, upper and
lower bounds for symbol-error probability were found, with de-
tails provided in [2]. Since the bounds are also very complex
analytical expressions, it is not clear that they can efficient-
ly be used, in the way that those for NCFSK can, for extensive
parametric studies and system optimization. Instead, it is
recommended that this remain an open area for additional ana-
lytical effort in any future methodology developments. As a
result of the above, no further comments for this case are
given. Instead, in the next section are represented new results
for the very important MSK case.

5.0 FH/DS MSK

Minimum Shift Keying has been adequately described in the
earlier interim reports, along with certain of its properties
which make it a leading candidate for army tactical multichannel
systems of the 1980's. The emphasis of this section remains
that of vulnerability analysis.

In order to fix some of the notation to be used in the

following analysis, the MSK receiver will be briefly described, and error probability will be re-derived for a white-noise environment. This will be followed by the derivation of certain "building-block" probabilities that apply to the noise-jamming and tone-jamming cases. This, in turn, leads to the desired results for the frequency-hopped (both "fast" and "slow" cases, and, finally, the FH/DS hybrid-spread cases.

The MSK signal is given by

$$s(t) = A_s \cdot d(K-1) \cdot \cos \frac{\pi t}{2T_b} \cdot \cos \omega_c t$$

$$+ A_s \cdot d(K) \cdot \sin \frac{\pi t}{2T_b} \cdot \sin \omega_c t \quad , \quad o < t < T_b$$

$$\tag{20}$$

$$= A_s \cdot d(K) \cdot \cos \frac{\pi t}{2T_b} \cdot \cos \omega_c t$$

$$+ A_s \cdot d(K+1) \cdot \sin \frac{\pi t}{2T_b} \cdot \sin \omega_c t \quad , \quad T_b < t < 2T_b$$

where $d(K-1)$, $d(K)$, $d(K+1)$ are three consecutive data symbols. The receiver processing involves multiplying the incoming waveform (signal, noise, jamming) by $2\sin \frac{\pi t}{2T_b} \cdot \sin \omega_c t$ during $o < t < T_b$ and by $2 \cos \frac{\pi t}{2T_b} \cdot \cos \omega_c t$ during $T_b < t < 2T_b$, followed by integration and sampling. The assumed white-noise component at the input has single-sided spectral density η.

First we consider, for completeness and for reference to the later results, the white-noise only case (no jamming, no spreading). For the first interval, the correlator's output

is directly shown to be

$$Y_1(T_b) = \frac{A_s T_b}{2} \cdot d(K) + n_1(T_b) \tag{21}$$

with $n_1(t)$ zero mean, Gaussian, with variance $\eta \frac{T_b}{2}$.
The output for the second interval is similarly seen to be

$$Y_2(2T_b) = \frac{A_s T_b}{2} \cdot d(K) + n_2(2T_b) \tag{22}$$

with $n_2(t)$ also zero-mean, Gaussian, variance $\eta \frac{T_b}{2}$, and
independent of $n_1(t)$. The total signal component is $A_s T_b \cdot d(K)$
and the total noise is $n_T(t) = n_1(t) + n_2(t)$.

Probability-of-error for this case follows immediately,
and is

$$P(err) = P_r[A_s T_b < n_T]$$

$$= \frac{1}{\sqrt{2 \pi \sigma_T^2}} \int_{A_s T_b}^{\infty} e^{-\frac{x^2}{2\sigma_T}} \cdot dx$$

$$= \frac{1}{2} \, erfc \left[\frac{A_s^2 T_b^2}{2 \sigma_T^2} \right]^{\frac{1}{2}} \tag{23}$$

$$= \frac{1}{2} \, erfc \left[\frac{E_b}{\eta} \right]^{\frac{1}{2}}$$

$$= \frac{1}{2} \, erfc \left[\frac{S}{N} \right]^{\frac{1}{2}}$$

The following "building-block" probabilities, based on (23), are listed for later use in considering spectrum-spreading.

(a) Jamming misses both time-intervals

$$P_{ao} = \frac{1}{2} \text{ erfc } \left[\frac{S}{N}\right]^{\frac{1}{2}} \tag{24}$$

(b) Jamming (in equal amounts of power) hits both intervals

$$P_{a2} = \frac{1}{2} \text{ erfc } \left[\frac{S}{N+J_s}\right]^{\frac{1}{2}}$$

$$= \frac{1}{2} \text{ erfc } \left[\frac{\left(\frac{S}{N}\right)\left(\frac{S}{J_s}\right)}{\left(\frac{S}{N}\right) + \left(\frac{S}{J_s}\right)}\right]^{\frac{1}{2}} \tag{25}$$

(J_s is the average jammer power per frequency slot.)

(c) Jamming hits only one of the two time intervals

$$P_{a1} = \frac{1}{2} \text{ erfc } \left[\frac{S}{N + J_{s/2}}\right]^{\frac{1}{2}}$$

$$= \frac{1}{2} \text{ erfc } \left[\frac{2\left(\frac{S}{N}\right)\left(\frac{S}{J_s}\right)}{\left(\frac{S}{N}\right) + 2\left(\frac{S}{J_s}\right)}\right]^{\frac{1}{2}} \tag{26}$$

The effects of frequency hopping are accounted for by weighting these probabilities by appropriate discrete probabilities. The weights, assuming that the jammer is also hopping, are

(a) $\quad P(\text{Misses Both}) = \left(\dfrac{N_s - K_s}{N_s}\right)^2 = P_H(0)$ \hfill (27)

(b) $\quad P(\text{Hits Both}) = \left(\dfrac{K_s}{N_s}\right)^2 = P_H(2)$ \hfill (28)

(c) $\quad P(\text{Hits One}) = \dfrac{2K_s(N_s - K_s)}{N_s^2} = P_H(1)$ \hfill (29)

If the jammer is not hopping, the weights are

(a) $\quad P(\text{Misses Both}) = \dfrac{(N_s - K_s)(N_s - K_s - 1)}{N_s(N_s - 1)} = P_H'(0)$ \hfill (30)

(b) $\quad P(\text{Hits Both}) = \dfrac{K_s(K_s - 1)}{N_s(N_s - 1)} = P_H'(2)$ \hfill (31)

(c) $\quad P(\text{Hits One}) = \dfrac{2K_s(N_s - K_s)}{N_s(N_s - 1)} = P_H'(1)$ \hfill (32)

Therefore, for partial-band noise-jamming of FH-MSK, we have

$$P(\text{err}) = P_H(0) \cdot P_{ao} + P_H(2) \cdot P_{a2} + P_H(1) \cdot P_{a1} \tag{33}$$

or

$$P(\text{err}) = P_H'(0) \cdot P_{ao} + P_H'(2) \cdot P_{a2} + P_H'(1) \cdot P_{a1} \tag{34}$$

with jammer hopping or not-hopping, respectively.

For a "slow" frequency-hopping case, we need consider

only two discrete probability weights:

(a) P(Misses Both) $= \dfrac{N_s - K_s}{N_s} = P_H''(0)$ (35)

(b) P(Hits Both) $= \dfrac{K_s}{N_s} = P_H''(2)$ (36)

The result for this case is

$$P(\text{err}) = P_H''(0) \cdot P_{a0} + P_H''(2) \cdot P_{a2} \tag{37}$$

We now derive similar results for tone-jamming. The first case of interest concerns a jamming tone which is centered at one of the two signaling frequencies and which is present for only one of the two tone-intervals. The jamming waveform is

$$\begin{aligned} j(t) &= A_j \cos\left(\omega_c t - \frac{\pi t}{2T_b} + \theta\right), & 0 < t < T_b \\ &= 0 &, & T_b < t < 2T_b \end{aligned} \tag{38}$$

with θ uniform $(0, 2\pi)$. The following result also holds for the jamming tone being the larger frequency of the two signaling frequencies. The correlator output, due to this $j(t)$, is seen to be

$$\frac{A_j T_b}{\pi} (\pi^2 + 4)^{\frac{1}{2}} \cdot \cos\theta. \quad \text{This leads to}$$

$$P(err) = P_r\left[n_T > A_s T_b + \frac{A_j T_b}{2\pi}(\pi^2+4)^{\frac{1}{2}} \cdot \cos\theta\right]$$

(39)

$$= E\left\{\frac{1}{2} \text{erfc}\left[\left(\frac{S}{N}\right)^{\frac{1}{2}} + \left(\frac{J_s}{N}\right)^{\frac{1}{2}} \cdot \frac{(\pi^2+4)^{\frac{1}{2}}}{2\pi}\cos\theta\right]\right\}$$

This is more explicitly written as

$$P'_{b1} = \frac{1}{2\pi}\int_0^\pi \text{erfc}\left[\left(\frac{S}{N}\right)^{\frac{1}{2}} + \frac{\left(\frac{S}{N}\right)^{\frac{1}{2}}}{\left(\frac{S}{J_s}\right)^{\frac{1}{2}}} \cdot \frac{(\pi^2+4)^{\frac{1}{2}}}{2\pi}\cos\theta\right] \cdot d\theta$$

(40)

Before continuing with the general development, we consider that the jamming tone is centered at a frequency half-way between the two signaling frequencies. That is,

$$j(t) = A_j \cos(\omega_c t + \theta) \qquad , \quad 0 < t < T_b$$

$$= \quad 0 \qquad\qquad , \quad T_b < t < 2T_b$$

(41)

The correlator output now becomes $- \dfrac{2A_j T_b}{\pi}\sin\theta$

and the associated error-probability is

$$P_{b1} = \frac{1}{2\pi}\int_0^\pi \text{erfc}\left[\left(\frac{S}{N}\right)^{\frac{1}{2}} + \frac{\left(\frac{S}{N}\right)^{\frac{1}{2}}}{\left(\frac{S}{J_s}\right)^{\frac{1}{2}}} \cdot \frac{2}{\pi}\cos\theta\right] \cdot d\theta$$

(42)

A comparison of P_{b1}' and P_{b1}'' shows that, for equal error-probability, the jammer power for the latter is less, by a factor $\frac{\pi^2 + 4}{16}$, than that required using the first strategy. For the remainder of tone-jamming we will, therefore, assume the latter as the jamming waveforms.

Next we find the "building block" for tones in both intervals. That is,

$$j(t) = A_j \cos(\omega_c t + \theta_1) \qquad , \quad 0 < t < T_b$$

$$= A_j \cos(\omega_c t + \theta_2) \qquad , \quad T_b < t < 2T_b \tag{43}$$

Now the correlator output, due to $j(t)$, is

$\frac{-2A_j T_b}{\pi} (\sin\theta_1 + \cos\theta_2)$, and the error probability is

$$P_{b2} = \frac{1}{2\pi^2} \int_0^\pi \int_0^\pi erfc \left[\left(\frac{S}{N}\right)^{\frac{1}{2}} + \frac{\left(\frac{S}{N}\right)^{\frac{1}{2}}}{\left(\frac{S}{J_s}\right)^{\frac{1}{2}}} \cdot \frac{2}{\pi} (\cos\theta_1 + \cos\theta_2) \right] d\theta_1 \cdot d\theta_2 \tag{44}$$

Therefore, for partial-band tone jamming of FH-MSK, we have

$$P(err) = P_H(0) \cdot P_{a0} + P_H(2) \cdot P_{b2} + P_H(1) \cdot P_{b1} \tag{45}$$

or

$$P(err) = P_H'(0) \cdot P_{a0} = P_H'(2) \cdot P_{b2} + P_H'(1) \cdot P_{b1} \tag{46}$$

with jammer hopping or not-hopping, respectively.

Again, we treat separately the "slow hop" case, whereby

$$j(t) = A_j \cos(\omega_c t + \theta) \quad , \quad 0 < t < 2T_b \tag{47}$$

Now the correlator's output is $\dfrac{-2A_j T_b}{\pi} (\sin\theta + \cos\theta)$,

and the error probability is

$$P_{c2} = \frac{1}{2\pi} \int_{0}^{\pi} \mathrm{erfc} \left[\left(\frac{S}{N}\right)^{\frac{1}{2}} + \frac{\left(\frac{S}{N}\right)^{\frac{1}{2}}}{\left(\frac{S}{J_s}\right)^{\frac{1}{2}}} \cdot \frac{2\sqrt{2}}{\pi} \cos\theta \right] \cdot d\theta \tag{48}$$

The result, for partial-band tone-jamming of "slow" FH-MSK, is

$$P(\mathrm{err}) = P_H''(0) \cdot P_{ao} + P_H''(2) \cdot P_{c2} \tag{49}$$

The last step is replacement of $J_s = \dfrac{J}{K_s}$ by $\dfrac{J}{K_s} \cdot \dfrac{R_I}{R_c}$ in equations (33), (34), (37), (45), (46), and (49) to convert them to the FH/DS hybrid-spreading cases.

6.0 Summary and Conclusion

The analytical tools discussed and/or developed here provide the means for very extensive and complete susceptibility analyses of the systems/techniques which are likely candidates for the tactical multichannel system of the 1980s. Conventional NCFSK and DPSK (binary and M-ary), along with the newer MSK, are covered. In the companion report of Telecommunications

Associates, a Gray-Coded QAM was also covered. Spreading includes frequency-hopping and/or direct sequence types. Jamming analyses were performed for representative noise and tone cases, with a partial-band strategy included. While difficult to predict, it seems likely that still other modulation types will also become candidates for tactical applications, as studies progress. Also it is likely that more complex jamming waveforms and/or strategies will require investigation, allowing for good choices from both ECM and ECCM viewpoints. The tools developed here should be programmed on computers for ease in studying system sensitivities and in choosing optimum parameter values.

7.0 <u>References</u>

1. "Adaptive Techniques in Multichannel Transmission,"
Report DAAB07-78-C-0173-0002, January 31, 1979,
S. Consulting Services for U.S. Army CORADCOM.

2. R.A. Yost, "Susceptibility of DS/FH, M-ary DPSK to
Partial and Full-Band Noise, CW-Tone, and Periodic FM
Jamming, Interim Technical Report, February 1978, for
Headquarters, U.S. Air Force, Contract No. F30602-75-
0118.

3. R.H. Pettit, "A Susceptibility Analysis of Frequency-
Hopped M-ary NCFSK--Partial-Band Noise or CW Tone
Jamming," Southeastern Symposium on System Theory,
March 12-13, 1979.

IV.   PROBABILITIES OF ERROR WHEN CHANNEL BANDWIDTH IS FIXED

1.0   Introduction

In [4.1, Chap. IV, of Interim Report 2 (R2)], an analysis was presented which derived the average probability of symbol error for three different direct sequence (DS) spread spectrum systems, one employing BPSK modulation, one employing QPSK, and one employing 16-ary QASK. In all cases, the information rate, total bandwidth, and average transmitted power were held constant. The receiver was a coherent inphase/quadrature detector employing matched filter detection, and perfect carrier, bit, and chip synchronization was assumed. The systems were stressed by the presence of an intentional jammer, and expressions for the probability of error were determined. Two types of jammers were considered, a tone jammer at the center frequency of the signal, and a broadband noise jammer.

In addition to the above direct sequence systems, a noncoherent FSK frequency hopped (FH) system was analyzed in the presence of partial band tone jamming and partial band noise jamming. The FSK-FH system was fairly general in that the MARK and SPACE frequencies were not assumed to be orthogonal. That is, by allowing a certain degree of overlap between the MARK and SPACE channels, more slots over which to hop could be used in a given fixed total bandwidth.

In this chapter, the results of evaluating the probability of error expressions of (4.1, Chap. IV, R2] will be presented and qualitative comparisons will be made between the different

systems. It will be seen that the best DS system is the QPSK system. In addition, while the FSK-FH system performs quite poorly if used without any error-correction coding, once coding is employed the FH system yields results comparable to the DS system.

2.0 M-ary Direct Sequence Spread Spectrum Systems

When the jammer is a single tone located at the carrier frequency of the signal, the appropriate expressions for probability of error are given by Eqs. (62),(66), and (72) of [R2, 4.1, Chap. IV] for noise jamming and by Eqs. (81), (82) and (86) for tone jamming. Figures 4.1-4.14 illustrate how the three systems under consideration perform. The expressions plotted are for symbol error probability, but these can easily be used to provide bit error rate (BER) results. First of all, symbol error rate is an upper bound on BER, since making a symbol error does not necessarily result in every bit comprising that symbol being in error. Indeed, from [4.2],

$$\frac{P_s}{\log_2 M} \leq P_b \leq P_s \tag{4.1}$$

where P_b is the probability of making a bit error, P_s is the probability of making a symbol error, and M is the alphabet size. For high signal-to-noise ratio conditions and Gray encoding [4.3] of bits to symbols, the lower bound of (4.1) is quite tight. However, to be conservative, the BER can always be taken as the upper bound of (4.1).

Fig. 4.1 Tone jammer N=15 J/S=13 db
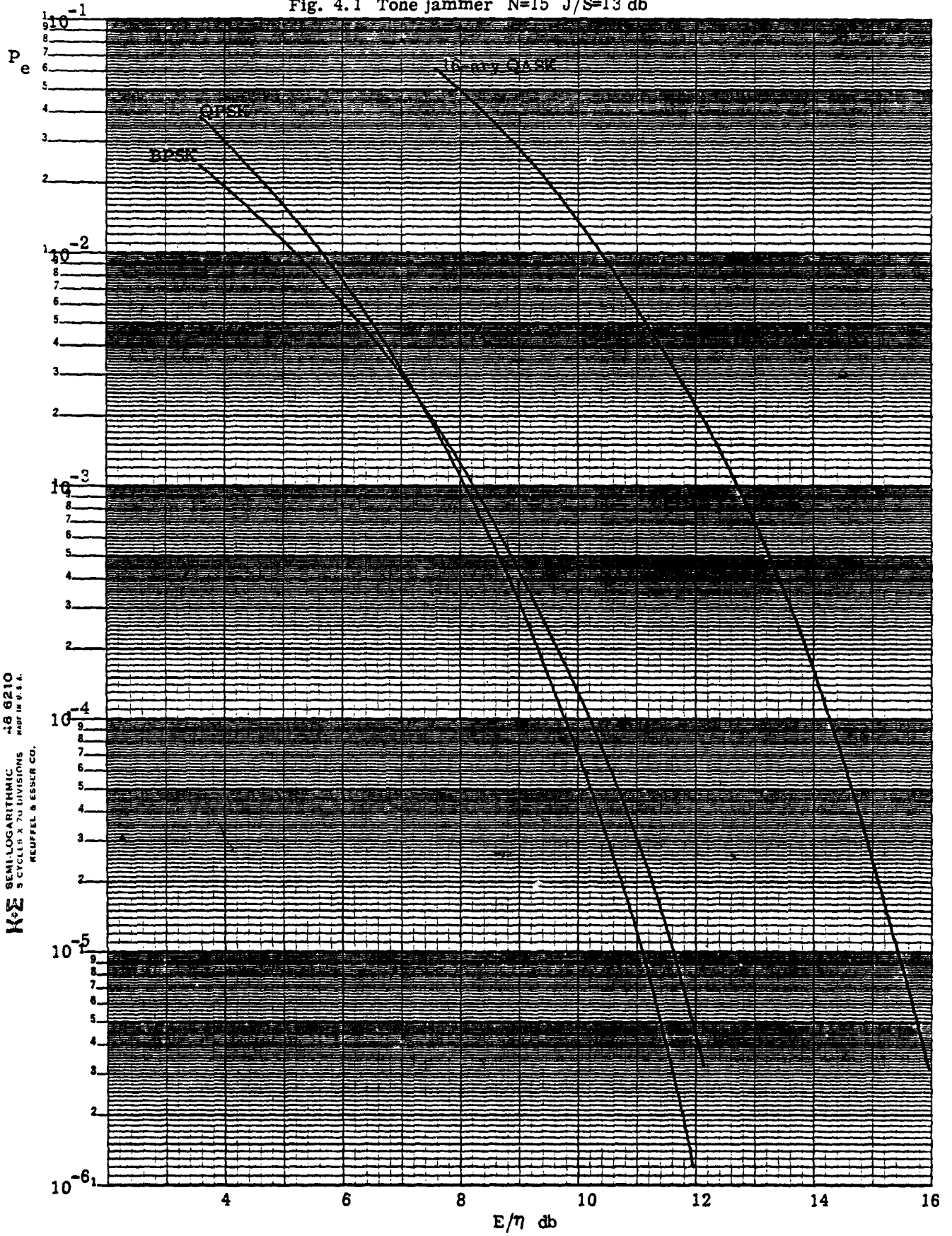
P_e

10^{-1}

10^{-2}

10^{-3}

10^{-4}

10^{-5}

10^{-6}

BPSK

QPSK

16-ary QASK

E/η db

4   6   8   10   12   14   16

Fig. 4.2 Tone jammer N=15 J/S=23 db
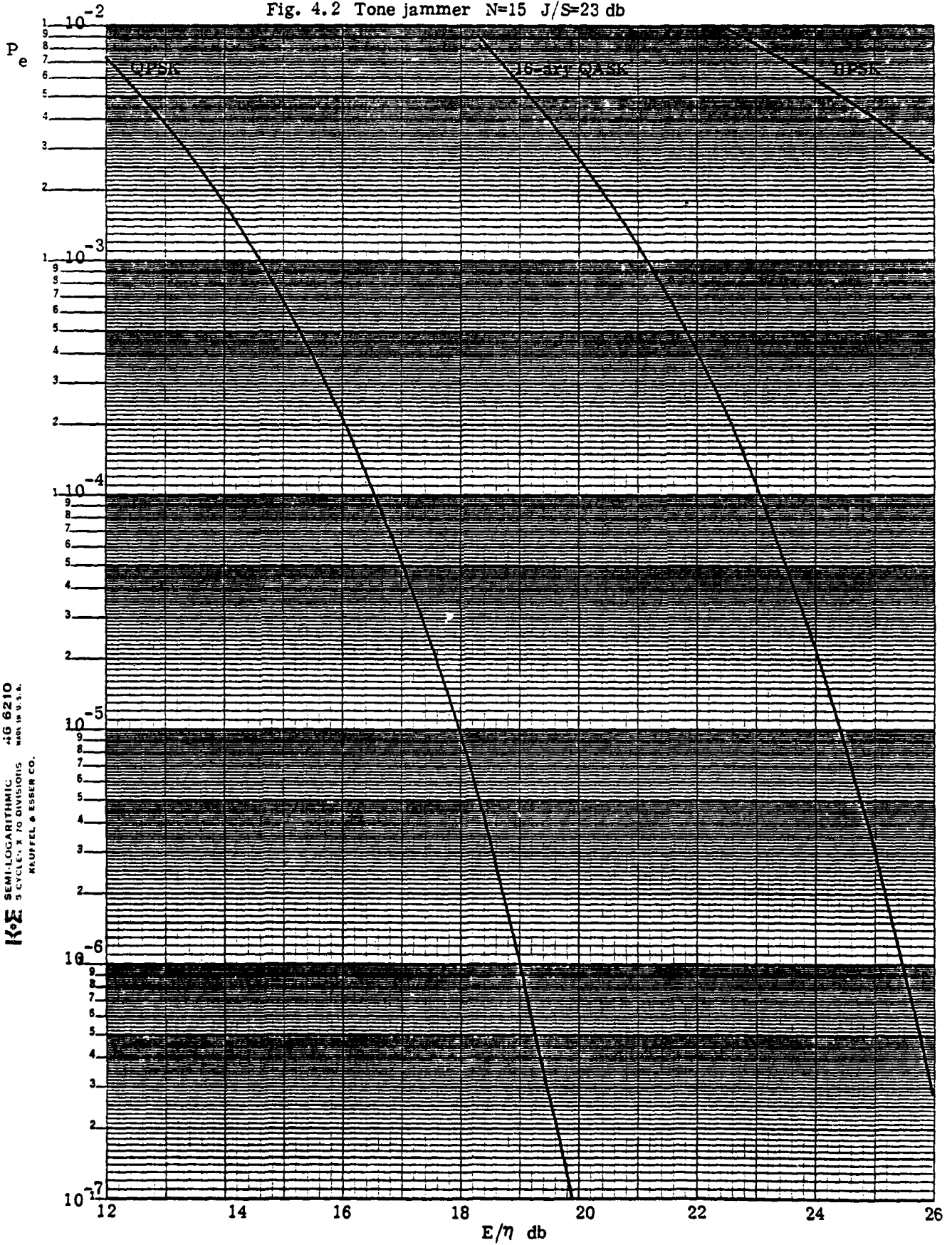
P_e

QPSK

16-ary QASK

QPSK

E/η db

Fig. 4.3 Tone jammer N=255 J/S=43 db
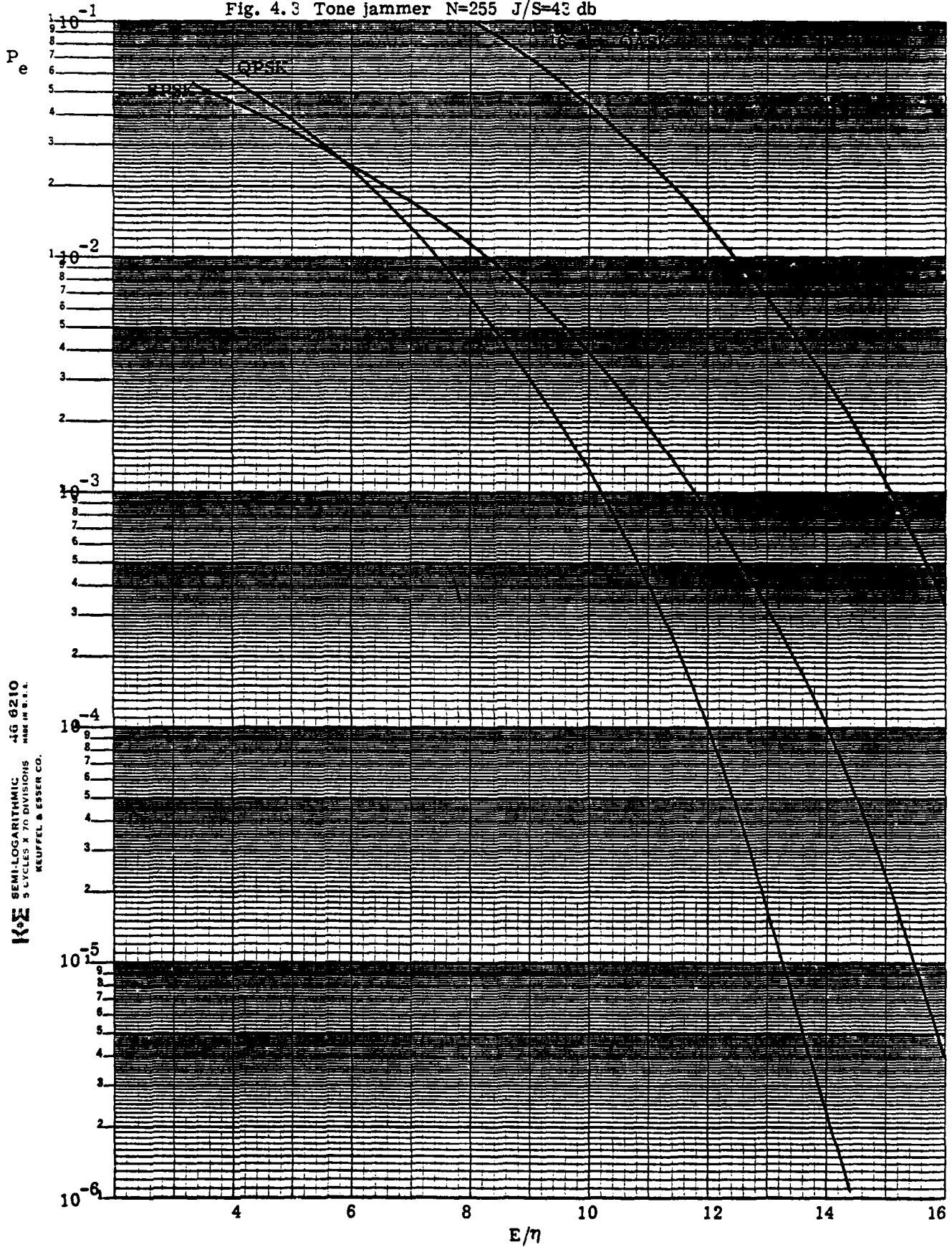
Fig. 4.4   Tone jammer   N=511   J/S=33db

Fig. 4.5 Tone jammer N=511 J/S=43 db

P_e

E/η db

Fig. 4.6   Tone jammer   N=511   J/S=53 db

Fig. 4.7 Tone jammer N=1000 J/S=33 db
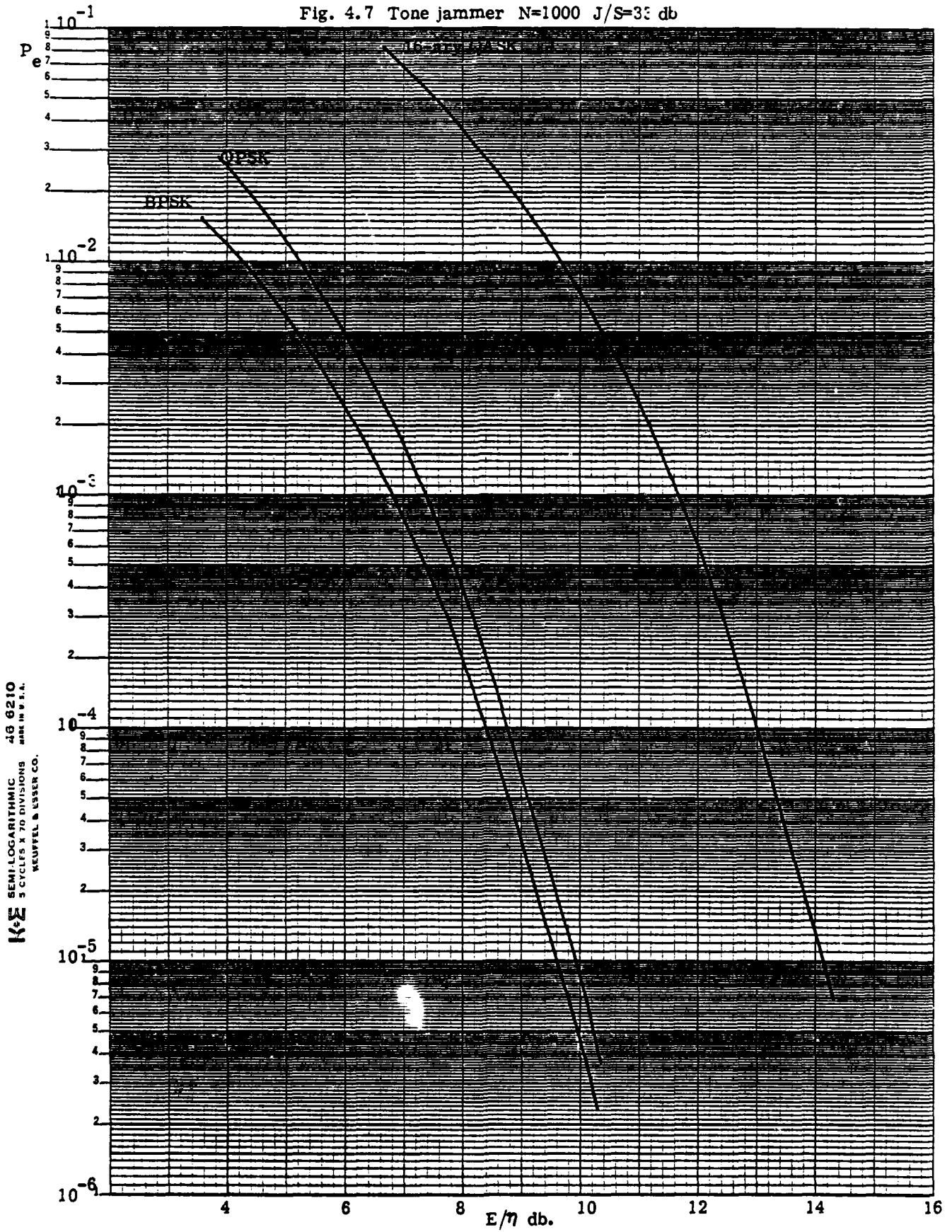
Fig. 4.8 Tone jammer N=1000 J/S=43 db
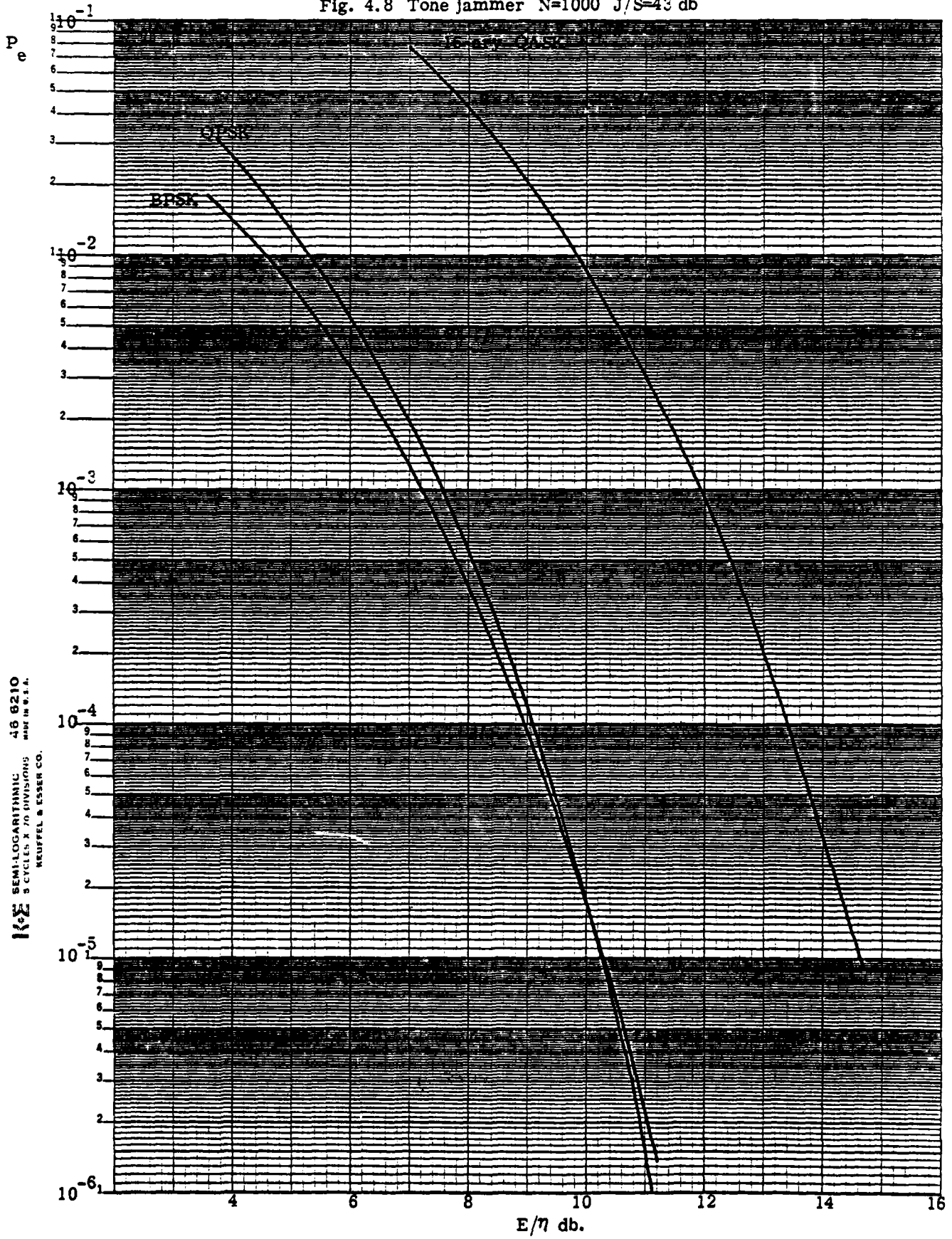
P_e

QPSK

BPSK

E/η db.

Fig. 4.9   Tone jammer   N=1000   J/S=53 db

P_e

E/η db

BPSK

QPSK

16-ary QASK

Fig. 4.10   Noise jammer   N=511   J/S=13 db

Fig. 4.11 Noise jammer N=511 J/S=23 db.

Vertical axis: P_e

Horizontal axis: E/η db.

16-ary Q.SK

QPSK

Fig. 4.12   Noise jammer   N=1000   J/S=13 db
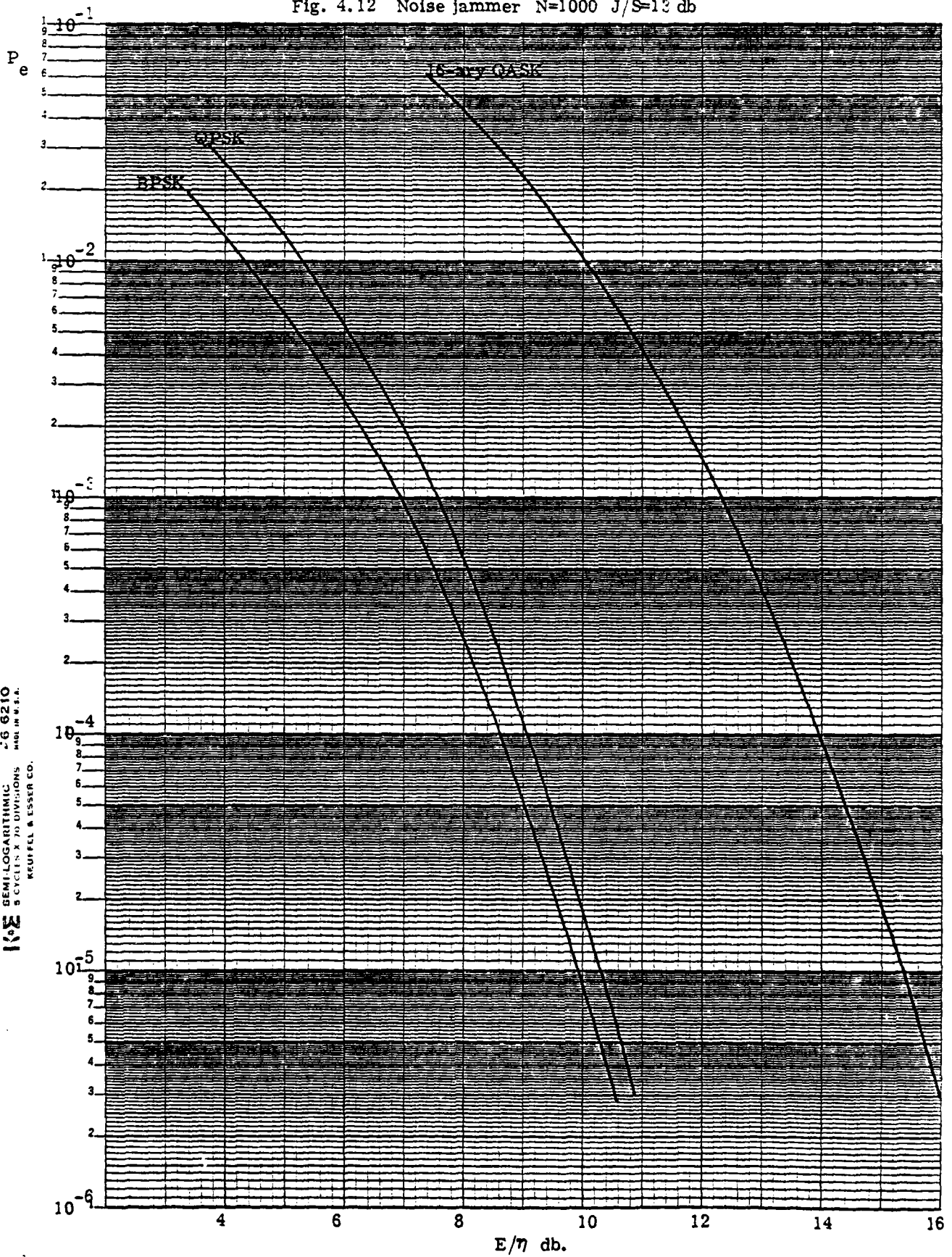
Fig. 4.13   Noise jammer   N=1000   J/S=33 db.

16-ary QASK

DPSK

E/η db
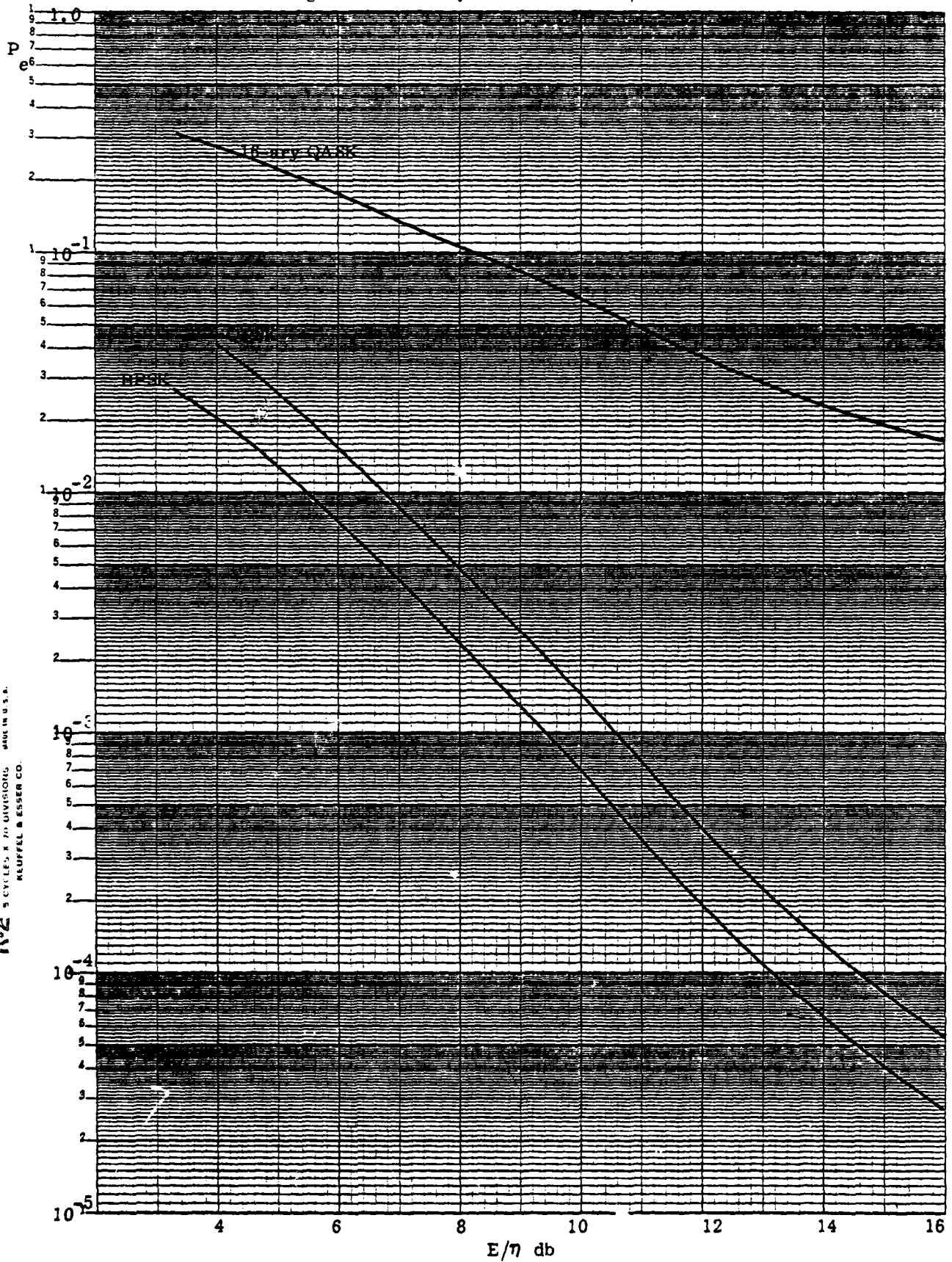
SEMI LOGARITHMIC   46 6210
5 CYCLES X 70 DIVISIONS   MADE IN U.S.A.
KEUFFEL & ESSER CO.

Fig. 4.14   Noise jammer   N=1000   J/S=33 db
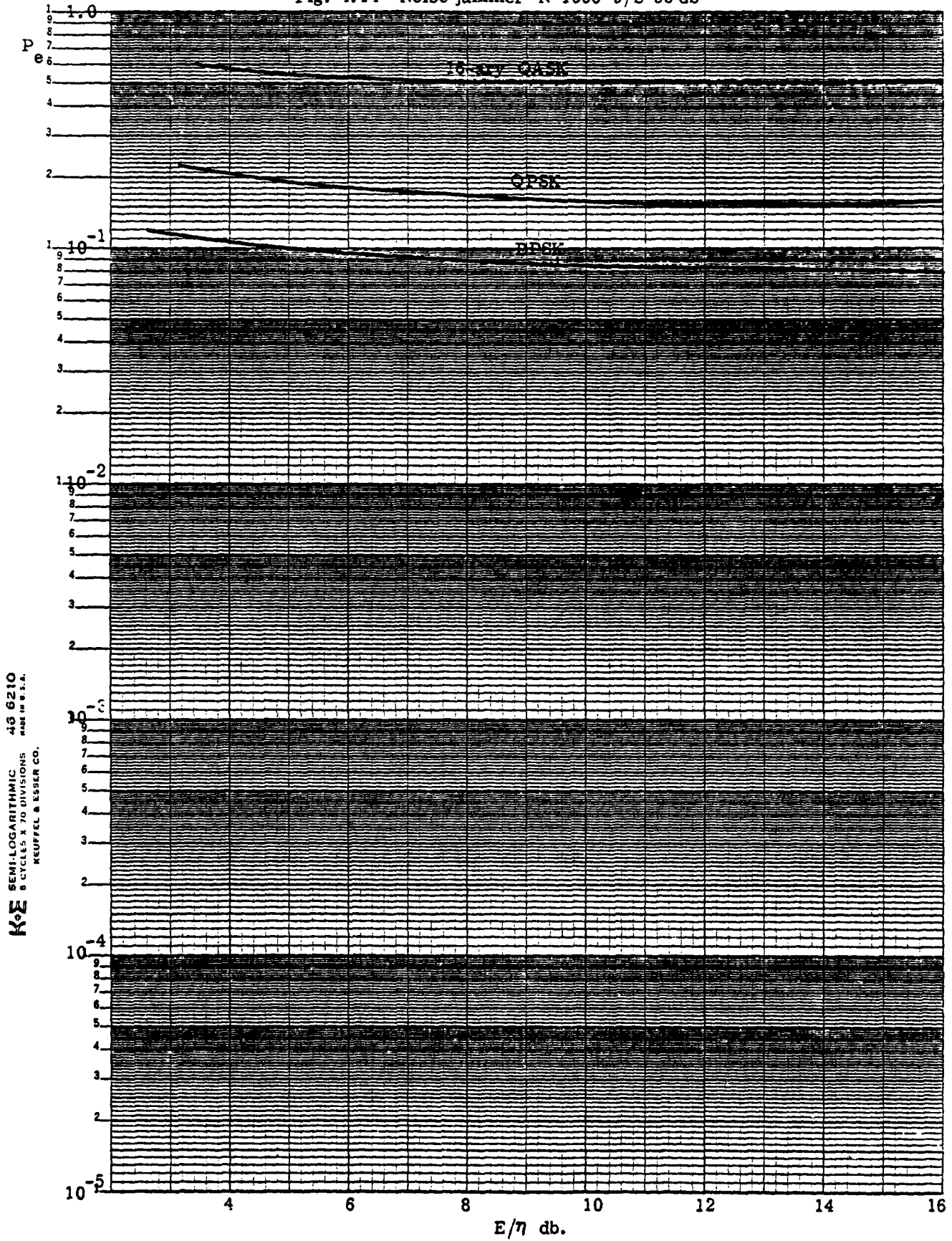
16-ary QASK

QPSK

BPSK

P_e

E/η db.

Let us consider first the effects of tone jamming. The BER for the three systems are shown in Figures 4.1-4.9 for different values of J/S and of processing gain. It can be seen from the figures that when a system is not overly stressed (i.e. when the amount of processing gain is sufficient to significantly attenuate the jammer), BPSK and QPSK perform roughly the same, while 16-ary QASK is noticeably worse. This is to be expected since the 16-ary QASK signal constellation packs the signal points much closer together than do either the BPSK or the QPSK constellations (assuming average power is fixed). Hence the 16-ary system is much more susceptible to errors due to thermal noise.

As the jammer increases in strength, the performance of the 16-ary system eventually surpasses that of the BPSK system due to its larger amount of processing gain in the fixed bandwidth. However, the QPSK system performs the best of the three. That is, while the 16-ary QASK system has 3dB more processing gain with respect to the jammer than does the QPSK system, the QPSK system still has a smaller vulnerability to thermal noise and this latter property proves to be the decisive factor.

Before examining the effects of a noise jammer, one further point should be explained for the tone jammer. For simplicity, the model used in the [4.1] assumed that the frequency of the tone was equal to the carrier frequency of the signal and that furthermore one entire period of the PN

sequence was contained in each data symbol. This allowed exact results to be derived. However, this combination of assumptions leads to very optimistic results of system performance relative to situations in which the period of the PN sequence is much larger than the duration of a data symbol and/or the frequency of the tone jammer is displaced from carrier frequency of the signal by some amount in the vicinity of the symbol rate.

This can be seen quite easily by considering the power that falls within the main lobe of the final integrate-and-dump filter due to the jammer. The power spectrum of a PN sequence N chips in length which has a period of T_1 seconds is given by

$$S(\omega) = \frac{1}{N^2} \delta(\omega) + \frac{N+1}{N^2} \left[\frac{\sin\left(\frac{\omega T_1}{2N}\right)}{\frac{\omega T_1}{2N}} \right]^2 \sum_{\substack{i=-\infty \\ i\neq 0}}^{\infty} \delta\left(\omega - \frac{2\pi i}{T_1}\right) \qquad (4.2)$$

If $T_1 = T$, where T is the duration of a data symbol, then when the frequency of the jammer equals the carrier frequency, only the component of $S(\omega)$ centered at $\omega = 0$ (i.e. $\frac{1}{N^2} \delta(\omega)$ falls in the mainlobe of the integrate-and-dump and hence the power is $\frac{1}{N^2}$. If, however, the jammer's frequency is the carrier frequency plus $\frac{2\pi}{T}$, then the terms of $S(\omega)$ at $\pm \frac{2\pi}{T}$ will fall within the mainlobe and the power contributed by the jammer will then be approximately

$$2\left(\frac{N+1}{N^2}\right) \simeq \frac{2}{N}$$

which is a factor of 2N times as great as what it was when the jammer was at the carrier frequency.

A similar result can be shown to hold almost independently of the jammer's frequency (providing, of course, it is not <u>too</u> far removed from the carrier's frequency) when there are many symbols contained in one period of the PN sequence (in this case N is taken to be the number of chips/symbol, not the number of chips/PN code period). Therefore, for these situations, a reasonable approximation is to use the results of Figures 4.1-4.9 with the J/S ratio changed from whatever it was (say $(J/S)_1$ to $(J/S)_2$, where $(J/S)_2$ is given by

$$(J/S)_2 = (J/S)_1 - 3 - 10 \log_2 N$$

and where all quantities are in dB.

Consider now the effects of a noise jammer. The appropriate figures in this case are Figures 4.10-4.14. At first glance it appears that in this case the BPSK system yields the best result. However, it is well known that in additive white gaussian noise both BPSK and QPSK perform identically if the probability of a bit error (as opposed to a symbol error) is considered. In other words, for this situation, the lower bound of (4.1) should be used with the equality. Notice that in this case, the noise spectral density due to the jammer is the same for all three systems despite the fact that, for example, the data rate of the 16-ary QASK system is only one-fourth that of the BPSK system. This is because the bandwidth

over which the noise jammer spreads its energy is the same in all cases (i.e., the total bandwidth of the system). Hence for equal noise powers, the noise spectral densities must similarly be equal.

The results presented in the figures are meant to illustrate the typical behavior of the systems under different operating conditions. The systems vary from one with very low processing gain (17.6 dB) to one with a processing gain of 30 dB. The following table summarizes the results that are presented in Figures 4.1-4.14.

Finally, for a somewhat different perspective on the same results, consider Figures 4.15-4.18. These figures show the performance of the QPSK system when the processing gain is increased by increments of approximately 3 dB. By comparing Figure 4.15 with Figure 4.16 (or correspondingly Figure 4.17 and 4.18), it is seen that the amount of improvement the system gets by, say, doubling the processing gain is highly dependent on the state of the system (i.e. the combination of J/S, E/η_0, and current processing gain).

## 3.0 Noncoherent Frequency-Shift Keying with Frequency Hopping

The FSK-FH System was evaluated in the presence of partial-band noise jamming and partial-band tone jamming. In particular, the jammer was allowed to jam K out of the N slots the signal could hop over, with K an integer between 1 and N. As in the DS case, the results presented here are based on the equations derived in [R2, 4.1, Chap. IV].

Table 4.1

Figure	Processing Gain	$\frac{J}{S}^*$ (dB)	Type of Jammer
4.1	15	13	Tone
4.2	15	23	Tone
4.3	255	43	Tone
4.4	511	33	Tone
4.5	511	43	Tone
4.6	511	53	Tone
4.7	1000	33	Tone
4.8	1000	43	Tone
4.9	1000	53	Tone
4.10	511	13	Noise
4.11	511	23	Noise
4.12	511	13	Noise
4.13	1000	23	Noise
4.14	1000	33	Noise

*Assuming that the tone jammer frequency equals the carrier
frequency of the signal and that the entire period of the
spreading code is contained in one data symbol

Fig. 4.15 Tone jammer J/S=33 db
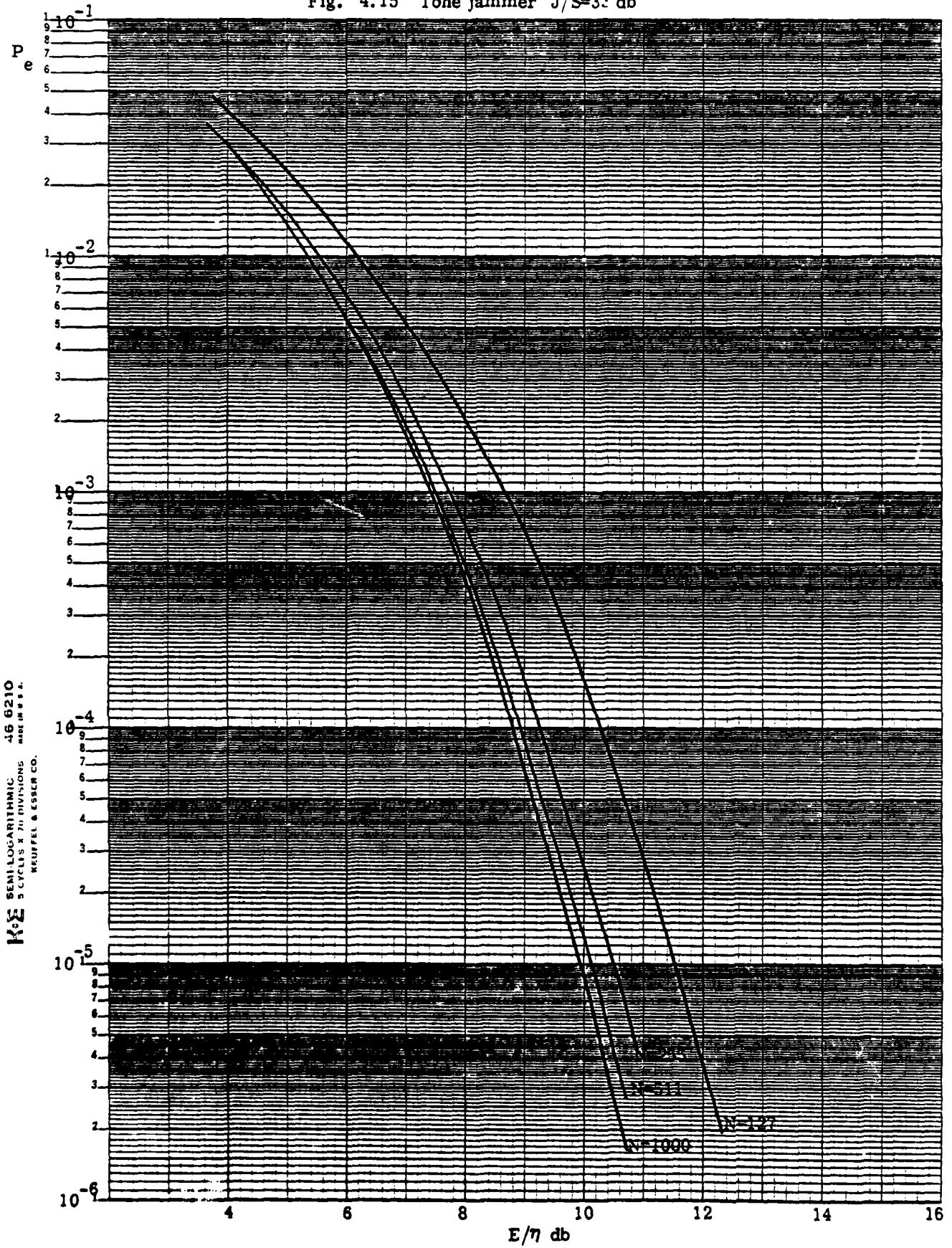
Fig. 4.16 Tone jammer J/S=43 db.

Fig. 4.16 Tone jammer J/S=43 db.
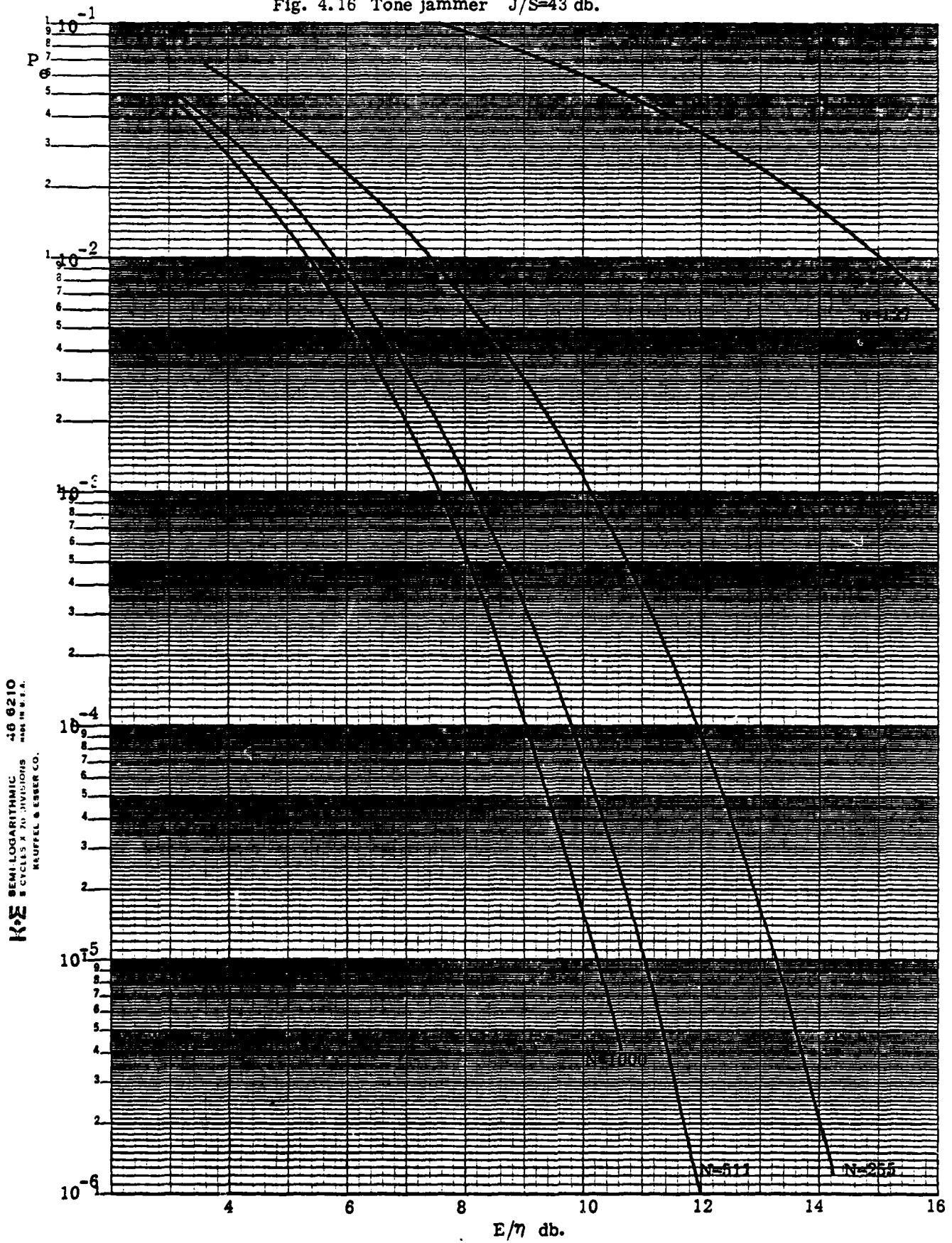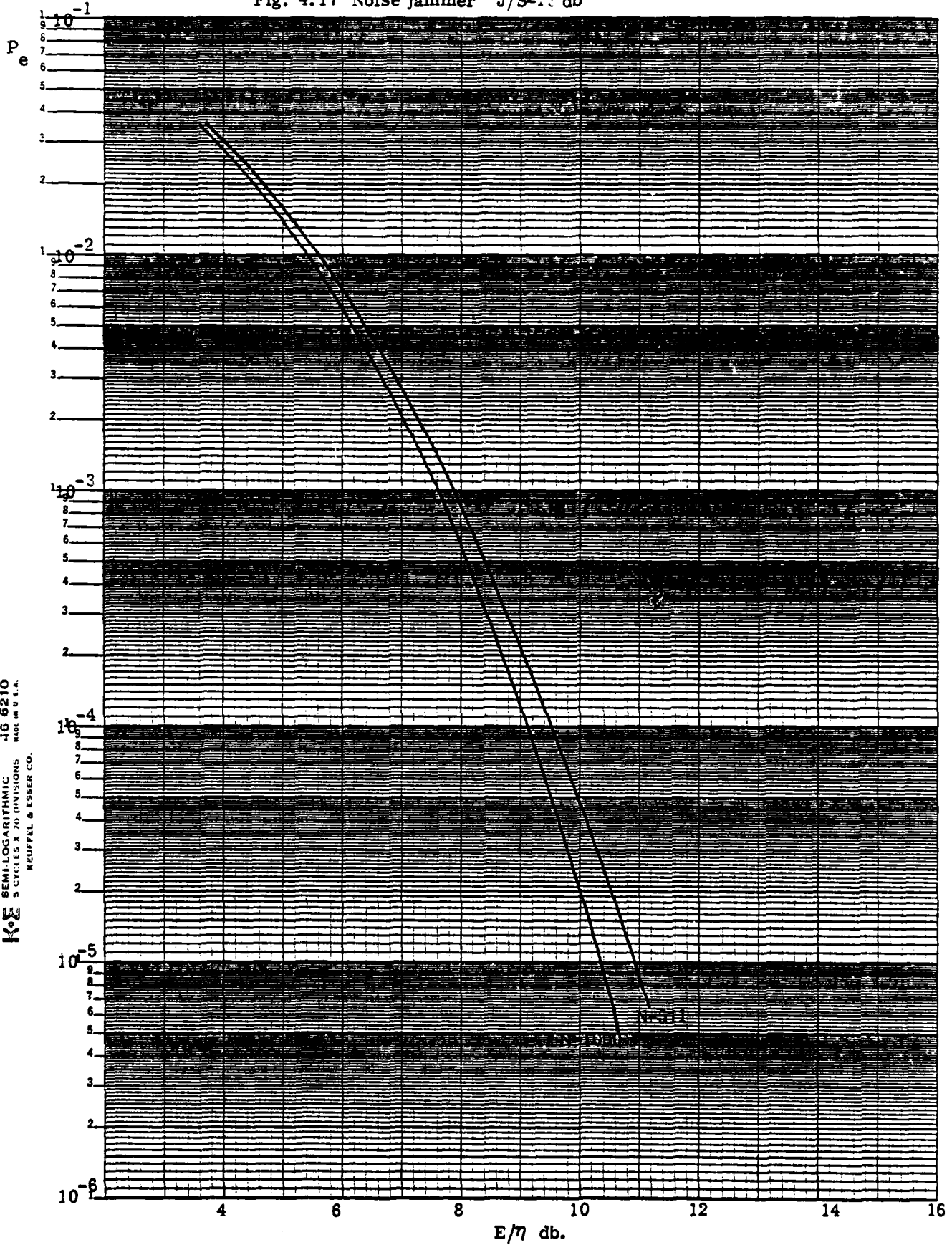
Fig. 4.17 Noise jammer J/S=13 db

Fig. 4.18 Noise jammer J/S=23 db
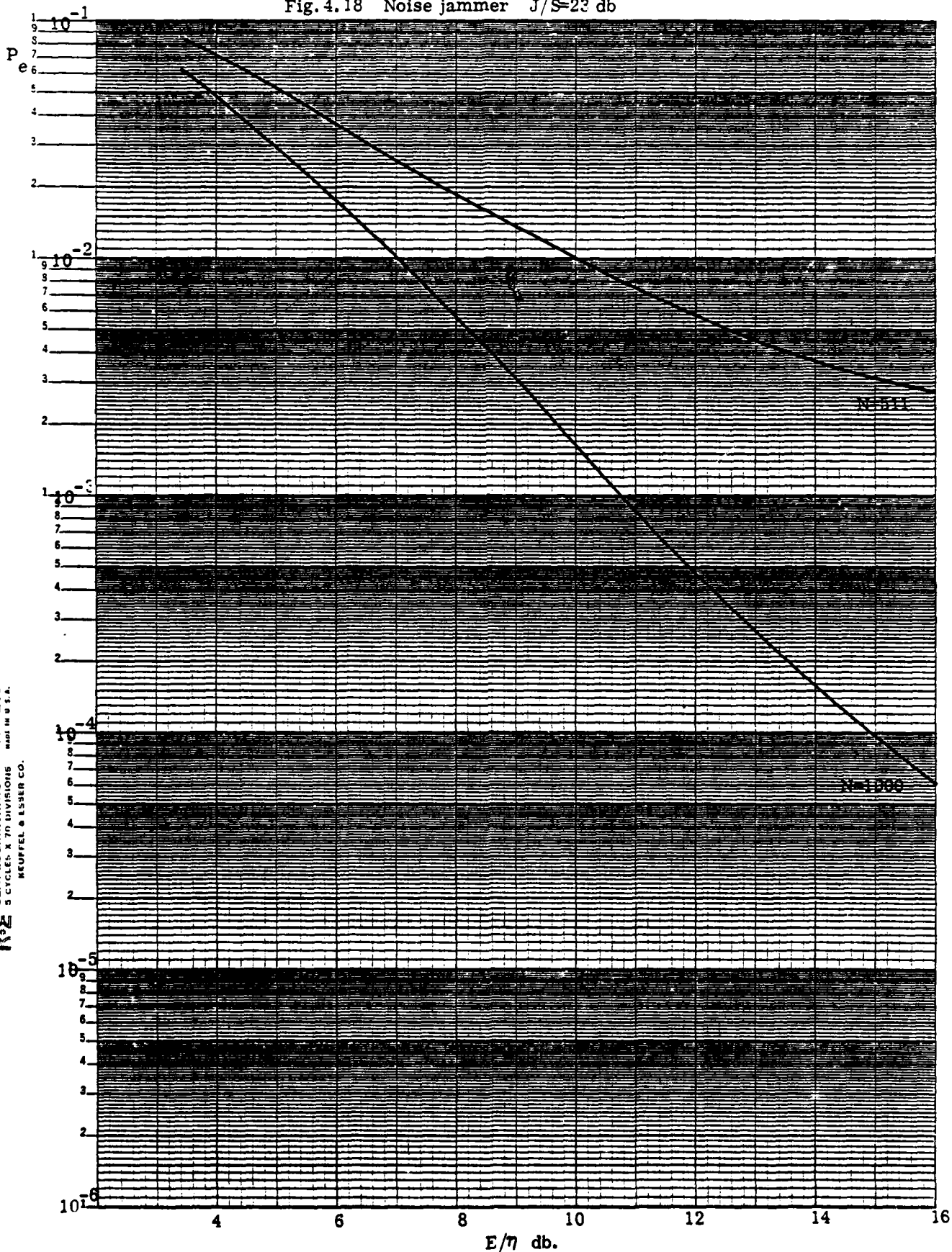
P_e

E/η db.

N=511

N=1000

In order to obtain reasonable performance with an FH-
FSK system in the presence of an intentional jammer, it is
well known that some type of error-correction coding must be
used. This can be seen very simply by assuming the jammer
is much stronger than the desired signal and that he chooses
to put all his power in a single slot (i.e. the jammer jams
one out of N slots). Then with no error-correction coding,
the system will make an error (with high probability) every
time it hops to that particular frequency being jammed. This
will happen on the average one out of every N hops, so that
the probability of error of the system will be approximately
1/N, independent of signal-to-noise ratio.

In light of this, all FH systems considered will be
evaluated uncoded, encoded with a (7,4) Hamming code, and en-
coded with a (23,12) Golay code [4.4]. As is well known, the
(7,4) Hamming code corrects all single errors, while the (23,
12) Golay code corrects all combinations of three or fewer
errors.

Since the addition of parity check bits required in error
correcting codes results in an increased bandwidth (assuming
the information rate is constant), to make the overall compari-
son fair, the amount of spread spectrum processing gain will
be decreased by the same proportion that the error-correcting
code expands the bandwidth. For example, if the uncoded FH-FSK
system uses N slots, the (7,4) Hamming encoded system will use
4N/7 slots.

The probability of making a word error can be computed very simply as follows: Let P_e be the probability of making an error on an individual bit. Under the assumption that the frequency being hopped to during the ith interval is independent of where it was at the $(i-1)^{th}$ interval (or any other interval), it can be shown that

$$P_e = \left(\frac{N-K}{N}\right)^2 P_e(a_o,b_o,0) + \frac{K}{N}\frac{N-K}{N}\left[P_e(a_{11},b_{11},A_{11}) + P_e(a_{12},b_{12},A_{12})\right]$$

$$+ \left(\frac{K}{N}\right)^2 P_e(a_o,b_o,0) \tag{4.3}$$

for a partial-band noise jammer, and

$$P_e = \left(\frac{N-K}{N}\right)^2 P_e(a_o,b_o,0) + \frac{K(N-K)}{N^2}\frac{1}{2\pi}\left[\int_0^{2\pi} P_e(a_{11},b_{11},0)d\theta_1 + \int_0^{2\pi} P_e(a_{12},b_{12},0)d\theta_2\right]$$

$$+ \left(\frac{K}{N}\right)^2\frac{1}{4\pi^2}\int_0^{2\pi}\int_0^{2\pi} P_e(a,b,0)d\theta_1 d\theta_2 \tag{4.4}$$

for a partial-band tone jammer. In (4.3) and (4.4), the notation is that introduced in Chapter IV of [4.1], in which all the a's, b's, and A's are explicitly defined.

With P_e as given by (4.3) or (4.4), the probability of making a word error in an n-bit code that can correct up to e errors is given by

$$P_{ew} = \sum_{i=e+1}^{n} \binom{n}{i} P_e^i(1-P_e)^{n-i} \tag{4.5}$$

The final probability of bit error in the decoded sequence is somewhat more difficult to calculate. It is shown in [4.5] that the following is a reasonable approximation:
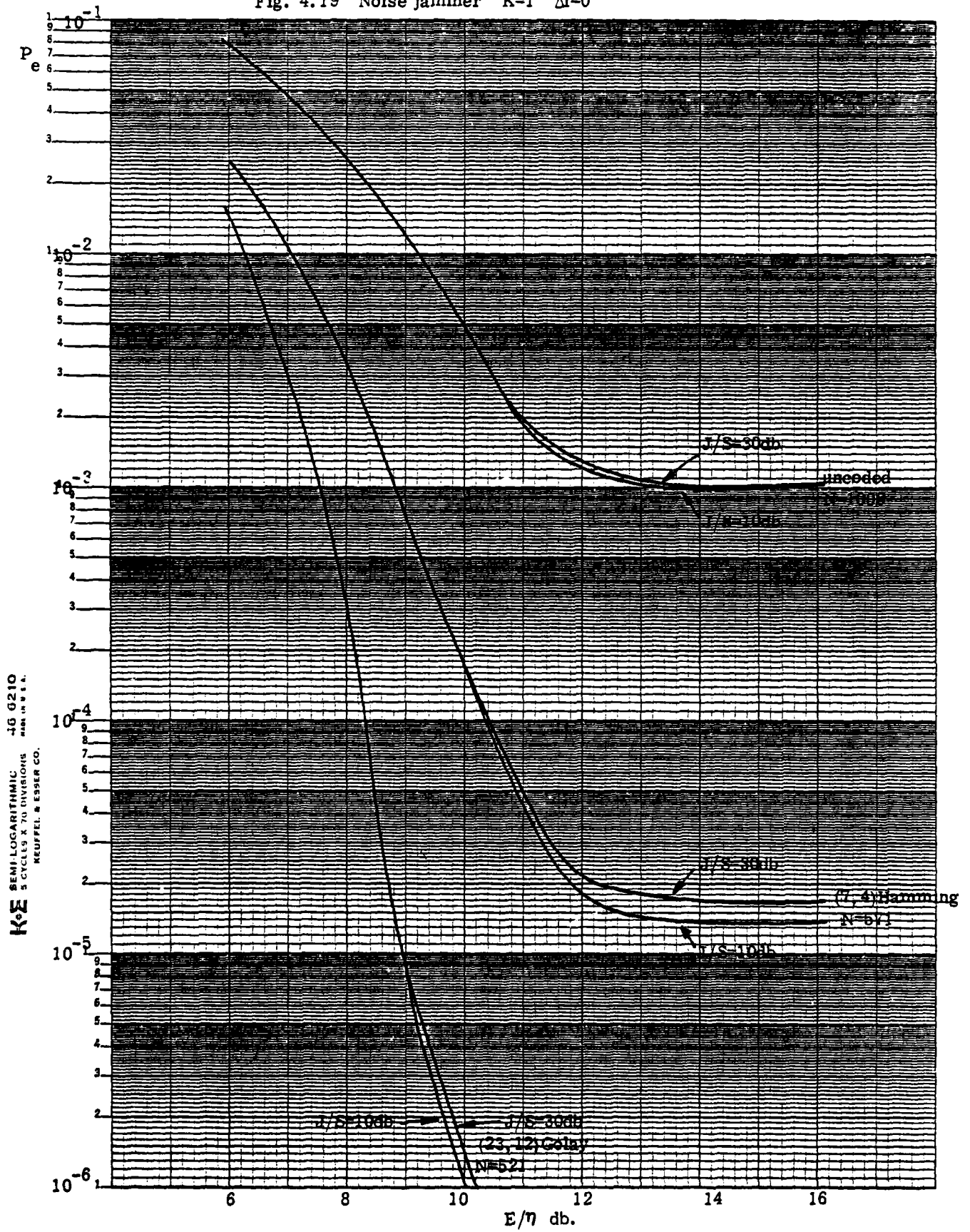
$$P_b \simeq \frac{1}{n} \sum_{i=e+1}^{n} i \binom{n}{i} \; P_e^i \; (1-P_e)^{n-i} \tag{4.6}$$

Equation (4.6) will be computed for the two coded systems and both will be compared to the results obtained for the uncoded system.

The results of such a comparison are shown in Figures 4.19-4.30. There are two different comparisons illustrated in these figures. The first considers the performance of an orthogonal (i.e. $\Delta f = 0$) noncoherent FSK-FH system under the three coding situations listed above, and the second picks the best of those conditions, namely the (23,12) Golay code, and considers the effect of varying Δf (recall from [4.1] that Δf is a measure of the degree of overlap between the MARK and SPACE frequencies).
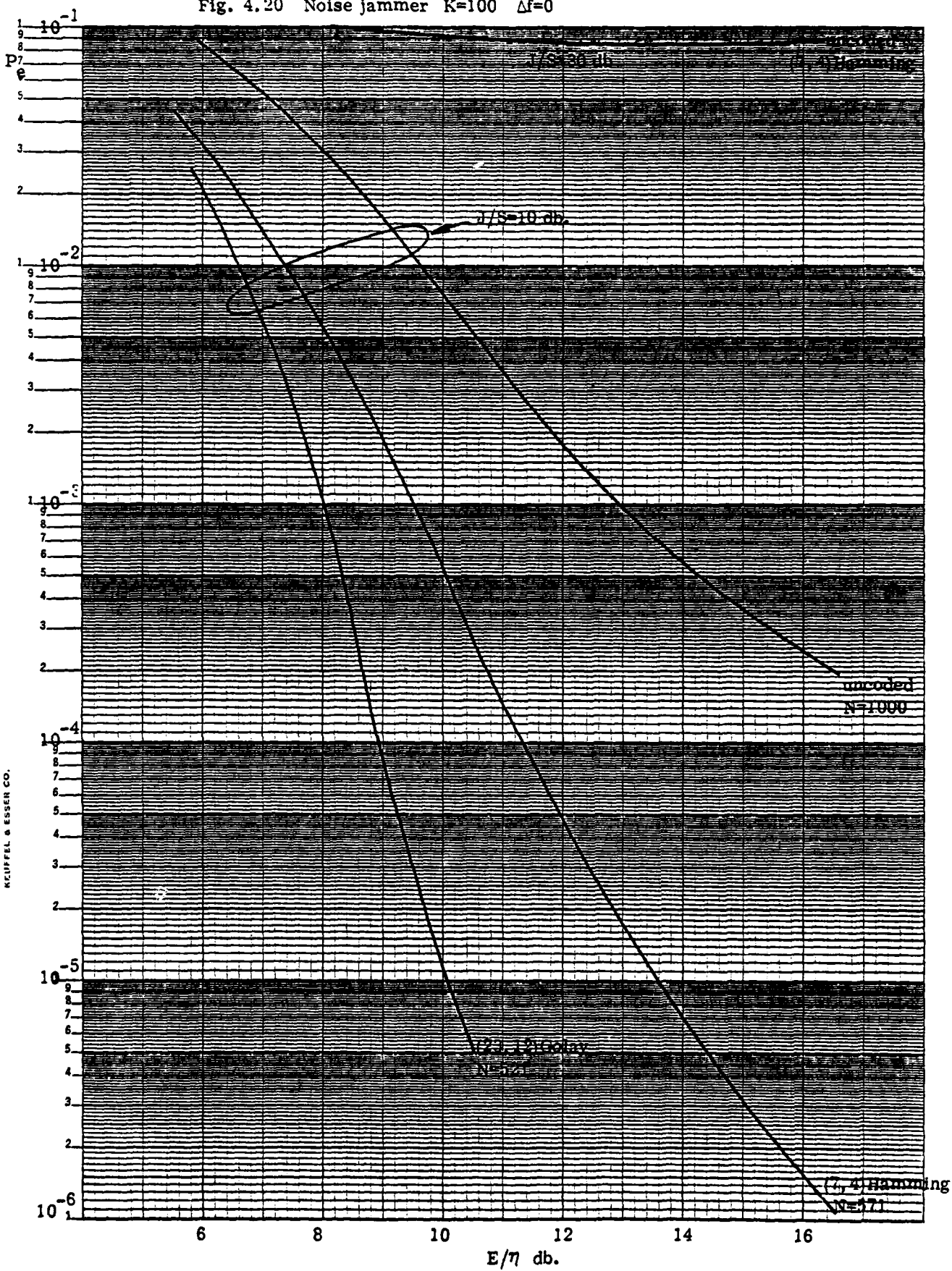
Consider the first comparison illustrated in Figures 4-19-4.22 and 4.27-4.28. Figures 4.19 and 4.20 show the effect of partial bound noise jamming when K, the total number of slots being jammed, is equal to 1 and 100, respectively. The total number of slots which were available for use by the uncoded system was N = 1000. This resulted in 571 slots for the system employing the (7,4) Hamming code and 521 slots for the system using the (23,12) Golay code. From Figure 4.19, it can

Fig. 4.19   Noise jammer   K=1   Δf=0

Fig. 4.19   Noise jammer   K=1   Δf=0

Fig. 4.20   Noise jammer   K=100 $\Delta f=0$

P_e

J/S=30 db

(7,4)Hamming

J/S=10 db

uncoded
N=1000

(23,12)Golay
N=529

(7,4)Hamming
N=171

E/η db.

Fig. 4.21 Tone jammer K=1 $\Delta f=0$

P

10^{-1}
9
8
7
6
5
4
3
2

10^{-2}
9
8
7
6
5
4
3
2

J/S=20 db

uncoded
N=1000

10^{-3}
9
8
7
6
5
4
3
2

J/S=10 db

10^{-4}
9
8
7
6
5
4
3
2

J/S=20 db

(7,4)
Hamming
N=571

J/S=10 db

10^{-5}
9
8
7
6
5
4
3
2

J/S=10db   J/S=20 db

(23, 12) Golay
N=521

10^{-6}

6   8   10   12   14   16

E/η

K&E SEMI-LOGARITHMIC 46 6210
5 CYCLES X 70 DIVISIONS MADE IN U.S.A.
KEUFFEL & ESSER CO.

Fig. 4.21 Tone jammer K=1 $\Delta f=0$
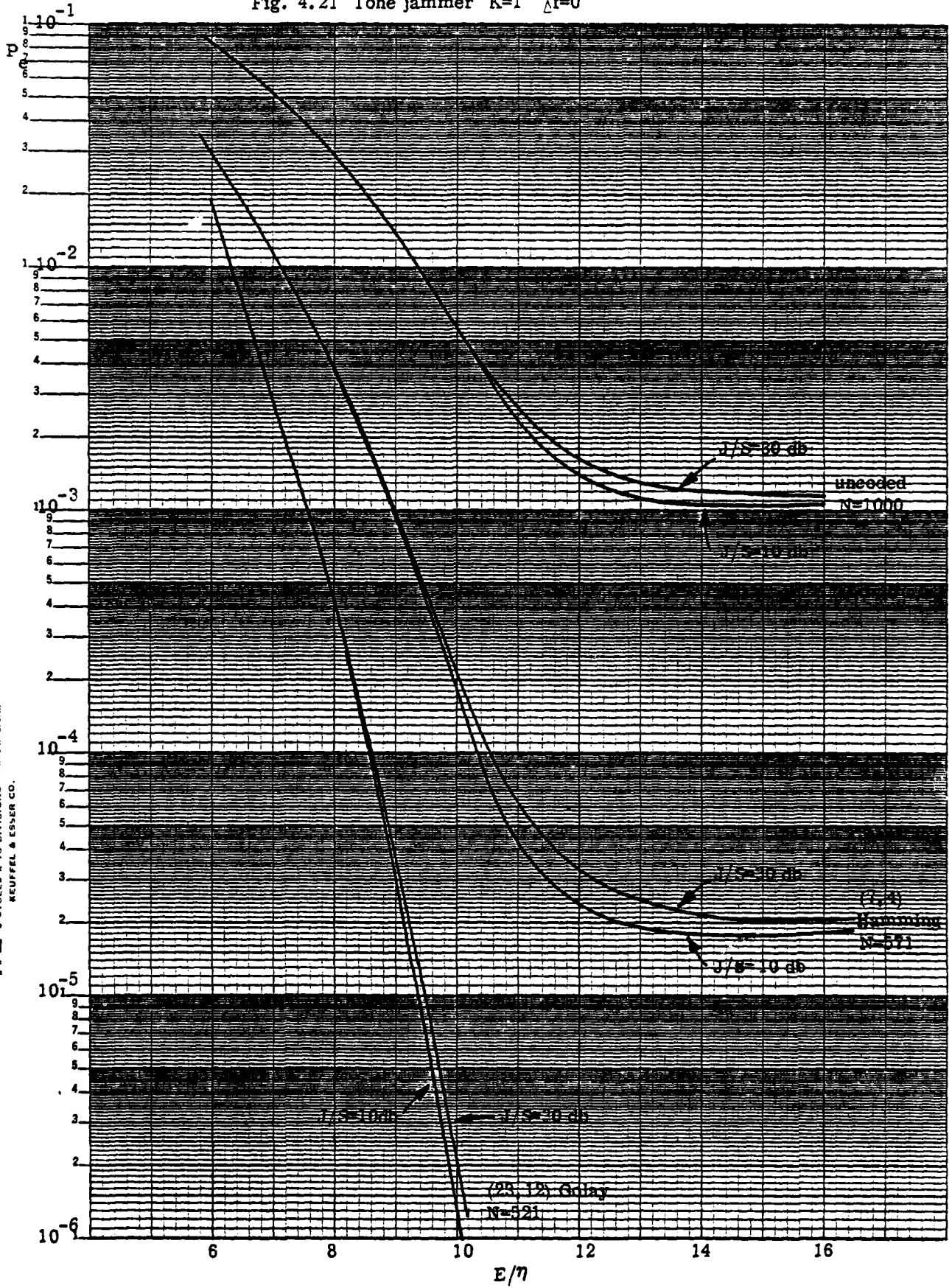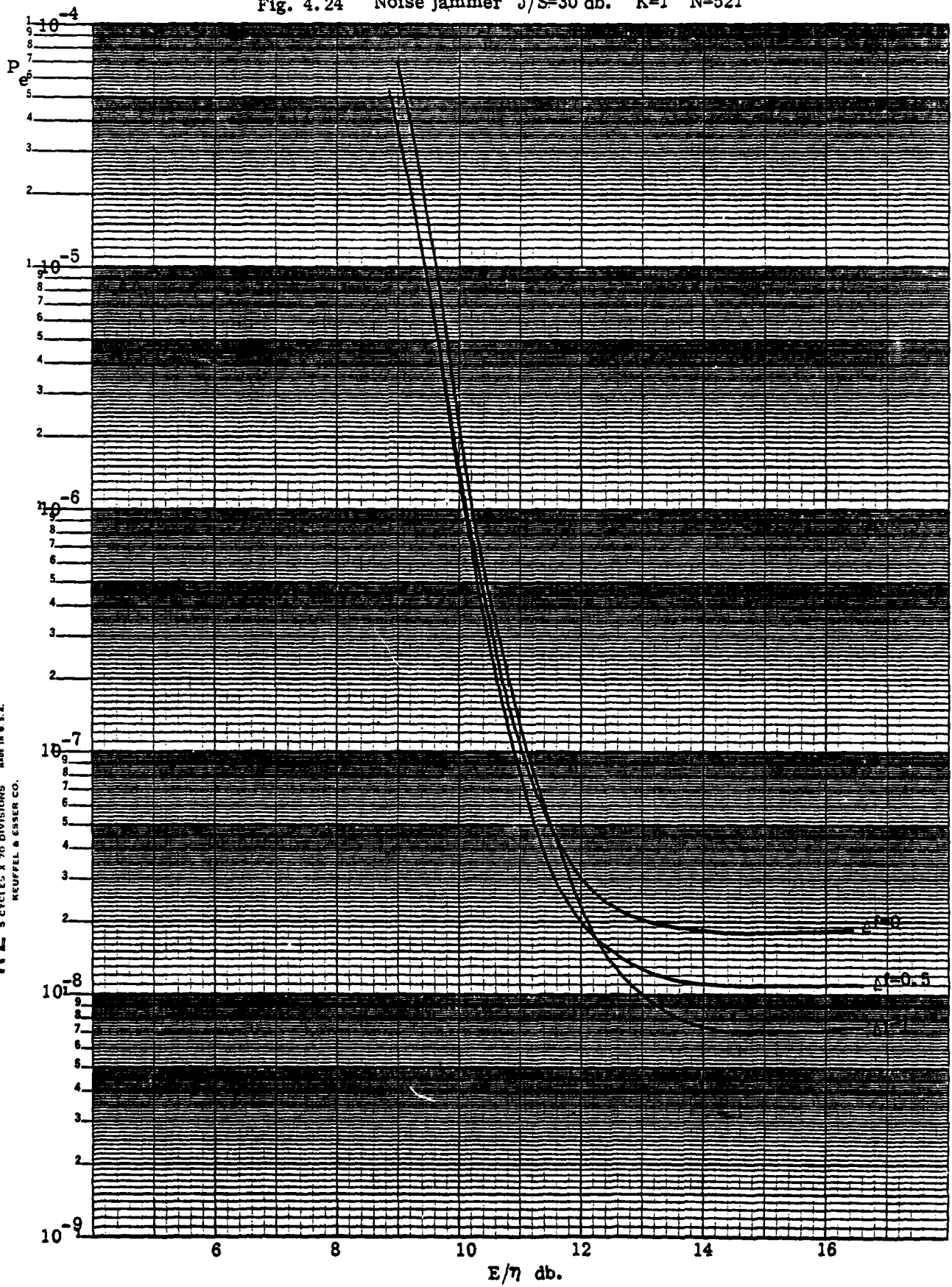
Fig. 4.22   Tone jammers   K=100 $\Delta f=0$
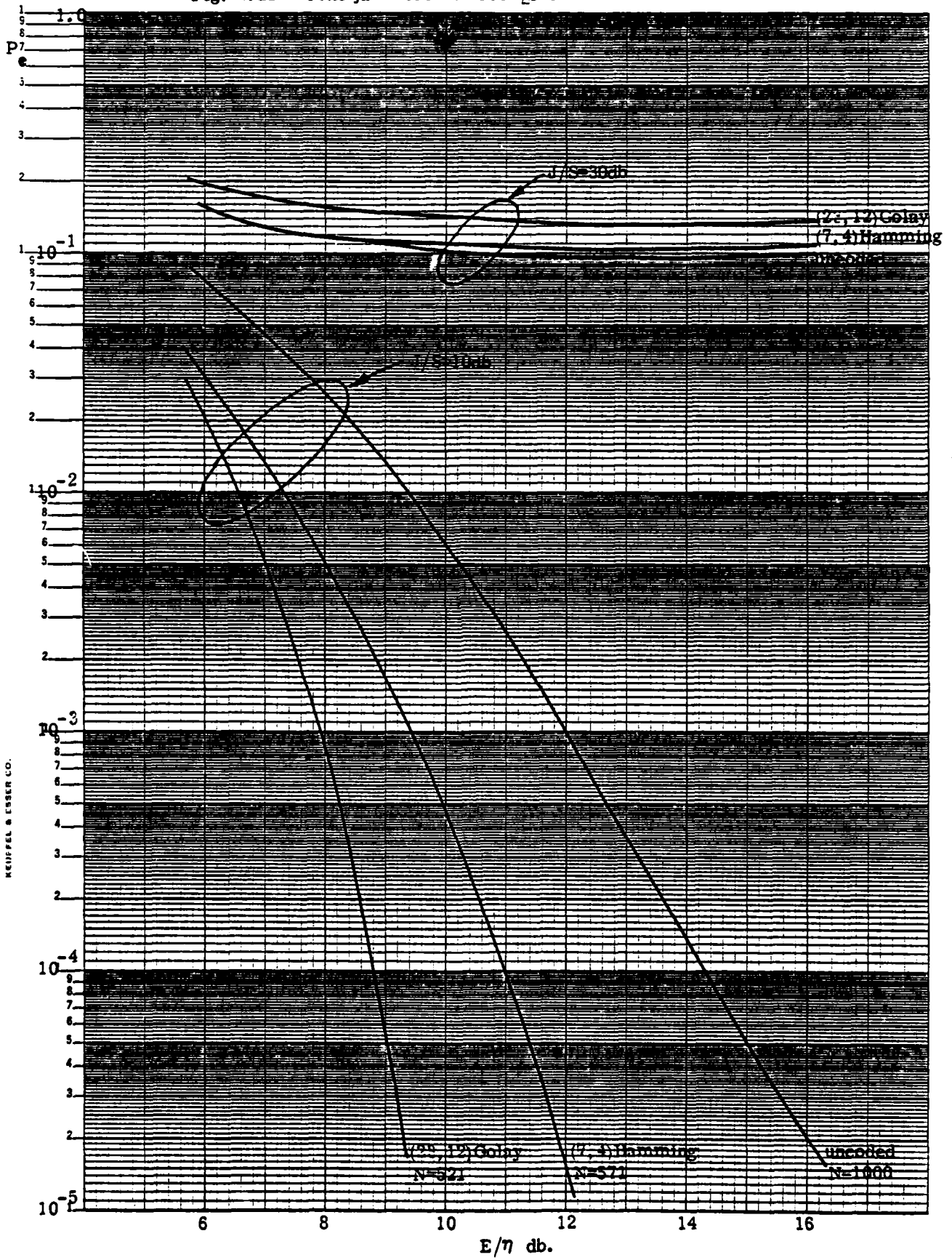
P e

J/S=30db

(23, 12)Golay
(7, 4)Hamming
uncoded

J/S=10db

(23, 12)Golay
N=521

(7, 4)Hamming
N=571

uncoded
N=1000

E/η db.

6   8   10   12   14   16

Fig. 4.23 Noise jammers K=100 N=521

J/S=30 db
Δf=0
Δf=0.5

J/S=20 db
Δf=0
Δf=0.5
Δf=1

J/S=10 db

Δf=1
Δf=0
Δf=0.5

P_e

E/η db.
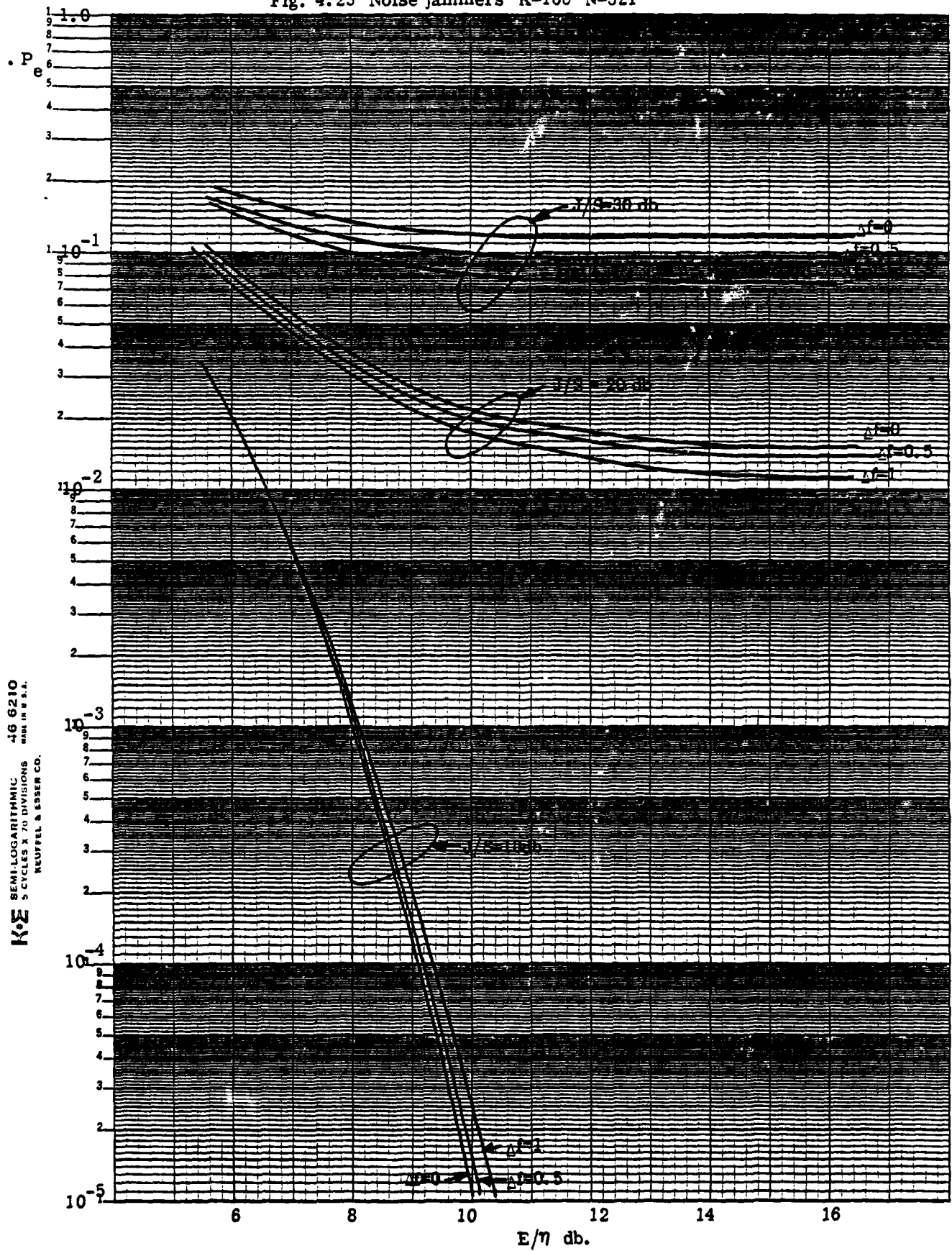
SEMI-LOGARITHMIC   46 6210
5 CYCLES X 70 DIVISIONS   MADE IN U.S.A.
KEUFFEL & ESSER CO.

Fig. 4.24   Noise jammer   J/S=30 db.   K=1   N=521

Fig. 4.25 Tone jammer J/S=30 db K=1 N=521
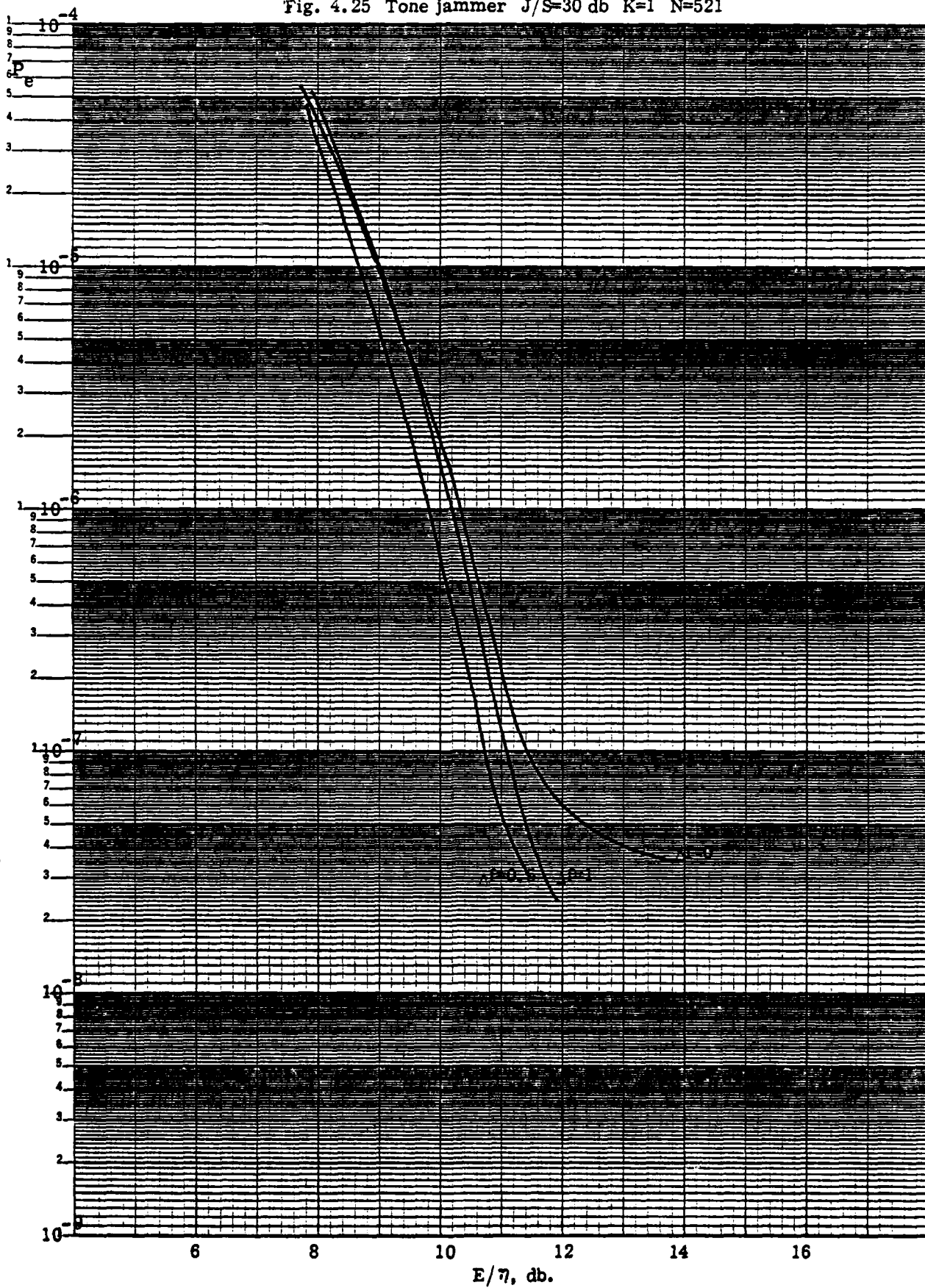
Fig. 4.26 Tone jamming K=100 N=521
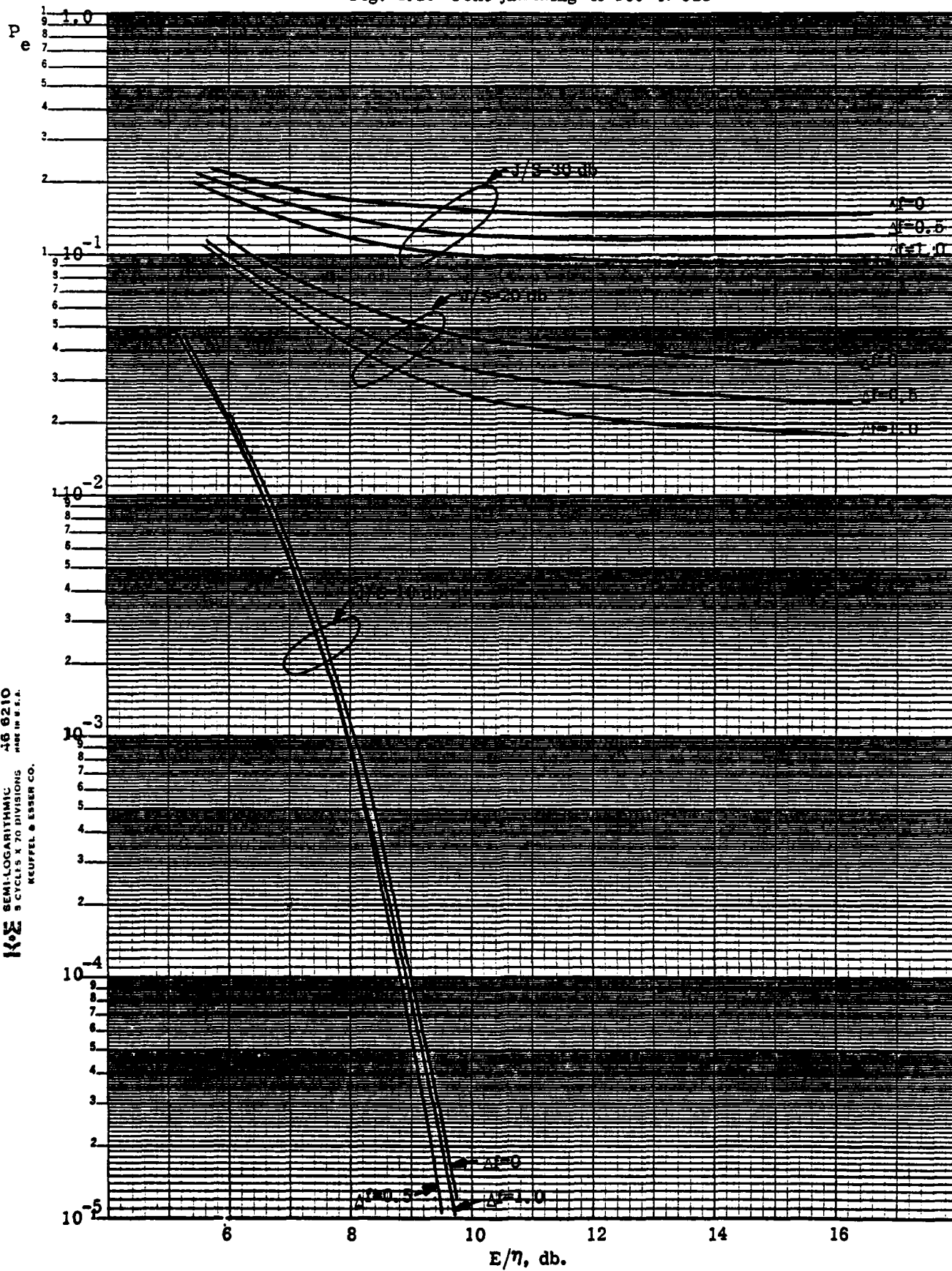
Fig. 4.27 Noise jammer K=1 $\triangle$f=0
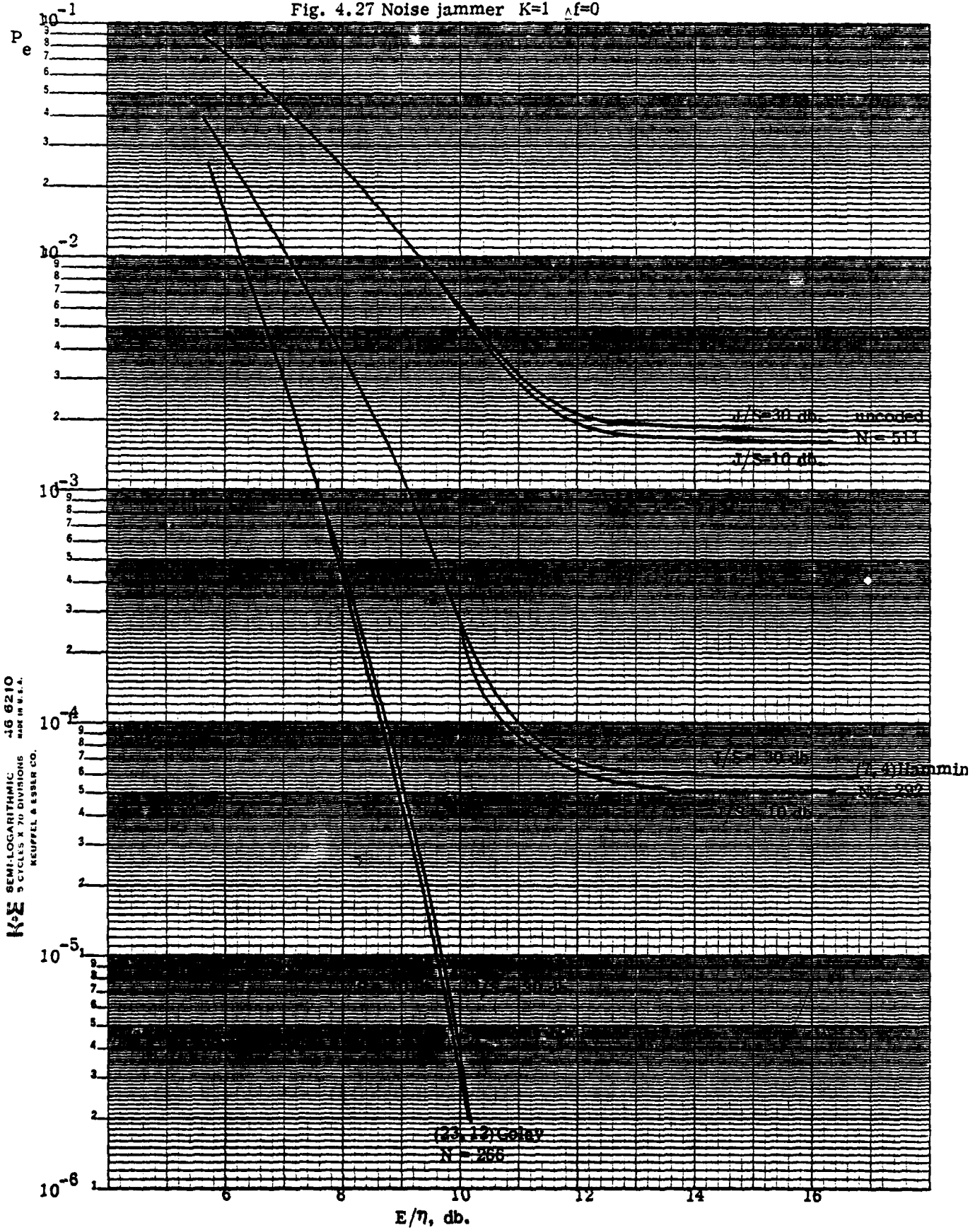
Fig. 4.28 Noise jammer K=100 ∧f=0
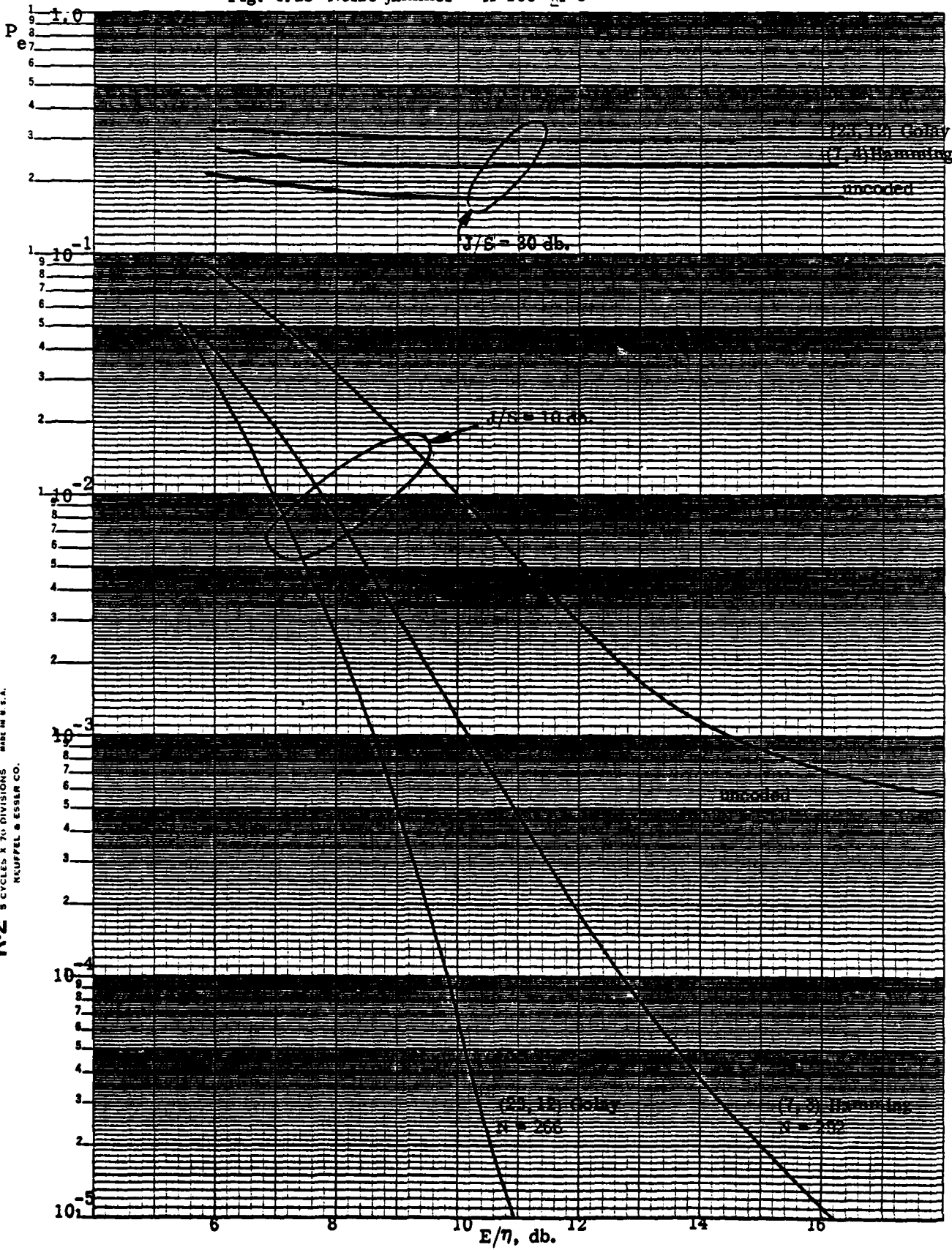
Fig. 4.29 Noise jammer   J/S = 30 db K=1 N=266
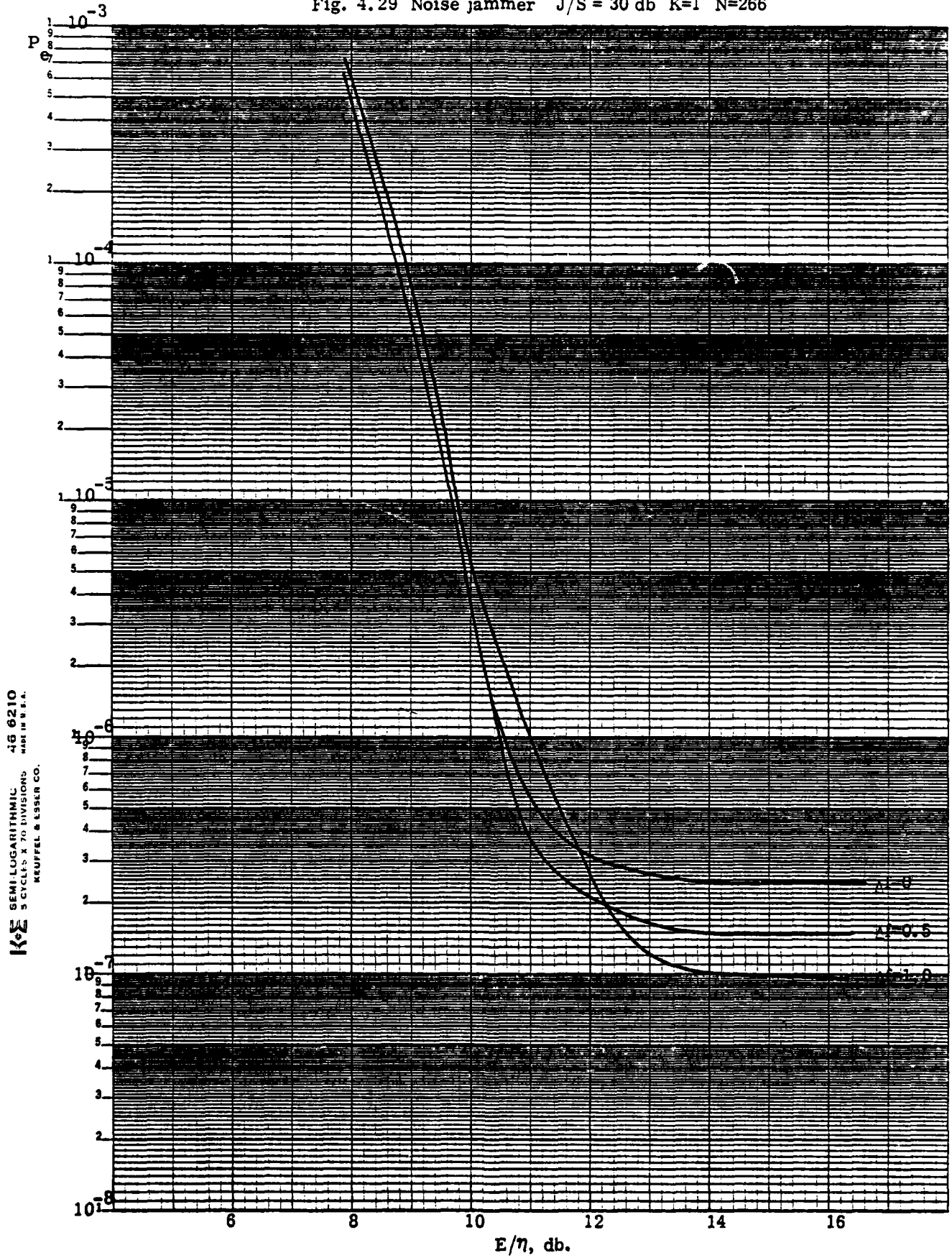
E/η, db.

Fig. 4.30   Noise jammers   K=100   N=266
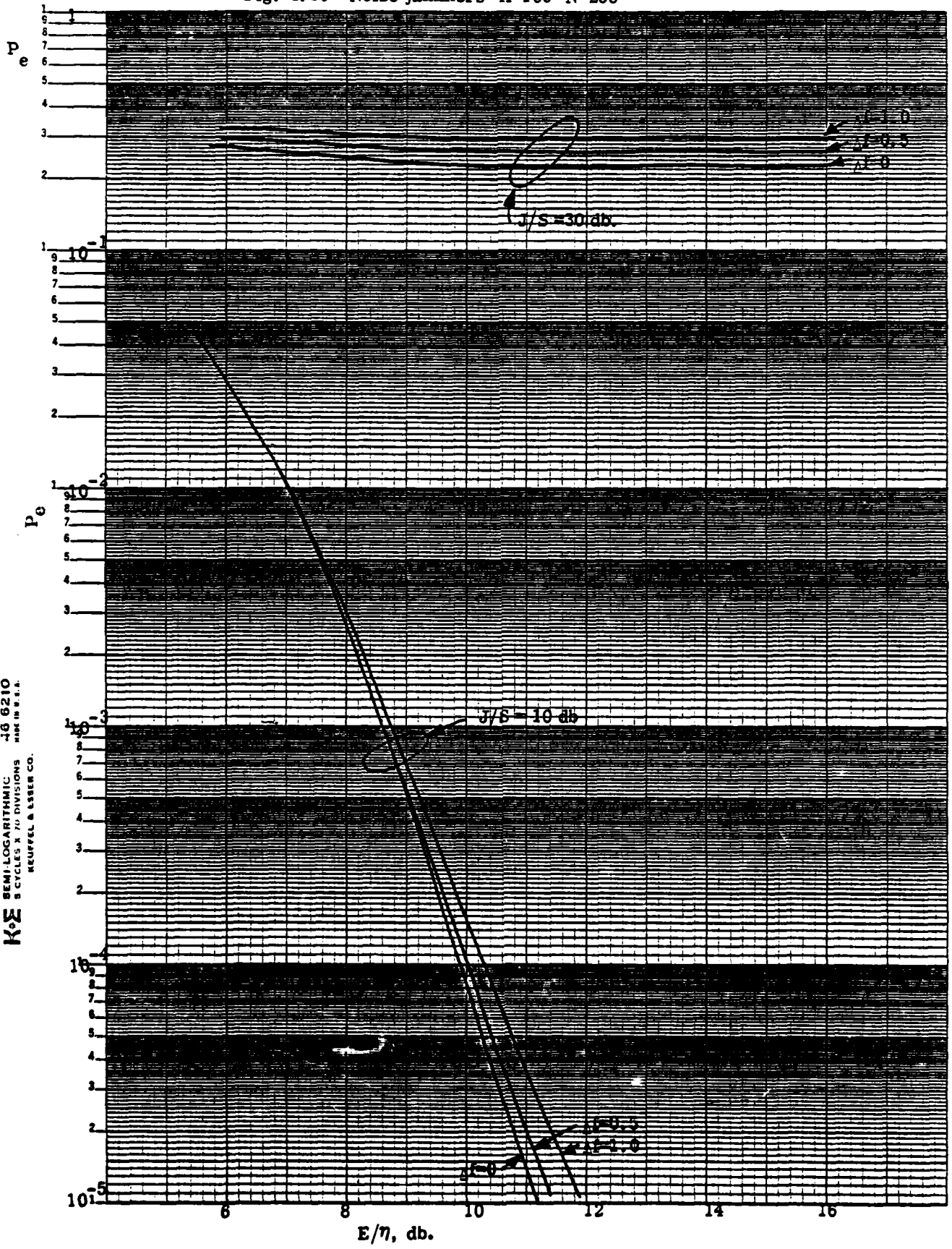
P_e

P_e

J/S =30 db.

J/S = 10 db

J=1.0
J=0.5
J=0

J=0.5
J=1.0
J=0

K+E SEMI-LOGARITHMIC 46 6210
3 CYCLES X 70 DIVISIONS MADE IN U.S.A.
KEUFFEL & ESSER CO.

E/η, db.

be seen that the difference in system performance when J/S = 10 dB

from when J/S ≈ 30 dB was negligible for each of the three cod-

ing situations. On the other hand, whereas the curves, for the

uncoded system, flatten out at $P_e = \frac{1}{N} = 10^{-3}$, the coded sys-

tems perform markedly better. In particular, the advantage

of using the three-error correcting Golay code is evident.

From Figure 4.20, one can see a clear qualitative differ-

ence from the results of Figure 4.19. There is now a tremen-

dous difference in the effect of the jammer when the J/S is

increased from 10 dB to 30 dB. In fact, for the J/S = 30 dB

case, the Golay encoded system was actually the poorest and

resulted in an error rate of slightly greater than 10^{-1}. It

is for this reason that that particular curve is missing from

Figure 4.20. Also, it is clear from Figures 4.19 and 4.20

that for the same jammer power it is much more advantageous to

the jammer to jam 100 of the slots rather than just a single

slot.

If the noise jammers are replaced with tone jammers, the

analogous results are shown in Figures 4.21 and 4.22. It can

be seen that there is no qualitative difference from the noise

jamming case and relatively little quantitative difference.

Considering now Figures 4.23-4.26, it can be seen that

the effect of going from a perfectly orthogonal ($\Delta f = 0$), Golay

encoded, noncoherent FSK system to one with a 50% overlap

($\Delta f - 1.0$) between MARK and SPACE frequencies (with a correspond-

ing 50% increase in the number of slots over which to hop) is

is relatively small, with again no significant difference in system performance under noise and tone jamming conditions.

Finally, Figures 4.27-4.30 show similar results for the noise jamming case when the processing gain for the uncoded system was reduced to 511. This resulted in a processing gain of 292 for the system using the (7,4) Hamming code and 266 for the system using the (23,12) Golay code. In particular, it is again seen that for the Golay encoded system there is not a significant difference in system performance when the overlap in the MARK and SPACE channels is increased from 0 to 50%.

The following table summarizes the results presented in the figures for the coded and the uncoded FH-FSK systems.

Figure	Processing Gain	$\frac{J}{S}$ (dB)	Type of Jammer	Number of Slots Jammed
4.19	1000	10, 30	Noise	1
4.20	1000	10, 30	Noise	100
4.21	1000	10, 30	Tone	1
4.22	1000	10, 30	Tone	100
4.23**	1000	30	Noise	1
4.24**	1000	10, 20, 30	Noise	100
4.25**	1000	30	Tone	1
4.26**	1000	10, 20, 30	Tone	100
4.27	511	10, 30	Noise	1
4.28	511	10, 30	Noise	100
4.29**	511	30	Noise	1
4.30**	511	10, 30	Noise	100

*This is the processing gain of the uncoded system.

**Shows curve for different values of frequency overlap between MARK and SPACE channels

4.0   Conclusion

In this chapter, results have been presented for the per-
formance of various coherent DS spread spectrum systems as well
as for certain noncoherent FSK-FH systems. The underlying
constraint in all the analysis presented here is the assump-
tion that the total bandwidth of the channel is fixed. There-
fore, if some technique is used to alter the required signal
bandwidth before any spread spectrum processing gain is applied
(e.g. using an M-ary signal alphabet or using an error-correct-
ing code), the amount of processing gain itself must correspond-
ingly be eltered to keep the total bandwidth constant.

Under this constraint, it appears from the results that
have been obtained to date that a DS system employing coher-
ent QPSK modulation yields the best overall performance. In-
deed, the performance of the QPSK system (or for that matter
any of the DS systems) could probably still be improved
further over what is shown in the figures by combining PN cod-
ing with error-correction coding as was done with the FSK-FH
systems.

Relative to the FH systems, it is clear that if one does
employ some type of error-correction coding, the improvement
in system performance can be substantial. On the other hand,
one does not really gain very much by going to a system in
which the MARK and SPACE frequencies overlap, at least not
when one is employing error-correction coding as well.

Finally, there are certain areas which still must be

investigated in order to have a complete picture as to how the tradeoffs should be made. One area was alluded to above, namely that of combining error-correction coding with spread spectrum coding for a DS system and then evaluating system performance. Other areas include more precise results of the effect of a tone jammer on a DS system when the jammer is off-set in frequency from the carrier frequency of the modulation, and the effect of a comb jammer on a DS system.

5.0   References

[4.1]   "Adaptive Techniques in Multichannel Transmission,"
         Interim Report 2 for 9/30/78 - 1/31/79, prepared for
         U.S. Army CORADCOM by S Consulting Services.

[4.2]   Arthurs, E. and H. Dym, "On the optimum detection of
         digital signals in the presence of white gaussian
         noise," IRE Trans. Comm. Systems, vol. CS-10, pp. 336-
         372, December 1962.

[4.3]   Lucky, R.W., J. Salz and E.J. Weldon, Jr., Principles
         of Data Communication, McGraw-Hill, 1968.

[4.4]   R.G. Gallager, Information Theory & Reliable Communi-
         cation. Wiley, 1968.

[4.5]   "Error Control Coding Handbook," Final report prepared
         by Linkabit Corporation for U.S. Air Force, July 15,
         1976.